

DEVELOPMENT OF PAPER-BASED ANALYTICAL DEVICES FOR SIMULTANEOUS NAKED-  
EYE DETECTION OF HEAVY METAL IONS



A Dissertation Submitted in Partial Fulfillment of the Requirements  
for the Degree of Doctor of Philosophy in Chemistry

Department of Chemistry

FACULTY OF SCIENCE

Chulalongkorn University

Academic Year 2020

Copyright of Chulalongkorn University

การพัฒนาอุปกรณ์วิเคราะห์ฐานกระดาษสำหรับการตรวจวัดไอออนโลหะหนักพร้อมกันด้วยตาเปล่า



วิทยานิพนธ์นี้เป็นส่วนหนึ่งของการศึกษาตามหลักสูตรปริญญาวิทยาศาสตรดุษฎีบัณฑิต

สาขาวิชาเคมี ภาควิชาเคมี

คณะวิทยาศาสตร์ จุฬาลงกรณ์มหาวิทยาลัย

ปีการศึกษา 2563

ลิขสิทธิ์ของจุฬาลงกรณ์มหาวิทยาลัย

Thesis Title	DEVELOPMENT OF PAPER-BASED ANALYTICAL DEVICES FOR SIMULTANEOUS NAKED-EYE DETECTION OF HEAVY METAL IONS
By	Miss Pornphimon Kamnoet
Field of Study	Chemistry
Thesis Advisor	Associate Professor WANLAPA AEUNGMAITREPIROM, Ph.D.

---

Accepted by the FACULTY OF SCIENCE, Chulalongkorn University in Partial  
Fulfillment of the Requirement for the Doctor of Philosophy

..... Dean of the FACULTY OF SCIENCE  
(Professor POLKIT SANGVANICH, Ph.D.)

DISSERTATION COMMITTEE

..... Chairman  
(Associate Professor VUDHICHAJ PARASUK, Ph.D.)

..... Thesis Advisor  
(Associate Professor WANLAPA AEUNGMAITREPIROM,  
Ph.D.)

..... Examiner  
(Professor THAWATCHAI TUNTULANI, Ph.D.)

..... Examiner  
(Associate Professor FUANGFA UNOB, Ph.D.)

..... External Examiner  
(Assistant Professor Yupaporn Sameenoi, Ph.D.)

พรพิมล กำเนิด : การพัฒนาอุปกรณ์วิเคราะห์ฐานกระดาษสำหรับการตรวจวัดไอออนโลหะหนักพร้อมกันด้วยตาเปล่า. ( DEVELOPMENT OF PAPER-BASED ANALYTICAL DEVICES FOR SIMULTANEOUS NAKED-EYE DETECTION OF HEAVY METAL IONS) อ.ที่ปรึกษาหลัก : รศ. ดร.วัลภา เอื้องไมตรีภรณ์

ประดิษฐ์อุปกรณ์วิเคราะห์ฐานกระดาษด้วยวิธีการพิมพ์พอลิเมอร์และการพิมพ์ซีดี ออกแบบอุปกรณ์หลายชนิดสำหรับการตรวจวัดไอออนโลหะหนักพร้อมกันในตัวอย่างน้ำสังเคราะห์ที่ไม่ทราบและตัวอย่างน้ำจริง ประยุกต์วิธีวิเคราะห์เชิงสีเพื่อตรวจวัดไอออนโลหะหนักโดยใช้ 1-(2-ไพริดีลาโซ)-2-แนพทอล บาโทฟีแนนโทรลีน 1, 5-ไดเฟนิลคาร์บาไซด์ บาโทคิวโปรอิน ไดมethylไกลออกซิม ไดโทโซน และ 4-(2-ไพริดีลาโซ) เรเซอร์ซินอล เป็นคอมเพลกซิงก์เอเจนต์ อย่างไรก็ตามคอมเพลกซิงก์เอเจนต์ต้องการการเลือกเฉพาะสูงมาก เพื่อปรับปรุงการเลือกเฉพาะสำหรับการตรวจวัดไอออนโลหะหนัก จึงออกแบบอุปกรณ์ให้มีโซนปรับสภาพและใช้มาสคิงเอเจนต์เพื่อกำจัดไอออนรบกวน นำวิธีที่เสนอนี้ใช้สำหรับการตรวจวัดทองแดง โคบอลต์ สังกะสี แคดเมียม หรือ ตะกั่วไอออนพร้อมกันด้วยตาเปล่าบนอุปกรณ์ชนิด D และการตรวจวัดทองแดง โคบอลต์ นิกเกิล พรอท เหล็ก โครเมียม วาเนเดียม และแมงกานีสไอออนแบบพร้อมกันด้วยตาเปล่าบนอุปกรณ์ชนิด E ในตัวอย่างน้ำสังเคราะห์ที่ไม่ทราบได้อย่างประสบความสำเร็จสำหรับการวิเคราะห์ปริมาณทองแดง โคบอลต์ นิกเกิล พรอท และแมงกานีสไอออนพร้อมกันบนอุปกรณ์ชนิด F ประสิทธิภาพการวิเคราะห์ให้ค่าความเข้มข้นต่ำสุดที่ตรวจวัดได้เป็น 0.32, 0.59, 5.87, 0.20 และ 0.11 มิลลิกรัมต่อลิตร สำหรับทองแดง โคบอลต์ นิกเกิล พรอท และแมงกานีสไอออนตามลำดับ วิธีที่เสนอนี้มีการเลือกเฉพาะสูงและมีประสิทธิภาพสำหรับวิเคราะห์ปริมาณทองแดง โคบอลต์ นิกเกิล พรอท และแมงกานีสไอออนพร้อมกันในน้ำดื่ม น้ำประปา และน้ำบ่อจากจุฬาลงกรณ์มหาวิทยาลัย และการตรวจวัดด้วยตาเปล่า

จุฬาลงกรณ์มหาวิทยาลัย  
CHULALONGKORN UNIVERSITY

สาขาวิชา เคมี  
ปีการศึกษา 2563

ลายมือชื่อนิสิต .....  
ลายมือชื่อ อ.ที่ปรึกษาหลัก .....

# # 5772072023 : MAJOR CHEMISTRY

KEYWORD:

Pornphimon Kamnoet : DEVELOPMENT OF PAPER-BASED ANALYTICAL DEVICES FOR SIMULTANEOUS NAKED-EYE DETECTION OF HEAVY METAL IONS. Advisor: Assoc. Prof. WANLAPA AEUNGMAITREPIROM, Ph.D.

Paper-based analytical device was fabricated by a polymer screen printing and wax printing methods. The various types of device were designed for simultaneous heavy metal ions detection in synthetic unknown and real water samples. The colorimetric method was applied to detect the heavy metal ions using 1-(2-pyridylazo)-2-naphthol, bathophenanthroline, 1, 5-diphenylcarbazide, bathocuproine, dimethylglyoxime, dithizone, and 4-(2-pyridylazo) resorcinol as complexing agents. However, complexing agents require very highly selectivity. To improve the selectivity for heavy metal ion detection, a device was designed with pretreatment zones and the masking agents were applied to remove interfering ions. The proposed method was successfully applied for simultaneous Cu(II), Co(II), Zn(II), Cd(II)/Pb(II) detection on device type D and for simultaneous Cu(II), Co(II), Ni(II), Hg(II), Fe(III), Cr(VI), V(III), and Mn(II) detection on device type E in synthetic unknown water samples by naked-eye. For simultaneous Cu(II), Co(II), Ni(II), Hg(II), and Mn(II) determination on device type F, the analytical performance was achieved with the lowest detectable concentration of 0.32, 0.59, 5.87, 0.20, and 0.11 mg/L for Cu(II), Co(II), Ni(II), Hg(II), and Mn(II), respectively. The proposed method provided highly selective and efficient for simultaneous Cu(II), Co(II), Ni(II), Hg(II), and Mn(II) determination in drinking, tap, and pond-CU water samples and detection by naked-eye.

Field of Study: Chemistry

Student's Signature .....

Academic Year: 2020

Advisor's Signature .....

## ACKNOWLEDGEMENTS

This research was successfully completed with the cooperation and assistance by many institutions and people. Therefore, I would like to thank for all support and suggestion.

First, I am really appreciation my advisor, Associate Professor Dr. Wanlapa Aeungmaitrepirom for all suggestion, mental support, and encouragement and I would like to gratitude to my proposal and thesis committees including Associate Professor Dr. Vudhichai Parasuk, Professor Dr. Thawatchai Tuntulani, Associate Professor Dr. Fuangfa Unob, Assistant Professor Dr. Yupaporn Sameenoi for useful comment and suggestion.

Second, my grateful thanks present to Associate Professor Dr. Pichayada Katemake (Department of Imaging and Printing Technology, Faculty of Science, Chulalongkorn University) for all suggestions and spectrophotometer color i5 instrumentation support.

Third, I am grateful to Professor Dr. Charles S. Henry (Colorado State University, United States) for giving the valuable experience to join in Henry Group as an exchange student and also thanks to Henry members for advice and wonderful experience. My thanks extend to Professor Dr. Orawan Chailapakul (Electrochemistry and Optical Spectroscopy Research Unit (EOSRU), Department of Chemistry, Faculty of Science, Chulalongkorn University) and EOSRU members for partial device fabrication and beneficial idea and recommendation.

This research was financially supported by The Development and Promotion of Science and Technology Talents Project (DPST) under Environmental Analysis Research Unit (EARU). My thanks present to EARU members for all suggestion and advice.

Finally, I am thankful my beloved parents and family for mental support and all support to succeed of this research.

Pornphimon Kamnoet

## TABLE OF CONTENTS

	Page
ABSTRACT (THAI).....	iii
ABSTRACT (ENGLISH).....	iv
ACKNOWLEDGEMENTS.....	v
TABLE OF CONTENTS.....	vi
LIST OF TABLES.....	x
LIST OF FIGURES.....	xiii
CHAPTER I INTRODUCTION.....	1
CHAPTER II THEORY AND LITERATURE REVIEW.....	6
2.1 Heavy metals in environment.....	6
2.2 Heavy metal determination methods.....	7
2.3 Microfluidic paper-based analytical device.....	8
2.4 Colorimetric methods for heavy metal determination.....	10
2.5 Complexing agents.....	13
2.6 Masking agents.....	16
CHAPTER III EXPERIMENTAL SECTION.....	20
3.1 Chemicals and instruments.....	20
3.2 Metal complex study in solution phase.....	24
3.2.1 PAN-metal complexes at pH 1-7.....	24
3.2.2 PAN-metal complexes at pH 5.....	24
3.3 Metal complex study on paper-based analytical device: polymer screen printing method.....	24

3.3.1 Device design and fabrication method: device type A, B, C, and D.....	24
3.3.2 Metal complex study on paper-based device type A .....	26
3.3.3 Simultaneous detection for four metal ions by naked-eye on paper-based device type B and C .....	27
3.3.4 Simultaneous detection for four metal ions by naked-eye on paper-based device type D.....	28
3.3.4.1 Optimization conditions.....	28
3.3.5 Application of simultaneous detection of four metal ions in synthetic unknown samples .....	29
3.4 Metal complex study on paper-based analytical device: wax printing .....	36
method.....	36
3.4.1 Device design and fabrication method: device type E and F.....	36
3.4.2 Metal complex study on paper-based analytical device type E.....	37
3.4.2.1 Optimization conditions.....	37
3.4.3 Application of simultaneous detection for eight metal ions in synthetic unknown samples .....	40
3.4.4 Metal complex study on paper-based analytical device type F.....	43
3.4.4.1 Optimization conditions.....	43
3.4.4.2 Colorimetric detection and interference study under optimal conditions .....	45
3.4.4.3 Simultaneous detection of five metal ions .....	45
3.4.4.4 Application of simultaneous determination of five metal ions in water samples.....	46
CHAPTER VI RESULTS AND DISCUSSIONS .....	48
4.1 Metal complex study in solution phase.....	48



4.1.1 PAN-metal complexes at pH 1-7.....	48
4.1.2 PAN-metal complexes at pH 5.....	49
4.2 Metal complex study on paper-based analytical device: polymer screen printing method .....	50
4.2.1 Device design and fabrication method: device type A, B, C, and D.....	50
4.2.2 Metal complex study on paper-based device type A .....	51
4.2.3 Simultaneous detection for four metal ions by naked-eye on paper-based device type B and C .....	57
4.2.4 Simultaneous detection for four metal ions by naked-eye on paper-based device type D.....	60
4.2.4.1 Optimization conditions.....	61
4.2.4.2 Application of simultaneous detection of four metal ions in synthetic unknown samples.....	65
4.3 Metal complex study on paper-based analytical device: wax printing .....	73
method .....	73
4.3.1 Device design and fabrication method: device type E and F.....	73
4.3.2 Metal complexes study on paper-based analytical device type E.....	74
4.3.2.1 Optimization conditions.....	74
4.3.2.2 Application of simultaneous detection for eight metal ions in synthetic unknown samples.....	90
4.3.3 Metal complex study on paper-based analytical device type F.....	93
4.3.3.1 Optimization conditions.....	93
4.3.3.2 Colorimetric detection and interference study under optimal conditions .....	103
4.3.3.3 Simultaneous detection of five metal ions .....	115

4.3.3.4 Application of simultaneous determination of five metal ions in water samples.....	118
CHAPTER V CONCLUSIONS.....	123
REFERENCES .....	125
VITA.....	135



## LIST OF TABLES

	Page
<b>Table 2.1</b> Table Heavy metal ions toxicity.....	6
<b>Table 2.2</b> The maximum permissible level of heavy metal ions in drinking water. ....	7
<b>Table 2.3</b> Properties of paper as substrates of $\mu$ PAD. ....	8
<b>Table 2.4</b> The fabrication methods for $\mu$ PAD. ....	9
<b>Table 2.5</b> The optimal pH of various complexing agent for heavy metals detection.	15
<b>Table 2.6</b> Cumulative formation constants for some metal complexing agent. ....	16
<b>Table 2.7</b> Cumulative formation constants for some metal masking agent. ....	19
<b>Table 3.1</b> Chemicals and suppliers. ....	20
<b>Table 3.2</b> Instruments and software. ....	23
<b>Table 3.3</b> Types of synthetic unknown water samples. ....	30
<b>Table 3.4</b> Specific hazard. ....	31
<b>Table 3.5</b> Identification of metal ion in unknown samples by comparison with the photograph of the color chart and the color chart in computer display by naked-eye. ....	35
<b>Table 3.6</b> Types of synthetic unknown samples. ....	41
<b>Table 4.1</b> The complexing and masking agent preparations for metal ion detection (50 mg/L) on the device type D. ....	65
<b>Table 4.2</b> The optimal conditions for simultaneous Cu(II), Co(II), Zn(II), Cd(II)/Pb(II) detection on the device type D. ....	65
<b>Table 4.3</b> The accuracy (student's results, n=10) for metal ion identification in 24 types of unknown samples. ....	71

<b>Table 4.4</b>	The summary of the accuracy for metal ion identification in comparison with photograph of the color chart.....	72
<b>Table 4.5</b>	The summary of the accuracy for metal ion identification in comparison with the color chart in computer display.....	73
<b>Table 4.6</b>	The reagent preparations and optimal conditions for metal ion detection on the device type E.....	86
<b>Table 4.7</b>	The masking agents for metal ion detection (0.40 mM) on the device type E.....	88
<b>Table 4.8</b>	The limit of detection (LOD) by naked-eye on device type E.....	91
<b>Table 4.9</b>	The optimal parameters for metal ion detection on device type F.....	102
<b>Table 4.10</b>	The reagent preparations and optimal conditions for metal ion detection on device type F.....	103
<b>Table 4.11</b>	The masking agents for metal ion detection on detection on the device type F.....	105
<b>Table 4.12</b>	Summary of the analytical performance of the proposed method for Cu(II), Co(II), Ni(II), Hg(II), and Mn(II) detection (n=5). .....	109
<b>Table 4.13</b>	Comparison of the performance between the proposed $\mu$ PAD and other $\mu$ PADs based on wax printing fabrication method for heavy metals detection by colorimetric methods. ....	118
<b>Table 4.14</b>	Summary of the recovery and RSD of the proposed sensor and the standard method (ICP-OES) for simultaneous Cu(II), Co(II), Ni(II), Hg(II), and Mn(II) determination in drinking water.....	120
<b>Table 4.15</b>	Summary of the recovery and RSD of the proposed sensor and the standard method (ICP-OES) for simultaneous Cu(II), Co(II), Ni(II), Hg(II), and Mn(II) determination in tap water.....	121

<b>Table 4.16</b> Summary of the recovery and RSD of the proposed sensor and the standard method (ICP-OES) for simultaneous Cu(II), Co(II), Ni(II), Hg(II), and Mn(II) determination in pond-CU water.....	122
--	-----



## LIST OF FIGURES

	Page
<b>Figure 2.1</b> Complexing agent structures in this research.....	14
<b>Figure 2.2</b> Masking agent structures in this research. ....	18
<b>Figure 3.1</b> Screen patterns design for device type A, B, C, and D.....	25
<b>Figure 3.2</b> Screen patterns on a wooden frame for (A-D) the device type A, B, C, and D, and (E) a squeegee. ....	25
<b>Figure 3.3</b> The polymer screen printing fabrication processes <sup>16</sup> . ....	26
<b>Figure 3.4</b> The components of device type B. ....	27
<b>Figure 3.5</b> The components of device type C.....	27
<b>Figure 3.6</b> The components of device type D.....	28
<b>Figure 3.7</b> Device components and type of reagents for simultaneous Cu(II), Co(II), Zn(II), Cd(II)/Pb(II) detection on one device.....	34
<b>Figure 3.8</b> The components of device type E. ....	36
<b>Figure 3.9</b> The components of device type F. ....	37
<b>Figure 3.10</b> ImageJ processes for image analysis. ....	44
<b>Figure 4.1</b> Color changes of PAN-metal complexes in solution phase at pH 1-7. ....	49
<b>Figure 4.2</b> Color changes of PAN-metal, PAN-thiourea-metal, PAN-KCl-metal complexes in solution at pH 5.....	50
<b>Figure 4.3</b> The device type A, B, C, and D after fabrication by using polymer screen-printing method. ....	51
<b>Figure 4.4</b> Color changes of metal-DTZ (left) and metal-PAN (right) complexes on device type A at pH 1-7. ....	52
<b>Figure 4.5</b> Cu(II), Co(II), and Zn(II)-PAN reaction. ....	53
<b>Figure 4.6</b> Cd(II) or Pb(II)-DTZ reaction.....	53

<b>Figure 4.7</b> Color changes of PAN-metal complexes on device type A.....	53
<b>Figure 4.8</b> Color changes of PAN-masking agent-metal complexes (left) and DTZ- masking agent-metal complexes (right) on device type A at pH 5. ....	55
<b>Figure 4.9</b> Color changes of (A) PAN-tartaric acid-metal complexes, (B) PAN-sodium citrate-metal complexes, and (C) PAN-sodium sulphate-metal complexes on device type A at pH 1-7. ....	55
<b>Figure 4.10</b> Effect of reaction time on the color response of Zn(II) and Cd(II) complexes on device type A.....	56
<b>Figure 4.11</b> The design components for simultaneous Cu(II), Co(II), Zn(II), Cd(II)/Pb(II) detection on device type B. ....	57
<b>Figure 4.12</b> The design components for simultaneous Cu(II), Co(II), Zn(II), Cd(II)/Pb(II) detection on device type C.....	57
<b>Figure 4.13</b> Type of complexing agents and masking agents on device type B and C for simultaneous Cu(II), Co(II), Zn(II), Cd(II) detection.....	58
<b>Figure 4.14</b> Color changes of metal complexes at pH 5 on device type B and C for simultaneous Cu(II), Co(II), Zn(II), Cd(II) detection.....	58
<b>Figure 4.15</b> Complexing agents and masking agents on device types B for simultaneous Cu(II), Co(II), Zn(II), Cd(II) detection.....	60
<b>Figure 4.16</b> Color changes of metal complexes at pH 5 on device type B for simultaneous Cu(II), Co(II), Zn(II), Cd(II) detection.....	60
<b>Figure 4.17</b> The design components for simultaneous Cu(II), Co(II), Zn(II), Cd(II)/Pb(II) detection on device type D.....	61
<b>Figure 4.18</b> Type of complexing agents and masking agents on device type D for simultaneous Cu(II), Co(II), Zn(II), Cd(II)/Pb(II) detection. ....	61
<b>Figure 4.19</b> Effect of acetate buffer concentrations (A) 1 M, (B) 2 M, (C) 3 M, (D) 5 M at pH 5 on color response of Cu(II), Co(II), Zn(II), Cd(II), and Pb(II) complexes on device type D.....	62

<b>Figure 4.20</b> Effect of DTZ solvent and concentration on the color responses of Cd(II) and Pb(II) complexes on device type D. ....	63
<b>Figure 4.21</b> Effect of NaOH concentration as DTZ solvent (A) 2.5 M, (B) 2 M, (C) 1 M, (D) 0.1 M on the color response of Cd(II) and Pb(II) complexes on the detection zone 4 for simultaneous Cu(II), Co(II), Zn(II), Cd(II)/Pb(II) detection on device type D. ....	64
<b>Figure 4.22</b> Color changes of metal complexes (24 types) for simultaneous Cu(II), Co(II), Zn(II), Cd(II)/Pb(II) detection on device type D. ....	67
<b>Figure 4.23</b> Color chart of metal complexes (24 types) for simultaneous Cu(II), Co(II), Zn(II), Cd(II)/Pb(II) detection on device type D. ....	68
<b>Figure 4.24</b> Pathway for simultaneous Cu(II), Co(II), Zn(II), Cd(II)/Pb(II) identification on device type D. ....	69
<b>Figure 4.25</b> The design components of device type E for simultaneous detection of eight metal ions. ....	73
<b>Figure 4.26</b> The design components of device type F for simultaneous detection of five metal ions. ....	74
<b>Figure 4.27</b> Color changes of metal-BC complexes on the device type E for Cu(II) detection. ....	75
<b>Figure 4.28</b> Cu-Bathocuproine reaction. ....	75
<b>Figure 4.29</b> Color changes of metal-DMG complexes on the device type E for Ni(II) detection. ....	76
<b>Figure 4.30</b> Ni-Dimethylglyoxime reaction. ....	76
<b>Figure 4.31</b> Color changes of metal-PAR complexes on the device type E for V(III) detection. ....	77
<b>Figure 4.32</b> Color changes of metal-PAR complexes on the device type E for Mn(II) detection. ....	77



<b>Figure 4.33</b> Color changes of metal-PAN complexes on the device type E for Mn(II) detection.....	78
<b>Figure 4.34</b> Mn-PAN reaction <sup>28</sup> .....	78
<b>Figure 4.35</b> Color changes of metal-DTZ complexes by using en as a making agent on the device type E for Hg(II) detection.....	79
<b>Figure 4.36</b> Color changes of metal-DTZ complexes by using DCTA, KCN, and en as making agents on the device type E for Hg(II) detection.....	80
<b>Figure 4.37</b> Hg-Dithizone reaction <sup>80</sup> .....	80
<b>Figure 4.38</b> Color changes of metal-DPC complexes on the device type E for Cr(VI) detection.....	81
<b>Figure 4.39</b> Color changes of metal-DPC complexes by using thiourea and NaF as masking agents on the device type E for Cr(VI) detection. ....	81
<b>Figure 4.40</b> Cr-DPC reaction <sup>91</sup> .....	82
<b>Figure 4.41</b> Color changes of metal-Bphen complexes on the device type E for Fe(III) detection.....	82
<b>Figure 4.42</b> Fe-Bphen reaction <sup>34</sup> .....	83
<b>Figure 4.43</b> Color changes of metal-PAR complexes on the device type E for Co(II) detection.....	84
<b>Figure 4.44</b> Co-4-(2-Pyridylazo) resorcinol reaction <sup>39</sup> .....	84
<b>Figure 4.45</b> Effect of metal ion volume (120.0-160.0 $\mu$ L) on the color response for Mn(II) detection on the device type E.....	85
<b>Figure 4.46</b> Pathway for simultaneous Cu(II), Co(II), Hg(II), Ni(II), Fe(III), Cr(VI), V(III), and Mn(II) identification on the device type E.....	89
<b>Figure 4.47</b> Color changes for limit of detection study of each metal ion detection on the device type E.....	90

<b>Figure 4.48</b> Color chart for simultaneous detection of eight metal ions on the device type E.....	91
<b>Figure 4.49</b> Color changes of metal complexes on the device type E from 46 unknown samples.....	92
<b>Figure 4.50</b> Color changes of metal-Bc complexes on the device type F for Cu(II) detection.....	93
<b>Figure 4.51</b> Color changes of metal-PAR complexes on the device type F for Co(II) detection.....	94
<b>Figure 4.52</b> Color changes of metal-DMG complexes on the device type F for Ni(II) detection.....	94
<b>Figure 4.53</b> Color changes of metal-DMG complexes by using hydroxylamine hydrochloride as a masking agent on the device type F for Ni(II) detection. ....	95
<b>Figure 4.54</b> Color changes of metal-DTZ complexes on the device type F for Hg(II) detection.....	96
<b>Figure 4.55</b> Color change of metal-PAR complexes on the device type F for Mn(II) detection.....	96
<b>Figure 4.56</b> The color intensity optimization for Cu(II) calibration on the device type F.....	97
<b>Figure 4.57</b> The color intensity optimization for Co(II) calibration on the device type F.....	97
<b>Figure 4.58</b> The color intensity optimization for Ni(II) calibration on the device type F. ....	98
<b>Figure 4.59</b> The color intensity optimization by for Hg(II) calibration on the device type F.....	98
<b>Figure 4.60</b> The color intensity optimization for Mn(II) calibration on the device type F.....	99

- Figure 4.61** Effect of reaction time on the color response for (A) Cu(II), (B) Co(II), (C) Ni(II), (D) Hg(II), (E) Mn(II) detections on the device type F. .... 100
- Figure 4.62** Effect of metal ion volume for (A) 200.0  $\mu\text{L}$ , (B) 250.0  $\mu\text{L}$ , (C) 300.0  $\mu\text{L}$  Mn(II) on the color response for Mn(II) detection on the device type F. 101
- Figure 4.63** Effect of complexing agent volume on the color response for (A) Cu(II), (B) Co(II), (C) Ni(II), (D) Hg(II), (E) Mn(II) detections on the device type F. . 102
- Figure 4.64** Visual calibration for semi-quantitative Cu(II) determination (top). Cu(II) Calibration curve (0.005-1.000 mM) by analyzing the gray intensity of the color response on the detection zone (bottom). .... 106
- Figure 4.65** Visual calibration for semi-quantitative Co(II) determination (top). Co(II) Calibration curve (0.010-0.080 mM) by analyzing the green intensity of the color response on the detection zone (bottom). .... 107
- Figure 4.66** Visual calibration for semi-quantitative Hg(II) determination (top). Hg(II) Calibration curve (0.001-0.060 mM) by analyzing the green intensity of the color response on the detection zone (bottom). .... 107
- Figure 4.67** Visual calibration for semi-quantitative Ni(II) determination (top). Ni(II) Calibration curve (0.100-6.000 mM) by analyzing the green intensity of the color response on the detection zone (bottom). .... 108
- Figure 4.68** Visual calibration for semi-quantitative Mn(II) determination (top). Mn(II) Calibration curve (0.0020-0.0100 mM) by analyzing the green intensity of the color response on the detection zone (bottom). .... 108
- Figure 4.69** The color intensities of 0.455 mM (A) Cu(II), (B) Co(II), (C) Ni(II), (D) Hg(II), (E) Mn(II) in the presence of 0.455 mM Cu(II), Co(II), Ni(II), Hg(II), Mn(II), and All-5 for Cu(II), Co(II), Ni(II), Hg(II), and Mn(II) detection, respectively. .... 110
- Figure 4.70** The color intensities of 0.455 mM (A) Cu(II), (B) Co(II), (C) Ni(II), (D) Hg(II), (E) Mn(II) in the presence of 0.455 mM Cd(II), Zn(II), Pb(II), Fe(II), Fe(III), Cr(VI), and V(III) for Cu(II), Co(II), Ni(II), Hg(II), and Mn(II) detection, respectively. 111

- Figure 4.71** The color intensities of 0.455 mM (A) Cu(II), (B) Co(II), (C) Ni(II), (D) Hg(II), (E) Mn(II) in the presence of 0.910 mM Cu(II), Co(II), Ni(II), Hg(II), Mn(II), and All-5 for Cu(II), Co(II), Ni(II), Hg(II), and Mn(II) detection, respectively. .... 112
- Figure 4.72** The color intensities of 0.455 mM (A) Cu(II), (B) Co(II), (C) Ni(II), (D) Hg(II), (E) Mn(II) in the presence of 0.910 mM Cd(II), Zn(II), Pb(II), Fe(II), Fe(III), Cr(VI), and V(III) for Cu(II), Co(II), Ni(II), Hg(II), and Mn(II) detection, respectively. 113
- Figure 4.73** The color intensities of 0.455 mM (A) Cu(II), (B) Co(II), (C) Ni(II), (D) Hg(II), (E) Mn(II) in the presence of 45.5 mM Na(I), K(I), Mg(II), Ca(II) for Co(II) detection..... 114
- Figure 4.74** The color intensities of 0.455 mM (A) Cu(II), (B) Co(II), (C) Ni(II), (D) Hg(II), (E) Mn(II) in the presence of 455 mM Na(I), K(I), Mg(II), Ca(II) for Co(II) detection..... 115
- Figure 4.75** Color changes of metal complexes (A) 1:1 ratio for All-5, (B) 1:2 for Cu(II):other metal ions, (C) 1:2 for Co(II):other metal ions, (D) 1:2 for Ni(II):other metal ions, (E) 1:2 for Hg(II):other metal ions, (F) 1:2 for Mn(II):other metal ions. .... 116
- Figure 4.76** Color changes of metal complexes using (A) 0.455 mM target metal ion (B) a mixture solution of five metal ions (mixing in the concentration ratio of 1:1) for each metal ion detection..... 117
- Figure 4.77** Color changes of metal complexes using (A) 0.455 mM target metal ion (B) a mixture solution of five metal ions (mixing in the concentration ratio of 1:2) for each metal ion detection..... 117

## CHAPTER I

### INTRODUCTION

There are many manufactories such as battery, electronics, and electroplating that have been continuously growth in developing countries. These manufactories are also releasing various toxic pollutants which impact on human health and environment processes. Heavy metals are a composition toxic pollutant which are released from many sources into environments. The contamination of heavy metals was found in water, soil, and air samples <sup>1, 2</sup>. In addition, these metals do not degrade which can be accumulated in various environmental samples. Heavy metals are toxic for human health and living organisms.

To evaluate water quality, there are many conventional methods for metal ions determination including atomic absorption spectrometry (AAS) <sup>3, 4</sup> fluorescent spectrometry <sup>5</sup>, inductively coupled plasma-optical emission spectrometry (ICP-OES) <sup>6</sup>, and electrochemical methods <sup>7-9</sup>. These techniques are very high selective and sensitive, low detection limit, applying for simultaneous determination. However, these methods are required an expensive instrumentation, sophisticated instruments, time consuming processes, and high skilled technicians. Therefore, the selective, sensitive, simple, and low-cost method has been concentrated to develop for toxic metal determination.

This work focused on the development of method on microfluidic paper-based analytical device ( $\mu$ PAD) as substrate materials to apply for toxic metal determination. The  $\mu$ PAD is low-cost materials, flexibility, high surface to volume ratio, light weight, disposability, miniaturization, and portability <sup>10-13</sup>. The  $\mu$ PAD fabrication methods have been reported including photolithography <sup>14</sup>, inkjet etching <sup>15</sup>, polymer screen printing <sup>16</sup>, wax printing <sup>17</sup>, and cutting <sup>18</sup>. However, these methods have some disadvantages. For example, photolithography includes an expensive instrumentation (e.g., spin coating and UV exposure system), complicated fabrication processes, and required solvent exposure to the hydrophilic, the device fabricated

with Inkjet etching is reduced channel reproducibility because it is difficult to align the paper for consecutive times, cutting is cost of the cutting machine and the inability to create small stable structures. Therefore, a polymer screen-printing method is attended to use in this work because the fabrication method has many advantages. For example, it can be performed by the deposition of polystyrene solution penetrated through screen patterns and paper in a single step, a hydrophobic barrier remains on paper after the evaporation of solvent, polystyrene is low-cost material and easy to obtain, the device is also flexible, bending, or folding after fabrication. In addition, wax printing is also applied to fabricate device in this work because it is widely used, simple, rapid and high-resolution fabrication method<sup>19</sup>.

The colorimetric method on  $\mu$ PAD was attracted to apply for simultaneous heavy metal ions detection in this work. There are various previous works which were developed  $\mu$ PADs for toxic metals detection such as development of a 3D origami paper-based analytical device combined with PVC membrane for heavy metals colorimetric detection and applied this method for Cu(II) determination<sup>20</sup>. A paper strip integrated with a smartphone for Zn(II), Cr(VI), Cu(II), Pb(II), and Mn(II) colorimetric detection in wastewater<sup>21</sup>. The colorimetric paper sensor based-on a cation-exchange (belt-like ZnSe nanoframes as colorimetric reagent) was applied for Ag(I), Cu(II), and Hg(II) visual determination<sup>22</sup>. The multilayer paper-based sensor was designed for Cd(II) and Pb(II) electrochemical detection and Fe(III), Ni(II), Cr(VI), and Cu(II) colorimetric detection<sup>23</sup>. A colorimetric paper-based device was used for semiquantitative Pb(II) detection with a smartphone<sup>24</sup>. Although these traditional colorimetric methods have been developed to detect toxic metals for on-site analysis by using a smartphone, they are limited metal ions detection, time consuming processes for reagent preparation or synthesis steps, complicated steps for some works, and narrow linearity.

To improve some limitation of previous works, this research focused on the development of tree types of paper-based sensor for simultaneous heavy metal ion detection including (1) Cu(II), Co(II), Zn(II), Cd(II)/Pb(II), (2) Cu(II), Co(II), Ni(II), Hg(II), Fe(III), Cr(VI), V(III), and Mn(II) in synthetic unknown water samples by naked-eye, and (3)

Cu(II), Co(II), Ni(II), Hg(II), and Mn(II) colorimetric determination couple with a scanner in real water samples. The colorimetric method was relied on using commercial complexing agents and masking agents that all reagents were applied on the device without complicated preparation and purification steps before use. The commercial complexing agents were applied to form color complex with target metal ion and the commercial masking agents were used to mask interfering ions to obtain the selectivity of target metal ion detection.

There are several complexing agents for colorimetric determination of heavy metals <sup>25-27</sup>. For example, 1-(2-pyridylazo)-2-naphthol (PAN) is a heterocyclic azo compound that is a possible complexing agent to detect heavy metal ions <sup>28</sup>. PAN forms various colored complexes with number of metal ions through the azo group and the nitrogen atom of pyridyl group <sup>28</sup>. Dithizone (DTZ) forms colored complexes with various metals through the azo group and the nitrogen atom of pyridyl group <sup>29</sup>. For example, Pb(II)-DTZ complexes was formed in an aqueous micellar medium which show high sensitivity and selectivity for Pb(II) determination <sup>30</sup>. Bathocuproine (Bc) is a sensitive and selective complexing agent for Cu(II) detection <sup>31</sup>. Cu(Bc)<sub>2</sub> complex is stable under a wide range of pHs <sup>31</sup>. Dimethylglyoxime (DMG) is an effectively complexing agent for Ni(II) detection <sup>32</sup>. 4-(2-Pyridylazo) resorcinol (PAR) is frequently applied as an analytical reagent for heavy metal ion analysis. PAR forms red complexes with numerous metal ions including Cu(II), Co(II), Ni(II), Hg(II), Zn(II), Mn(II), Cd(II), and Pb(II) <sup>33</sup>. PAR is highly selective and sensitive colorimetric reagent for Mn(II), Ni(II), Zn(II), and Pb(II) in strong basic condition <sup>33</sup>. Bathophenanthroline (Bphen) is sensitive, selective for Fe(II) detection, and Fe(II)-Bphen complex has low solubility in water <sup>34</sup>. 1, 5-Diphenylcarbazide (DPC) is a selective complexing agent for Cr(VI) detection <sup>35</sup>. However, these complexing agents are required the selectivity for target metal ion detection. Therefore, masking agents were applied to remove interfering ions. For example, thiourea was used as masking agent for Cu(II) <sup>36</sup>, *trans*-1,2-diaminocyclohexane-N,N,N',N'-tetraacetic acid (DCTA) was used mask Cu(II), Co(II), Ni(II), Cr(VI), Mn(II), Pb(II), and Zn(II) <sup>37</sup>, KCN was used for Cu(II), Zn(II), Cd(II), Ni(II), and Co(II) <sup>38</sup>, ethylenediaminetetraacetic acid (EDTA) was used to mask Mn(II), Ni(II), Zn(II), Cd(II), Pb(II), and Fe(III) <sup>39</sup>, and triethylenetetramine was used for Cu(II), Zn(II), Cd(II),

Pb(II)<sup>39</sup>. Therefore, these commercial complexing agents and masking agents were applied on the various types of devices for simultaneous colorimetric detection of Cu(II), Co(II), Zn(II), Cd(II), Pb(II), Ni(II), Hg(II), Fe(III), Cr(VI), V(III), and Mn(II).

For simultaneous Cu(II), Co(II), Zn(II), Cd(II)/Pb(II) detection in synthetic unknown water samples on device type D by naked-eye, the accuracy of proposed sensor was evaluated by a researcher and ten students. For simultaneous Cu(II), Co(II), Ni(II), Hg(II), Fe(III), Cr(VI), V(III), and Mn(II) detection in synthetic unknown water samples on device type E by naked-eye, the accuracy was studied by a researcher. The proposed method was successfully applied for simultaneous an anion (Cr(VI)) and seven cations (Cu(II), Co(II), Ni(II), Hg(II), Fe(III), V(III), and Mn(II)) detection. For simultaneous Cu(II), Co(II), Ni(II), Hg(II), and Mn(II) colorimetric determination on device type F couple with a scanner in real water samples, the selectivity of target ion complex was improved for simultaneous five metal ions determination by (1) device design with two pretreatment zones and (2) using various masking agents. The proposed method provided highly selective and efficient for simultaneous Cu(II), Co(II), Ni(II), Hg(II), and Mn(II) determination in drinking, tap, and pond-CU water samples.

#### **Objectives of this research**

1. Fabricate paper-based analytical devices by using polymer screen printing and wax printing methods.
2. Apply the various types of device for simultaneous heavy metal ions naked-eye detection in real water samples.

#### **Scope of this research**

The proposed methods were relied on colorimetric detection on microfluidic paper-based analytical device. A polymer screen-printing method was used to fabricate device types A, B, C, and D. The preliminary study of each heavy metal ion detection was studied on device type A. Device types B, C, and D were developed for simultaneous Cu(II), Co(II), Zn(II), Cd(II)/Pb(II) detection in synthetic unknown water samples by naked-eye. A wax printing method was also used to fabricate device



types E and F. Device type E was applied for Cu(II), Co(II), Ni(II), Hg(II), Fe(III), Cr(VI), V(III), and Mn(II) detection in synthetic unknown water samples by naked-eye. Device type F was used for simultaneous Cu(II), Co(II), Ni(II), Hg(II), and Mn(II) determination couple with a scanner in real water samples.

#### **Expected beneficial outcomes**

The various types of device were successfully fabricated and applied for simultaneous heavy metal ions detection in real water samples.



## CHAPTER II

### THEORY AND LITERATURE REVIEW

#### 2.1 Heavy metals in environment

Heavy metals are important for many industrial factories which release these metals into environment. Heavy metals can be contaminated in water samples. These heavy metals are toxic on human health and also impact on environment processes. Toxicity of some heavy metal ions on human health are shown in **Table 2.1**.

**Table 2.1** Table Heavy metal ions toxicity.

Metal ions	Toxicity	Ref.
Cu(II)	Low blood pressure, cancer, neurological disorder, and cardiovascular disease	40
Co(II)	Asthma	41
Ni(II)	Lung fibrosis, cardiovascular diseases, lung cancer, and nasal cancer	42
Zn(II)	Alzheimer, diabetes, and epilepsy diseases	
Pb(II)	High blood pressure, headache, mood disorders	
Cd(II)	Hypertension, kidney damage, bronchitis, and the risk of prostatic cancer	43
Hg(II)	Neurological disorder, and kidney failure	
Fe(III)	Toxic on gastrointestinal mucosa, resulting in nausea, vomiting, and diarrhea	
Cr(VI)	Lung cancer by inhalation, toxic on nephritis, renal failure, and liver damage	
Mn(II)	Permanent neurological disorder	44
V(III)	Toxic on lungs	

The maximum permissible level of heavy metals has been set to control water quality. The World Health Organization (WHO, 2017) has set the maximum concentrations for heavy metal ions in drinking water as illustrated in **Table 2.2**.

**Table 2.2** The maximum permissible level of heavy metal ions in drinking water.

Metal ions	Maximum permissible level (mg/L)
Cu(II)	2.00
Co(II)	0.05 <sup>1</sup>
Zn(II)	5.0 <sup>2</sup>
Ni(II)	0.07
Cd(II)	0.003
Pb(II)	0.01
Hg(II)	0.006
Fe(II)	0.03
Mn(II)	0.10
Cr(VI)	0.05
Total V	0.05 <sup>3</sup>

<sup>1</sup>Co(II) in effluent discharge by Environment Protection Regulations (2003).

<sup>2</sup>Zn(II) in industrial effluent by Ministry of Natural Resources and Environment in Thailand (MNRE, 2016).

<sup>3</sup>Total V in groundwater by the U.S. Environmental Protection Agency's (U.S. EPA).

## 2.2 Heavy metal determination methods

To assess water quality, conventional methods such as graphite furnace atomic absorption spectrometry (GFAAS), inductively coupled plasma-optical emission spectrometer (ICP-OES), inductively coupled plasma-mass spectrometry (ICP-MS), electrochemical, and laser-induced breakdown spectroscopy (LIBS) were applied for heavy metals determination. For example, Liu *et al.*<sup>45</sup> prepared L-cysteine functionalized magnetic mesoporous nanosorbent (Cys-Si-MNPs) for the sensitive quantification of Pb(II), Cd(II), Cu(II), Cr(III), and V(V) in food by graphite

furnace atomic absorption spectrometry (GFAAS), Rodrigues *et al.*<sup>46</sup> reported inductively coupled plasma optical emission spectrometer (ICP-OES) coupled with linear discriminant analysis, principal component analysis, and logistic regression to analyze Al, B, Ba, Ca, Cu, Fe, K, Li, Mg, Mn, Na, and Sr from 111 sparkling wine samples, Dalkiran<sup>47</sup> developed horseradish peroxidase (HRP) enzyme inhibition biosensor based on indium tin oxide (ITO) nanoparticles, hexaammineruthenium (III) chloride (RUT), and chitosan (CH) modified glassy carbon electrode (GCE) for amperometric determination of Pb(II), Ni(II), and Cd(II), and Liu *et al.*<sup>48</sup> evaluated ultrasound-assisted extraction sample pretreatment method (UAE) for laser-induced breakdown spectroscopy to detect Pb(II) and Cd(II) in low-quality cosmetics. These techniques show high sensitivity, good precision, and low detection limit. However, they are still required an expensive instrument and complicated step analysis.

### 2.3 Microfluidic paper-based analytical device

Microfluidic paper-based analytical device ( $\mu$ PAD) was applied for heavy metals determination. Filter papers and chromatography papers are widely used as substrates for  $\mu$ PAD. These papers are various properties which satisfy as the substrate for  $\mu$ PAD as illustrated in **Table 2.3**. The  $\mu$ PAD fabrication methods were reported as shown in **Table 2.4**.

**Table 2.3** Properties of paper as substrates of  $\mu$ PAD.

Properties	Impacts	Ref.
Low cost	Satisfy for the countries with low purchasing power	12
Lightweight	Suitable for on-site applications and portability	
Disposability	Reduce cost for post-treatment	
High surface area	Enhance loading amounts of reagents and sample on the surface substrates	10
Capillary force	Flow liquid without the requirement of pumps	13

**Table 2.4** The fabrication methods for  $\mu$ PAD.

Methods	Advantages	Disadvantages	Ref.
Polymer screen printing	A single step preparation, flexible for bending, or folding	Toxic of organic solvent (toluene)	16
Wax printing	Simple operation, cheap, no required mask	Requires special wax printer	19
Photolithography	High resolution	Inflexible for bending and folding, high cost for a cleanroom and chemicals	49
Plasma treatment	Retains the flexible of paper, components (switches and filters) can be built directly	Requires a mask, a heating step	11
Laser cutting	Simple operation, none chemical contamination	Requires expensive laser cutter, low resolution	18
Contact stamping	Fast, cheap, reproducible	Requires special inks, low resolution	50
Lamination	Low-cost, simple operation	Requires a digital crafter cutter and a roll laminator	51
Wax dipping	Low-cost, simple operation	Requires a mask, a heating step	52
Drawing	Low-cost	Low resolution	53

The  $\mu$ PAD was applied for heavy metals determination. For example, Sánchez-Calvo *et al.* <sup>54</sup> presented paper-based electrochemical modified with hybrids of carbon nanofibers (CNFs) and gold nanoparticles (AuNPs) to improve the selectivity and sensitivity for Hg(II) determination in river water samples. It was found that the CNFs/AuNPs modified paper-based electrode showed highly sensitive with the detection limit of 30 nM. Chaiyo *et al.* <sup>55</sup> reported a new microfluidic paper-

based analytical device coupled with dual electrochemical and colorimetric detection for the simultaneous determination of Pb(II), Cd(II), and Cu(II). It was found that the detection limit was 0.1 ng/mL for Cd(II) and Pb(II) and 5.0 ng/mL for Cu(II). However, these methods are still required external instruments for electrode fabrication and determination process.

## 2.4 Colorimetric methods for heavy metal determination

The colorimetric method is attracted to apply for heavy metal determination because the output of colorimetric detection is evaluated by naked-eye, software, and instruments. For example, Li *et al.*<sup>56</sup> developed the feasibility, specificity, and reliability based on periodic-table-style paper sensor for monitoring Cu(II), Ni(II), and Cr(VI) in water, Guo *et al.*<sup>57</sup> evaluated colorimetric probes based on gold nanoparticles (GNPs) with the combination of enzymatic inhibition for Cu(II) ions determination, and Wang *et al.*<sup>24</sup> reported a simple, instrument-free, paper-based sensor with dual-emission carbon dots for the semiquantitative, visual, and sensitive speciation analysis of Pb(II) in a real sample.

The colorimetric method was applied on  $\mu$ PAD using complexing agents to form colored complexes with heavy metals. Some previous colorimetric methods on  $\mu$ PAD for heavy metals analysis are listed below.

Wu *et al.*<sup>58</sup> reported that a solid phase extraction (SPE) column was filled with home-made sulfonated polystyrene-divinylbenzene (PS-DVB) microspheres for clean-up and preconcentration for Cu(II) colorimetric determination. 1-(2-Pyridylazo)-2-naphthol as colorimetric reagent was immobilized on paper-based microfluidic analytical device and combined with home-made SPE column. This method showed good selectivity and sensitivity for Cu(II) colorimetric determination with the limit of detection of 0.340  $\mu$ M.

Meredith *et al.*<sup>39</sup> evaluated a simple eight-armed microfluidic paper-based analytical device coupled with the non-specific colorimetric reagent 4-(2-pyridylazo)resorcinol for screening masking agents for simultaneous Mn(II) and Co(II) determination. It was found that dimercaptosuccinic acid and triethylenetetramine in pH 10 borate buffer was successfully used as masking agents for selective

determination of Mn(II) and the combination of ethylenediaminetetracetic acid and triethylenetetramine in pH 10 phosphate buffer was efficiently used as masking agents for selective determination of Co(II).

Pratiwi *et al.*<sup>59</sup> synthesized meso-tetrakis(1,2-dimethylpyrazolium-4-yl)porphyrin sulfonate (TDMPzP) as a colorimetric reagent for Cu(II) detection on distance-based paper analytical device. The results indicated that the lowest detectable concentration of Cu(II) was 1 mg/L and Al(III), Fe(III), Mg(II), Co(II), Mn(II), Zn(II), Pb(II), Cd(II), Sn(II), and Ni(II) showed no interferences with Cu(II) detection within reasonable tolerance ratios.

Huang *et al.*<sup>60</sup> presented the ion imprinted polymers (IIPs) using Cd(II) as the template grafted on the paper surface for selective and sensitive detection of Cd(II) ions. Dithizone solution (0.4 mM, pH 13) was added on the IIPs paper platform because it could form a colored complex with metal ions in a strong alkaline solution. IIPs-paper platform was effectively applied for highly selective and sensitive detection of Cd(II) without complex sample pretreatment and expensive instrument.

Cai *et al.*<sup>61</sup> studied a microfluidic paper-based analytical device based on distance-based detection for visual quantification of Hg. Dithizone in NaOH solution was used as a complexing agent onto paper channel. The distance of colored complex was measured using the printed ruler along each device. The effect of interfering ions (Na(I), K(I), Mg(II), Ca(II), Al(II), Fe(III), Ba(II), Pb(II), Cr(VI), Cd(II), Cr(III), Mn(II), Co(II), Zn(II), Ni(II), Cu(II), and Ag(I)) was studied for 5 µg/mL Hg determination. NaF and 1,10-phenanthroline were used as masking agents. The results showed that the tolerance concentrations are 100 µg/mL for Mg(II), Ca(II) and Ni(II), 20 µg/mL for Zn(II), and 10 µg/mL for Cu(II) and Ag(I). This method was free any electronic instruments which was very attractive for on-site and real time analysis.

Mentele *et al.*<sup>62</sup> reported a microfluidic paper-based analytical device for colorimetric detection of particulate metals. The colorimetric detection was relied on 1,10-phenanthroline, bathocuproine, and dimethylglyoxime as complexing agents for Fe(III), Cu(II), and Ni(II) detection, respectively. For Fe(III) detection, hydroxylamine was added onto the device to (1) reduce Fe(III) to Fe(II), and (2) mask possibly interfering ions of Zn(II), Cd(II), and Co(II). For Ni(II) detection, sodium fluoride was used to mask

Co(II) and Fe(III). The limit of detection was found in the range of 1.0-1.5  $\mu\text{g}$  for each metal ion.

Cate *et al.*<sup>34</sup> demonstrated the microfluidic paper-based analytical devices based on distance-based detection of Ni, Cu, and Fe in air borne particulate matter. To evaluate colorimetric measurements, dimethylglyoxime, dithiooxamide, and 4,7-diphenyl-1,10-phenanthroline (bathophenanthroline) were used as complexing agents for Ni, Cu, and Fe detection, respectively. It was found that the detection limits were 0.1  $\mu\text{g}$  (Ni), 0.1  $\mu\text{g}$  (Cu), and 0.05  $\mu\text{g}$  (Fe) in single channel device and the detection limits were 1  $\mu\text{g}$  (Ni), 5  $\mu\text{g}$  (Cu), and 1  $\mu\text{g}$  (Fe) in multi-channel device of all three metal ions.

Quinn *et al.*<sup>63</sup> presented the preconcentration with solid-phase extraction coupled with a microfluidic paper-based analytical device to quantify trace Cu(II) in drinking water by naked-eye based on color distance. Dithiooxamide was printed on the detection zone to form colored complex with Cu(II) and hydroxylamine as a reducing agent was applied onto the pretreatment zone. This method was rapid screening and low-cost technique for Cu(II) detection in water systems.

Hofstetter *et al.*<sup>64</sup> used a new paper analytical devices based on the radial distance measurements which was applied for quantifying copper, total iron, and zinc using zincon, bathophenanthroline, and dithizone as complexing agents, respectively. Sample solution rapidly flowed to outwards and reacted with colorimetric complexing agents. This design evaluated the detection limits as low as 0.1 mg/L within 3 minutes.

Cate *et al.*<sup>65</sup> applied the paper-based analytical devices for Fe(III), Cu(II), Ni(II), and Cr(VI) colorimetric detection in welding fumes. 1,10-Phenanthroline, bathocuproine, dimethylglyoxime, and 1,5-diphenylcarbazide were used to react with Fe(III), Cu(II), Ni(II), and Cr(VI), respectively. The results from the  $\mu\text{PAD}$  showed good agreement with ICP-OES analysis.

These previous works on various types of microfluidic paper-based analytical device integrated with complexing agents and masking agents were applied to mask interfering ions for heavy metal detection.



## 2.5 Complexing agents

Complexing agents used in this research are listed below.

- 1-(2-Pyridylazo)-2-naphthol (PAN)

1-(2-Pyridylazo)-2-naphthol can be dissolved in various organic solvents including methanol, ethanol, and carbon tetrachloride which given a yellow color <sup>56</sup>. PAN forms colored complex with Cu(II), Co(II), Zn(II), Cd(II), Pb(II), Ni(II), Hg(II), Fe(III), Fe(II), and Mn(II) <sup>56</sup>. The alkali and alkaline earth metals do not form colored complex with PAN <sup>56</sup>.

- Dithizone (DTZ)

Dithizone is soluble in ketone, alcohol, hydrocarbon, and chlorinated hydrocarbon such as chloroform and carbon tetrachloride <sup>66</sup>. It also dissolves in alkaline aqueous media (>20 g/L) but it is insoluble in water at pH less than 7 <sup>67</sup>. Metal-dithizone forms different colored complexes and insoluble in water <sup>68</sup>. The sulfur, and nitrogen chelating groups of the dithizone bind tightly to metal ions in configurations which are square planar for [Cd(DTZ)<sub>2</sub>], tetrahedral for [Pb(DTZ)<sub>2</sub>] and [Hg(DTZ)<sub>2</sub>] <sup>68</sup>.

- Bathocuproine (Bc)

Bathocuproine is a complexing agent for copper by forming an orange colored 2:1 complex which is selective with Cu(I) <sup>69</sup>. Bc is typically used for spectrophotometric determination of Cu(I), or Cu(I)+Cu(II) in the presence of suitable reducing agent <sup>31</sup>. Ascorbic acid is an example of a reducing agent used to reduce Cu(II) to Cu(I) <sup>31</sup>.

- Dimethylglyoxime (DMG)

Dimethylglyoxime is considered as a specific complexing agent for Ni(II) detection because DMG provided specific, sensitive and not affected by moderate amounts of interfering ions <sup>70</sup>. DMG reacts with Ni(II) to produce bright pink water insoluble products <sup>71</sup>.

- 4-(2-Pyridylazo) resorcinol (PAR)

4-(2-Pyridylazo) resorcinol forms water soluble stable complexes with various metals. Metal ions react with PAR in wide pH values <sup>72</sup>. PAR has the reactive groups with a heterocyclic nitrogen group, azo group, and hydroxyl group available for

coordination with metal ions <sup>73</sup>. Molar absorption coefficients of PAR–metal ion complexes reported of 78,000 and 58,600 L mol<sup>-1</sup> cm<sup>-1</sup> for PAR–Mn(II) and PAR–Co(II), respectively <sup>74</sup>.

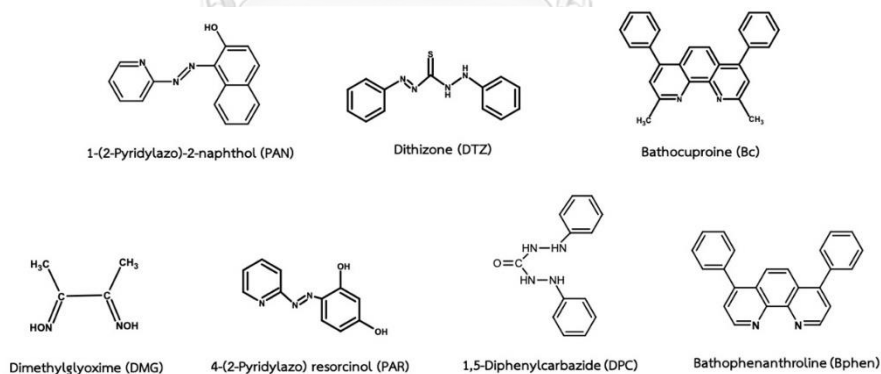
- Bathophenanthroline (Bphen)

Bathophenanthroline is selected to use as a complexing agent for iron over other 1,10-phenanthroline derivatives because Bphen showed highly sensitive to Fe more than 1,10-phenanthroline, the ferrous-Bphen complex is low water soluble, and Bphen showed highly selective with iron more than 1,10-phenanthroline <sup>34</sup>.

- 1, 5-Diphenylcarbazide (DPC)

1, 5-Diphenylcarbazide is considered to use for spectrophotometric determination of hexavalent chromium in the standard method <sup>35</sup>. DPC reacts with Cr(VI) in acidic conditions by forming violet red complex <sup>35</sup>. The formation of DPC–Cr complex is more complete under acidic condition with nitric acid <sup>35</sup>.

The structures of these complexing agents are shown in **Figure 2.1**.



**Figure 2.1** Complexing agent structures in this research.

The optimal pH of complexing agents is widely range for metal complex formation as summarized in **Table 2.5**.

**Table 2.5** The optimal pH of various complexing agent for heavy metals detection.

Complexing agent	Metal ion detection	Optimal pH	Ref.
PAN	Cu(II)	5.0	58
	Co(II)	3.5-5.0	28
	Zn(II)	3.5-5.0	
	Mn(II)	9.5	75
PAR	Co(II)	10.0	39
	Mn(II)	10.0	
DTZ	Cd(II)	11.0-12.0	29
	Pb(II)	7.5-8.5	
	Hg(II)	9.0-10.0	
DMG	Ni(II)	9.5	62
BC	Cu(II)	3.2-8.0	31
Bphen	Fe(II)	4.5	34
DPC	Cr(VI)	2.2	35

The formation constant ( $K_f$ ) is used to consider the stability of each metal complex. The Cumulative formation constants ( $\log K_f$ ) for some metal complexing agent are shown in **Table 2.6**.

**Table 2.6** Cumulative formation constants for some metal complexing agent.

Complexing agent	log K	Metal ion								Ref.
		Cu(II)	Co(II)	Ni(II)	Hg(II)	Mn(II)	Zn(II)	Cd(II)	Pb(II)	
PAN	log K <sub>1</sub>	16	>12	12.7	-	8.5	11.2	-	-	76
	log K <sub>2</sub>	-	-	25.3	-	16.4	21.7	-	-	
PAR	log K <sub>1</sub>	-	>12	13.2	-	9.7	12.4	-	-	
	log K <sub>2</sub>	-	-	26.0	-	18.9	23.5	-	-	
DTZ	log K <sub>1</sub>	9.35	7.52	7.42	20.64	4.94	6.93	7.52	7.31	
	log K <sub>2</sub>	19.18	13.97	14.17	40.3	9.55	13.96	15.10	14.16	
DMG	log K <sub>1</sub>	12	9.8	9.0 <sup>77</sup>	-	-	7.7	5.7	7.3	
	log K <sub>2</sub>	33.44	18.94	17.62 <sup>77</sup>	-	-	13.9	10.7	-	

### 2.6 Masking agents

Many previous works applied masking agents to eliminate interfering ions for metals determination as listed below.

Raoot *et al.*<sup>36</sup> evaluated a selective complexometric determination of palladium using thiourea as a masking agent for copper. It was found that thiourea showed effectively to mask copper in the pH range of 5-5.5.

Wuilloud *et al.*<sup>78</sup> reported the speciation and preconcentration of vanadium(V) and vanadium(IV) in water samples using flow injection-inductively coupled plasma optical emission spectrometry. The vanadium complexes of vanadium-2-(5-bromo-2-pyridylazo)-5-diethylaminophenol (V-5-Br-PADAP) were studied on an Amberlite XAD-7 resin. *trans*-1,2-Diaminocyclohexane-N,N',N'-tetraacetic acid (DCTA) was applied as a masking agent. It was found that the detection limit was 19 ng/L for the preconcentration of 10 mL of aqueous solution. Interference species of Cu(II), Zn(II), Cd(II), Ni(II), Co(II), Mn(II), and Fe(II) could be tolerated up to at least 2,500 µg/L.

Wilkins *et al.*<sup>79</sup> evaluated 2,6-bis-(z-pyridyl)-pyridine for the spectrophotometric determination of Fe(II). The interference of cobalt was eliminated by adding ethylene diamine (en) as a masking agent. The determination of iron in the

presence of cobalt, the use of ethylenediamine in the detection system was possible mask cobalt to detect iron.

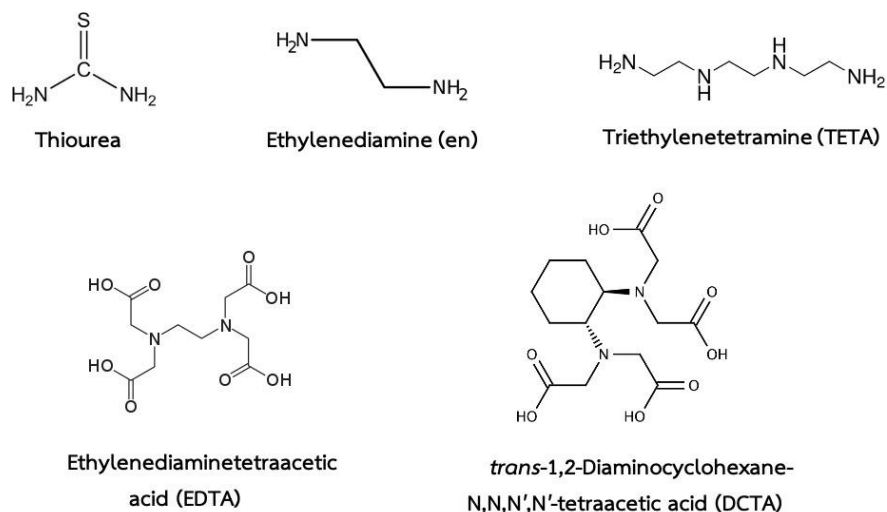
Takahashi *et al.*<sup>66</sup> presented the dithizone nanofiber-coated membranes for filtration-enrichment and colorimetric detection of trace Hg(II). Ethylenediamine tetraacetic acid (EDTA) was used as a masking agent to mask interferences. The presence of Na(I) (10,000 mg/L), K(I) (5,000 mg/L), Ca(II) (5,000 mg/L), Cu(II) (6.4 mg/L), Fe(II) (100 mg/L), Zn(II) (100 mg/L), Pb(II) (100 mg/L) and Cd(II) (10 mg/L) did not interfere for 10 µg/mL Hg(II) detection by using  $2.5 \times 10^{-4}$  M EDTA.

Shahat *et al.*<sup>29</sup> reported the Zr-based metal-organic frameworks (UiO-66) sensor for the visual detection and removal of ultra-traces of Bi(III), Zn(II), Pb(II), Hg(II) and Cd(II) in water. The addition of 0.15 M citrate, cyanide, thiosulphate, EDTA, or tartrate as masking agents to mask Cu(II), Ni(II), Co(II), Fe(III), and Pd(II) indicated that the tolerable concentration of each target ion detection increased. This sensor showed highly sensitivity and selectivity for metal detection up to  $10^{-10}$  M in solution.

Zargoosh and Babadi<sup>80</sup> evaluated a highly sensitive and selective optical membrane for Pb(II) and Hg(II) determination based on immobilization of dithizone on agarose membrane. Interfering ions as K(I), Li(I), Ag(I), Tl(I), Mg(II), Ca(II), Mn(II), and Cu(II) were investigated the selectivity of the proposed method for determination of Pb(II) and Hg(II). The addition of  $\text{CN}^-$  and  $\text{I}^-$  was used as masking agents. The results indicated that the proposed optical sensor can be applied for traces Hg(II) and Pb(II) determination in the presence of excess of several interfering ions.

Wang and Cheng<sup>81</sup> presented the spectrophotometric determination of iron in the presence of copper using 1,10-phenanthroline as a complexing agent. 1,10-Phenanthroline is commonly used for trace iron detection but it can tolerate with small amount of copper. Triethylenetetramine (TETA) was applied as a masking agent for copper. Maximum tolerance molar ratio (cupric ion to ferrous ion) was 25 for the determination 54.6 ng iron.

The structures of these masking agents are shown in **Figure 2.2**.



**Figure 2.2** Masking agent structures in this research.

The cumulative formation constants for some metal masking agent are shown in **Table 2.7**.

**Table 2.7** Cumulative formation constants for some metal masking agent.

Masking agent	log K	Metal ion										Ref.
		Cu(II)	Co(II)	Ni(II)	Hg(II)	Mn(II)	Zn(II)	Cd(II)	Pb(II)	Fe(II)	Fe(III)	
Thiourea*	log K <sub>1</sub>	-	-	-	-	-	-	0.6	1.4	-	-	76
	log K <sub>2</sub>	-	-	-	22.1	-	-	1.6	3.1	-	-	
	log K <sub>3</sub>	13	-	-	24.7	-	-	2.6	4.7	-	-	
	log K <sub>4</sub>	15.4	-	-	26.8	-	-	4.6	8.3	-	-	
en	log K <sub>1</sub>	10.67	5.91	7.52	14.3	2.73	5.77	5.47	-	4.34	-	
	log K <sub>2</sub>	20.00	10.64	13.84	23.3	4.79	10.83	10.09	8.66	7.65	-	
	log K <sub>3</sub>	21.00	13.94	18.33	-	5.67	14.11	12.09	-	9.70	-	
EDTA	log K <sub>1</sub>	18.7	16.31	18.56	21.80	13.8	16.4	16.4	18.3	14.33	24.23	
TETA	log K <sub>1</sub>	20.4	11.0	14.0	25.26	4.9	11.9	10.75	10.4	7.8	21.9	
	log K <sub>2</sub>	-	-	-	-	-	-	13.9	-	-	-	
DCTA	log K <sub>1</sub>	21.95	19.57	19.4	24.4	17.43	18.6	19.88	20.33	-	22.91	
Cyanide	log K <sub>1</sub>	-	-	-	-	-	-	5.48	20.33	-	-	
	log K <sub>2</sub>	24.0	-	-	-	-	-	10.60	-	-	-	
	log K <sub>3</sub>	28.59	-	-	-	-	-	15.23	-	-	-	
	log K <sub>4</sub>	30.30	-	31.3	41.1	-	16.7	18.78	-	-	-	
Fluoride	log K <sub>1</sub>	-	-	-	-	5.48	-	-	-	-	5.2	
	log K <sub>2</sub>	-	-	-	-	-	-	-	-	-	9.3	
Chloride	log K <sub>1</sub>	0.1	-	-	6.74	0.96	-	1.95	1.62	0.36	1.48	
	log K <sub>2</sub>	-	-	-	13.22	-	-	2.5	2.44	-	2.13	

\*Cumulative formation constants for thiourea-Cu(I)

## CHAPTER III

## EXPERIMENTAL SECTION

## 3.1 Chemicals and instruments

All chemicals used in this research are illustrated in **Table 3.1**.

**Table 3.1** Chemicals and suppliers.

Chemicals	Supplier
<b>1. Complexing agents</b>	
1-(2-Pyridylazo)-2-naphthol (PAN)	Sigma-Aldrich
4-(2-Pyridylazo) resorcinol (PAR)	Sigma-Aldrich
1, 5-Diphenylcarbazine (DPC)	Fluka
Dimethylglyoxime (DMG)	Merck
Dithizone (DTZ)	Fluka
Bathocuproine (Bc)	Aldrich
Bathophenanthroline (Bphen)	Aldrich
<b>2. Masking agents</b>	
2, 2'-Bipyridine	Sigma-Aldrich
<i>trans</i> -1,2-Diaminocyclohexane-N,N,N',N'-tetraacetic acid (DCTA)	Sigma-Aldrich
Thiourea	Sigma-Aldrich
Ethylenediamine (en)	Fluka
Tartaric acid	Merck
Sodium citrate	Merck
Sodium sulphate	Sigma-Aldrich
Citric acid	Merck



**Table 3.1** Chemicals and suppliers (cont.).

Chemicals	Supplier
Dimercaptosuccinic acid (DMSA)	Sigma-Aldrich
Hydroxylamine hydrochloride	Merck
Sodium fluoride	Merck
Potassium cyanide	Merck
Ethylenediaminetetraacetic acid (EDTA)	Sigma-Aldrich
Triethylenetetramine (TETA)	Aldrich
<b>3. Metal ions</b>	
Copper(II) nitrate monohydrate ( $\text{Cu}(\text{NO}_3)_2 \cdot \text{H}_2\text{O}$ )	Sigma-Aldrich
Cobalt(II) nitrate hexahydrate ( $\text{Co}(\text{NO}_3)_2 \cdot 6\text{H}_2\text{O}$ )	Sigma-Aldrich
Zinc(II) nitrate hexahydrate ( $\text{Zn}(\text{NO}_3)_2 \cdot 6\text{H}_2\text{O}$ )	Sigma-Aldrich
Nickel(II) nitrate hexahydrate ( $\text{Ni}(\text{NO}_3)_2 \cdot 6\text{H}_2\text{O}$ )	Sigma-Aldrich
Cadmium(II) nitrate tetrahydrate ( $\text{Cd}(\text{NO}_3)_2 \cdot 4\text{H}_2\text{O}$ )	Sigma-Aldrich
Lead(II) nitrate ( $\text{Pb}(\text{NO}_3)_2$ )	Sigma-Aldrich
Mercury(II) chloride ( $\text{HgCl}_2$ )	Sigma-Aldrich
Manganese(II) chloride hexahydrate ( $\text{MnCl}_2 \cdot 6\text{H}_2\text{O}$ )	Chem-Impex International Inc
Nickel(II) sulfate hexahydrate ( $\text{Ni}(\text{SO}_4) \cdot 6\text{H}_2\text{O}$ )	Alfa Aesar
Iron(III) chloride hexahydrate ( $\text{FeCl}_3 \cdot 6\text{H}_2\text{O}$ )	Sigma-Aldrich
Iron(II) sulfate heptahydrate ( $\text{Fe}(\text{SO}_4) \cdot 7\text{H}_2\text{O}$ )	Sigma-Aldrich
Potassium dichromate ( $\text{K}_2\text{Cr}_2\text{O}_7$ )	Alfa Aesar
Vanadium(III) chloride ( $\text{VCl}_3$ )	Sigma-Aldrich
Barium chloride dihydrate ( $\text{BaCl}_2 \cdot 2\text{H}_2\text{O}$ )	Sigma-Aldrich
Potassium nitrate ( $\text{KNO}_3$ )	Sigma-Aldrich
Sodium nitrate ( $\text{NaNO}_3$ )	Aldrich
Magnesium chloride hexahydrate ( $\text{MgCl}_2 \cdot 6\text{H}_2\text{O}$ )	Alfa Aesar
Calcium nitrate tetrahydrate ( $\text{Ca}(\text{NO}_3)_2 \cdot 4\text{H}_2\text{O}$ )	Alfa Aesar

**Table 3.1** Chemicals and suppliers (cont.).

Chemicals	Supplier
Dimercaptosuccinic acid (DMSA)	Sigma-Aldrich
Chromium(III) standard solution (1,000 mg/L)	Merck
Arsenic(III) standard solution (1,000 mg/L)	Merck
<b>4. Others</b>	
Sodium acetate anhydrous	Merck
Potassium chloride	Merck
Sodium chloride	Sigma-Aldrich
L-ascorbic acid	Ajax Finechem
Sodium tetraborate decahydrate	Sigma-Aldrich
Potassium phosphate monobasic	Merck
Potassium phosphate dibasic	Merck
Sodium hydroxide	Merck
Ammonium hydroxide	Sigma-Aldrich
Hydrochloric acid (37 %)	Merck
Nitric acid (65 %)	Merck
Acetic acid	Merck
Toluene	Merck
Ethanol	Merck
Methanol	Merck
Isopropanol	Merck
Acetone	Merck
Chloroform	RCI Labscan Limited
Polyethylene glycol (PEG 400)	Sigma-Aldrich
Poly (diallyldimethylammonium chloride) (PDDA)	Sigma-Aldrich
Polystyrene (average molecular weight of ~280,000 by GPC)	Aldrich

Instruments and software used in this research are shown in **Table 3.2**.

**Table 3.2** Instruments and software.

Instruments and software	Model	Mission
Analytical balance	Mettler Toledo and DENVER SI-234	Weight measurement
A benchtop pH meter with glass electrode	Mettler Toledo FE20 FiveEasy™ Plus, Switzerland	pH measurement
Spectrophotometer color i5	Color i5 Benchtop Spectrophotometer	L*, a*, b* values measurement
Inductively coupled plasma optical emission spectrometry (ICP-OES)	Thermo Scientific, model iCAP 6500 series ICP-OES Spectrometer	Cu(II), Co(II), Ni(II), Hg(II), and Mn(II) analysis
Scanner (metal ion group 2)	Xerox® DocuMate® 3320	Color response record
Scanner (metal ion group 3)	Brother MFC-8370DN	Color response record
Wax printer	Xerox Phaser 8860	Device fabrication
ImageJ-NIH software	-	Color intensity measurement
Microsoft PowerPoint	-	Device design
CorelDRAW software	-	Device design

### 3.2 Metal complex study in solution phase

#### 3.2.1 PAN-metal complexes at pH 1-7

1-(2-Pyridylazo)-2-naphthol (PAN) was selected as a complexing agent for preliminary study of metal complexes in solution phase. 2 mM PAN solution was prepared in ethanol. The buffer solution was used to prepare metal ion solutions which consisted of KCl-HCl buffer (pH 1-2), acetate buffer (pH 3-6), and phosphate buffer (pH 7). 200.0  $\mu\text{L}$  of PAN were added into a vial, followed by 200.0  $\mu\text{L}$  of 100 mg/L Cu(II), Ni(II), Co(II), Cd(II), Zn(II), Pb(II), Mg(II), Ba(II), Cr(III), and As(III) at pH 1-7. The color response of metal complexes in solution phase was recorded using digital camera (Nikon Coolpix P510).

#### 3.2.2 PAN-metal complexes at pH 5

For metal-PAN complexes study in solution phase at pH 5, 2 mM PAN solution was prepared in ethanol. 200.0  $\mu\text{L}$  of PAN were added into a vial, followed by 200.0  $\mu\text{L}$  of 100 mg/L Cu(II), Ni(II), Co(II), Cd(II), Zn(II), and a mixture solution of two metal ions (Cu(II)+Zn(II), Cu(II)+Co(II), Zn(II)+Cd(II)). Thiourea (1 M) and KCl (1 M) solutions were prepared in Milli-Q water and both reagents were used as masking agents. Thiourea (200.0  $\mu\text{L}$ ) or KCl (200.0  $\mu\text{L}$ ) solution was mixed into a vial. The color response of metal complexes in solution phase was recorded using digital camera.

### 3.3 Metal complex study on paper-based analytical device: polymer screen printing method

#### 3.3.1 Device design and fabrication method: device type A, B, C, and D

The screen patterns were designed into four types by using Microsoft PowerPoint as shown in **Figure 3.1**. The screen patterns were made from polyester fabric on a wooden frame for device type A, B, C, and D as shown in **Figure 3.2A-3.2D**. For the polymer screen printing fabrication method, the screen pattern was placed onto filter paper (Grade 1 or Grade 42). A solution of polystyrene (20 %w/v) was prepared by dissolving polystyrene pellets in toluene and polystyrene solution was applied onto screen pattern. Polystyrene solution was squeezed by a squeegee

(Figure 3.2E) to push the solution through screen pattern and this polystyrene solution was penetrated through a filter paper to generate hydrophobic barrier. The polymer screen printing fabrication processes are illustrated in Figure 3.3. The device was ready to use after drying by leaving in the hood (3 minutes). The screen pattern was cleaned with toluene during each filter paper fabrication. All steps were performed in a fume hood. The back side of paper was sealed with clear packing tape to prevent leakage of solution through filter paper during assay.

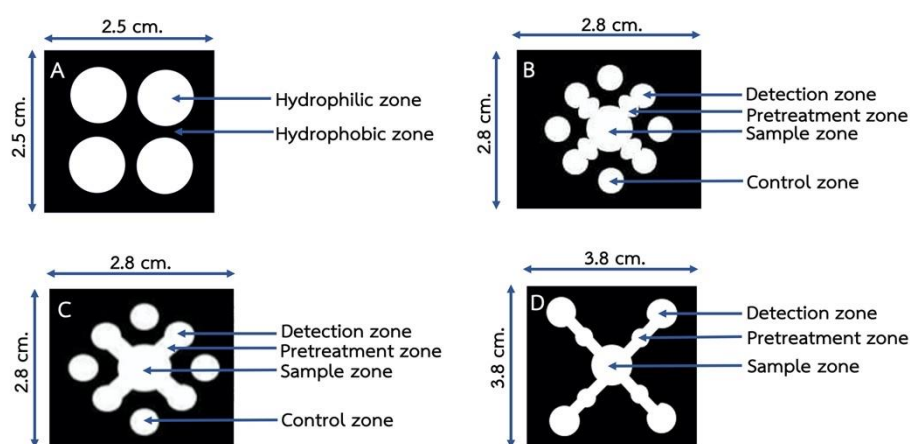


Figure 3.1 Screen patterns design for device type A, B, C, and D.

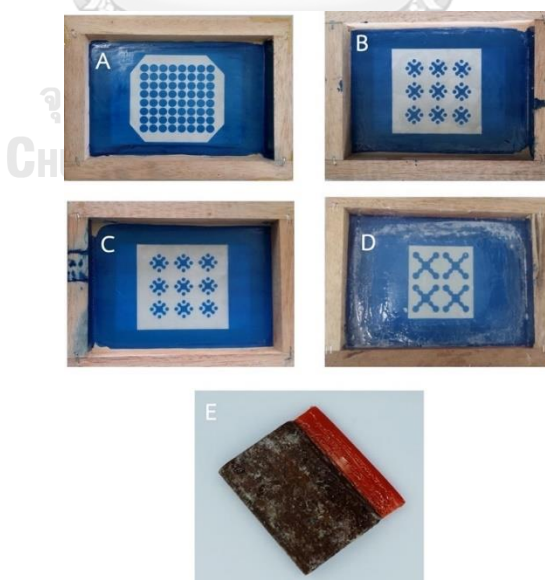


Figure 3.2 Screen patterns on a wooden frame for (A-D) the device type A, B, C, and D, and (E) a squeegee.

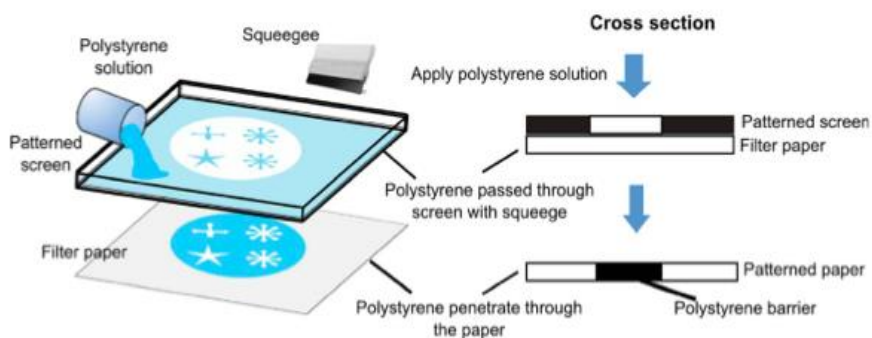


Figure 3.3 The polymer screen printing fabrication processes <sup>16</sup>.

### 3.3.2 Metal complex study on paper-based device type A

For each metal complex study, type of complexing agents, pH of metal ion solutions, paper type, type of masking agent, and reaction time were optimized. The complexing agents (PAN and DTZ) and pH of metal ion solutions at pH 1-7 were studied. DTZ was prepared in chloroform. 4.0  $\mu\text{L}$  of PAN or DTZ (2 mM) was added onto hydrophilic zones, followed by 10.0  $\mu\text{L}$  of 100 mg/L Cu(II), Ni(II), Co(II), Cd(II), Zn(II), Pb(II), Mg(II), Ba(II), Cr(III), and As(III). The color response of metal complexes on the device was recorded using digital camera.

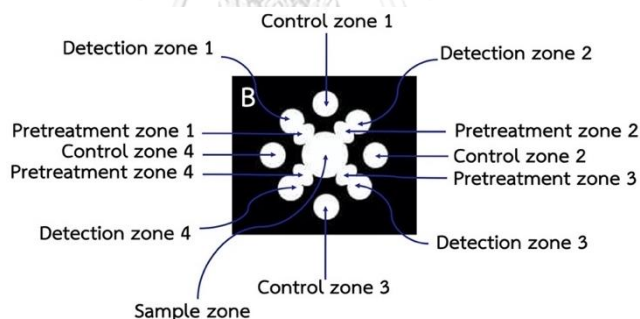
For paper type optimization, filter paper Grade 1 and Grade 42 were studied. 4.0  $\mu\text{L}$  of PAN (2 mM) was added onto hydrophilic zones, followed by 10.0  $\mu\text{L}$  of 100 mg/L Cu(II), Ni(II), Co(II), Cd(II), Zn(II), Pb(II), Mg(II), Ba(II), Cr(III), and As(III) at pH 5. The color response of metal complexes on device was recorded using digital camera.

For type of masking agents optimization, 1 M thiourea, 1 M KCl, and 0.1 M 2, 2' bipyridine were studied. 4.0  $\mu\text{L}$  of PAN or DTZ (2 mM) and 4.0  $\mu\text{L}$  of masking agent were added onto hydrophilic zones, followed by 10.0  $\mu\text{L}$  of a mixture solution of two Metals ions (Cu(II)+Zn(II), Cu(II)+Co(II), and Zn(II)+Cd(II) at pH 5). Each metal ion (100 mg/L) was mixed into a mixture solution. The color response of metal complexes on the device was recorded using digital camera under a lighting studio box. A similar experiment was performed with tartaric acid, sodium citrate, and sodium sulphate as masking agents and 100 mg/L Cu(II), Ni(II), Co(II), Cd(II), Zn(II) at pH 1-7. The color response of metal complexes on device was recorded using digital camera.

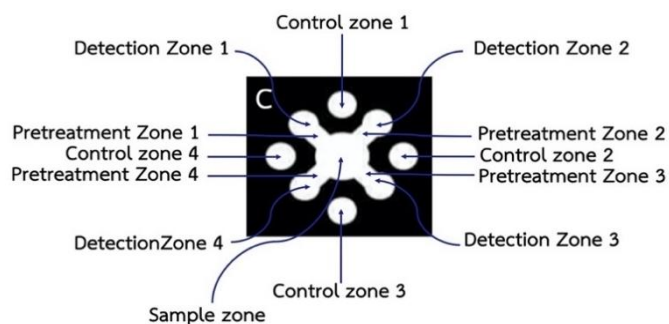
For the reaction time optimization, the color response of Zn(II) and Cd(II) complexes were studied on paper Grade 1. 4.0  $\mu\text{L}$  of PAN or DTZ (2 mM) was added onto hydrophilic zones, followed by 10  $\mu\text{L}$  of 100 mg/L Zn(II) for PAN as complexing agent and 10  $\mu\text{L}$  of 100 mg/L Cd(II) for DTZ as complexing agent. The color response of metal complexes on the device was measured by using spectrophotometer color i5 at the reaction time of 10-40 minutes.

### 3.3.3 Simultaneous detection for four metal ions by naked-eye on paper-based device type B and C

The device consisted of four detection zones (add complexing agent), four pretreatment zones (add masking agents), and one sample zone (add metal ion solution). The components of device type B and C are shown in **Figure 3.4.** and **Figure 3.5.** These devices were designed for simultaneous detection of four metal ions on one device.



**Figure 3.4** The components of device type B.



**Figure 3.5** The components of device type C.

The simultaneous Cu(II), Co(II), Zn(II), Cd(II)/Pb(II) detection on device type B and C were studied. For Cu(II) detection, 0.2  $\mu\text{L}$  of PAN (2 mM) was added onto the detection zone 1. For Co(II) detection, 0.2  $\mu\text{L}$  of PAN (2 mM) was added onto the detection zone 2, followed by 0.2  $\mu\text{L}$  of thiourea (1 M) onto the pretreatment zone. For Zn(II) detection, 0.2  $\mu\text{L}$  of PAN (2 mM) was added onto the detection zone 3, followed by 0.2  $\mu\text{L}$  of a solution of thiourea (1 M)/en (3 M) onto the pretreatment zone. For Cd(II)/Pb(II) detection, 0.2  $\mu\text{L}$  of PAN (2 mM) was added onto the detection zone 4, followed by 0.2  $\mu\text{L}$  of a solution of thiourea (1 M)/en (3 M) and 0.2  $\mu\text{L}$  of 2, 2' bipyridine (0.1 M) onto the pretreatment zone. A mixture solution of four metal ions (12.5  $\mu\text{L}$ , pH 4-6) was added onto the sample zone. Each metal ion (100 mg/L) was mixed into a mixture solution of four metal ions. The color response of metal complexes on the device was recorded using digital camera under optimal reaction time.

### 3.3.4 Simultaneous detection for four metal ions by naked-eye on paper-based device type D

The device components consisted of four detection zones, four pretreatment zones, and one sample zone as shown in Figure 3.6.

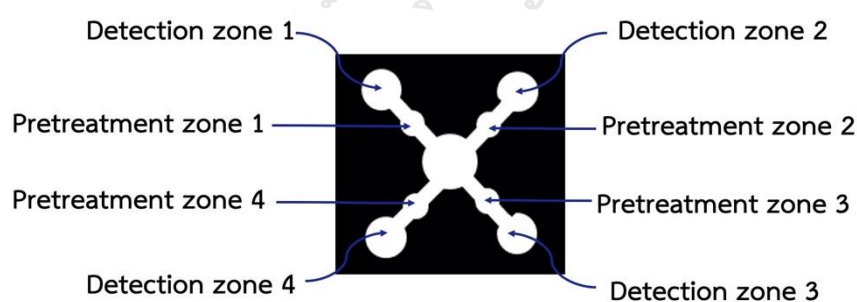


Figure 3.6 The components of device type D.

#### 3.3.4.1 Optimization conditions

The effect of acetate buffer concentrations (pH 5), solvents and concentrations of complexing agent (PAN and DTZ), and NaOH concentrations (DTZ solvent) on color response were studied. Acetate buffer concentrations of 1-5 M



were used to prepared metal ion solutions. PAN (2 mM) and DTZ (2 mM) were prepared in ethanol and chloroform, respectively. For Cu(II) detection, 1.0  $\mu\text{L}$  of PAN (2 mM) was added onto the detection zone 1. For Co(II) detection, 1.0  $\mu\text{L}$  of PAN (2 mM) was added onto the detection zone 2, followed by two aliquots of 3.0  $\mu\text{L}$  of thiourea (1 M) onto the pretreatment zone. For Zn(II) detection, 1.0  $\mu\text{L}$  of PAN (2 mM) was added onto the detection zone 3, followed by two aliquots of 3.0  $\mu\text{L}$  of a solution of thiourea (1 M)/en (3 M) onto the pretreatment zone. For Cd(II)/Pb(II) detection, 2.0  $\mu\text{L}$  of DTZ (2 mM) was added onto the detection zone 4, followed by two aliquots of 3.0  $\mu\text{L}$  a solution of thiourea (1 M)/en (3 M) onto the pretreatment zone. 80  $\mu\text{L}$  of each metal ion solution (50 mg/L) was added onto the sample zone. The color response of metal complexes on the device was recorded using digital camera under a lighting studio box at optimal reaction time of 15 minutes.

### **3.3.5 Application of simultaneous detection of four metal ions in synthetic unknown samples**

The synthetic unknown water samples were prepared in acetate buffer (2 M, pH 5). Each metal ion (50 mg/L) was used to mix into a mixture solution. The synthetic unknown water samples consisted of one metal ion, two metal ions, three metal ions, four metal ions, and none. Each metal ion was possibly mixed into 24 types as demonstrated in **Table 3.3** All synthetic unknown water samples were labeled No.1-24.

Table 3.3 Types of synthetic unknown water samples.

Unknown samples	Metal ions
None	-
One metal ion	Cu(II)
	Co(II)
	Zn(II)
	Cd(II)
	Pb(II)
Two metal ions	Cu(II)+Co(II)
	Cu(II)+Zn(II)
	Cu(II)+Cd(II)
	Cu(II)+Pb(II)
	Co(II)+Zn(II)
	Co(II)+Cd(II)
	Co(II)+Pb(II)
	Zn(II)+Cd(II)
Zn(II)+Pb(II)	
Three metal ions	Cu(II)+Co(II)+Zn(II)
	Cu(II)+Co(II)+Cd(II)
	Cu(II)+Co(II)+Pb(II)
	Co(II)+Zn(II)+Cd(II)
	Co(II)+Zn(II)+Pb(II)
	Cu(II)+Zn(II)+Cd(II)
	Cu(II)+Zn(II)+Pb(II)
Four metal ions	Cu(II)+Co(II)+Zn(II)+Cd(II)
	Cu(II)+Co(II)+Zn(II)+Pb(II)

The simultaneous detection of four metal ions on one device for 24 unknown samples was investigated under the optimal conditions by a researcher. The simultaneous detection of four metal ions on one device for 24 unknown samples was also studied under optimal conditions by and ten students (n=10). These students consisted of seven undergraduate students in the second year (n=2) and third year (n=5) and three graduated students (n=3). These students were advised about the specific hazard of all reagents as shown in **Table 3.4**. They were also briefly suggested about the safety and waste disposal, other notes, and the experimental procedures as below.

**Table 3.4** Specific hazard.

Chemicals	Specific Hazard <sup>1</sup>
1-(2-Pyridylazo)-2-naphthol (PAN)	Causes irritation to skin, eye, and respiratory tract. May be harmful if swallowed, inhaled or absorbed through skin.
Dithizone (DTZ)	Harmful if swallowed.
Thiourea	Harmful if swallowed. Suspected of causing cancer and damaging the unborn child.
Ethylenediamine (en)	Harmful if absorbed through the skin. May be harmful if swallowed or inhaled. May cause allergic respiratory and skin reaction.
Sodium acetate anhydrous	Harmful if swallowed. Suspected of causing cancer and damaging the unborn child.
Toluene	May be fatal if swallowed and enters airways. Causes skin and serious eye irritation. Causes respiratory irritation and damage to organs through prolonged or repeated exposure.
Acetic acid	Causes severe burns to skin, eyes, and digestive tract. Vapor cause extremely irritating to eyes and respiratory tract.

Table 3.4 Specific Hazard.

Chemicals	Specific Hazard <sup>1</sup>
Copper(II) nitrate	Harmful by ingestion. Cause skin irritation and serious eye damage.
Cobalt(II) nitrate	Acute oral toxicity. Respiratory sensitization, skin sensitization and reproductive toxicity.
Zinc(II) nitrate	Acute oral toxicity. Skin and eye irritation.
Nickel(II) nitrate	Acute oral toxicity. Cause skin irritation, serious eye damage, respiratory and skin sensitization.
Cadmium(II) nitrate	Acute oral and dermal toxicity. Reproductive Toxicity.
Lead(II) nitrate	Harmful by inhalation and if swallowed. May cause eye, skin, and respiratory tract irritation. May cause central nervous system effects. Danger of cumulative effects.
Barium chloride	Toxic if swallowed and harmful if inhaled.
Magnesium(II) (standard solution)	Acute oral toxicity. Skin corrosion and serious eye damage.
Chromium(III) (standard solution)	Skin and eye irritation.
Arsenic(III) (standard solution)	Carcinogenicity. Skin and eye irritation.

<sup>1</sup>Specific Hazard was achieved from Material Safety Data Sheet (MSDS).

### Safety and waste disposal

Personal protective equipment (PPE) should be used to handling chemicals which include safety glasses, glove, mask, and lab coat. Although this experiment required small volume of sample and reagents, students should be suggested about handling chemicals and waste. For example, heavy metal ions on the device were eluted with nitric acid and this metal waste was kept into appropriate container to further disposable. Complexing and masking agents on the device were eluted with appropriate solvent and stored in proper container before disposable.

### Other notes

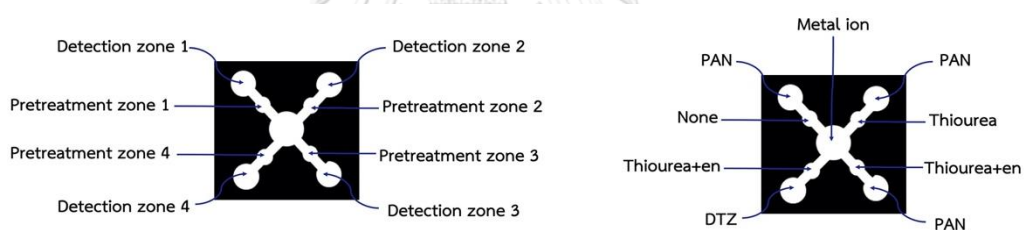
1. One student obtained two sets of 12 devices and 24 unknown samples labeled No.1-24.
2. Students were suggested about reagents adding onto center of each zone on device to avoid reagent reach to other zone.
3. Each zone on the devices (detection zone 1, 2, 3, 4, the pretreatment zone 1, 2, 3, 4, and sample zone) were suggested to label.
4. Experimental procedures were performed with one set of devices (12 devices and unknown samples No1-12) and then a similar experiment was proceeded with another set of devices (12 devices and unknown samples No. 13-24).
5. The color response of metal complexes on the device was recorded using digital camera under a lighting studio box at the reaction times of 15 minutes.
6. For metal ion identification, the color response on the device was compared to the photograph of the color chart of metal complexes by naked-eye and the color response of metal complexes on the device was compared to the color chart of metal complexes in computer display by naked-eye.
7. The detection zones 1, 2, and 3 were designed to detect Cu(II), Co(II), and Zn(II), respectively. The detection zone 4 was designed to detect Cd(II)/Pb(II). Briefly, the color response on device changed from yellow to the purple, green, and pink for Cu(II), Co(II), and Zn(II), respectively. The color response on device changed from orange to red or purple for Cd(II)/(Pb(II) in the detection zone 4 depending on metal ion.

### Instruction for student

Experimental procedures are followed as below.

1. Add reagent onto each zone (12 devices) according to **Figure 3.7**.
2. Add 5.0  $\mu\text{L}$  of DTZ onto the detection zone 4.
3. Add 1.0  $\mu\text{L}$  of PAN onto the detection zone 1, 2, 3.
4. Add 3.0  $\mu\text{L}$  of thiourea onto the pretreatment zone 2.
5. Add 3.0  $\mu\text{L}$  of a solution of thiourea/en onto the pretreatment zone 3 and 4.
6. Add 3.0  $\mu\text{L}$  of thiourea onto the pretreatment zone 2.

7. Add 3.0  $\mu\text{L}$  of a solution of thiourea/en onto the pretreatment zone 3 and 4.
8. Allow the device to dry during each reagent adding.
9. Add 80  $\mu\text{L}$  of unknown solutions (No.1-12) onto the sample zone.
10. Record the color response on the device using a digital camera under a lighting studio box at optimal reaction times of 15 minutes.
11. To identify metal ion, the color response on the device was compared to the photograph of the color chart of metal complexes by naked-eye and the color response of metal complexes on the device was compared to the color chart of metal complexes in computer display by naked-eye.
12. Mark  $\checkmark$ (certain),  $\times$ (none), and ? (uncertain) to identify each metal ion in unknown samples and note the results in **Table 3.5**.
13. Repeat 2-11 again for another set of devices for unknown of metal ion solutions No.13-24.



**Figure 3.7** Device components and type of reagents for simultaneous Cu(II), Co(II), Zn(II), Cd(II)/Pb(II) detection on one device.

**Table 3.5** Identification of metal ion in unknown samples by comparison with the photograph of the color chart and the color chart in computer display by naked-eye.

Each metal ion in unknown samples was identified by mark × (certain),  
 ✓ (none), and ? (uncertain).

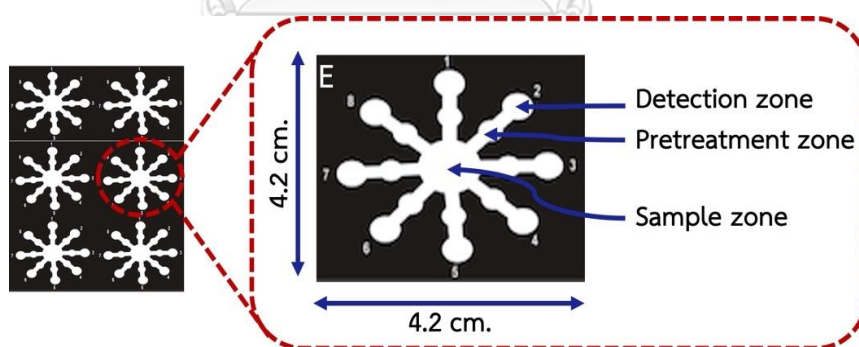
Unknown number	Metal ion identification					
	Cu(II)	Co(II)	Zn(II)	Cd(II)	Pb(II)	None
1						
2						
3						
4						
5						
6						
7						
8						
9						
10						
11						
12						
13						
14						
15						
16						
17						
18						
19						
20						
21						
22						
23						
24						

### 3.4 Metal complex study on paper-based analytical device: wax printing method

#### 3.4.1 Device design and fabrication method: device type E and F

These devices were designed by using CorelDRAW software. The wax printing was used for hydrophobic barrier fabrication on the filter paper Grade 1. The wax pattern was printed onto the filter paper using a Xerox Phaser 8860 wax printer<sup>19</sup>. This wax pattern was melted at 200 °C for 30 second on a hot plate to generate the three-dimensional hydrophobic barriers. The back side of device was sealed with clear packing tape to prevent leakage of solution through the paper during analysis.

The device type E consisted of eight detection zones, eight pretreatment zones, and one sample zone as illustrated in **Figure 3.8**. The design components consisted of the sample zone (10 mm diameter), the detection zone (5 mm diameter), the pretreatment zone (4 mm diameter), and channels (2.4 x 4 mm). The design of device type E was developed based on device type D by increasing the number of detection zone and the length of pretreatment zone for simultaneous Cu(II), Co(II), Hg(II), Ni(II), Fe(III), Cr(VI), V(III), and Mn(II) detection.



**Figure 3.8** The components of device type E.

The device type F consisted of five detection zones, ten pretreatment zones, and one sample zone as illustrated in **Figure 3.9**. The design components consisted of the sample zone (13 mm diameter), the detection zone (6 mm diameter), the pretreatment zone 1 and 2 (5 mm diameter), and channels (2x3 mm). The design for device type F was developed from device type E by increasing size of detection zone



and length of two pretreatment zone for simultaneous Cu(II), Co(II), Hg(II), Ni(II), and Mn(II) detection. The size of detection zone was increased to easy observe the color response by naked-eye. The pretreatment zone was extended into 2 zones to increase area for loading masking agent.

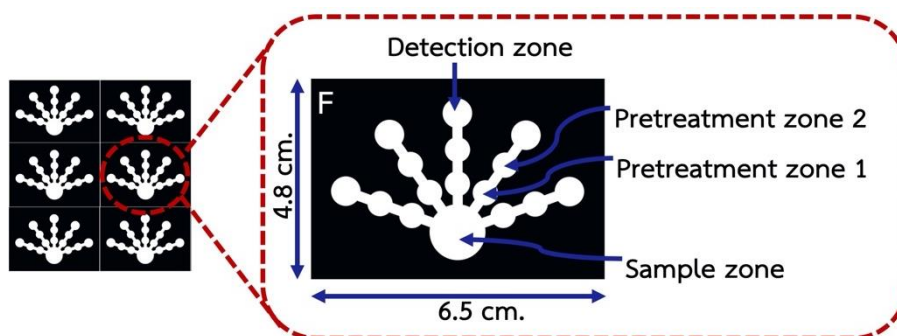


Figure 3.9 The components of device type F.

### 3.4.2 Metal complex study on paper-based analytical device type E

#### 3.4.2.1 Optimization conditions

##### - Types of complexing agent and masking agent

The effect of type of complexing agent and masking agent on the color response was optimized to achieve selectivity for simultaneous Cu(II), Co(II), Hg(II), Fe(II), Fe(III), Ni(II), Cr(VI), V(III), and Mn(II) detection by naked-eye. A set of reagents for single metal ion detection was added on one device by adding the same complexing agent onto eight detection zones and the same masking agent onto eight pretreatment zones. 140  $\mu\text{L}$  of each metal ion solution (25 mg/L) and a mixture solution of eight metal ions were added onto the sample zone. A mixture solution of eight metal ions was called **All-8**. Each metal ion solution was prepared in 0.1 M acetate buffer (pH 5). The device was allowed to dry and then the color response of metal complexes on the device was recorded by using a scanner (>50 minutes).

For Cu(II) detection, bathocuproine (Bc) was used as a complexing agent. Three 1.0  $\mu\text{L}$  aliquots of hydroxylamine hydrochloride (0.5 g/mL), 1.0  $\mu\text{L}$  of  $\text{CH}_3\text{COOH}/\text{NaCl}$  buffer (10 mM, pH 4.6), followed by 1.0  $\mu\text{L}$  of a solution of Bc (10 mM)/PEG 400 (80 mg/mL) onto eight detection zones. Four 2.0  $\mu\text{L}$  aliquots of NaF

(0.5 M) were added onto eight pretreatment zones. 140  $\mu\text{L}$  of each metal ion solution and **All-8** were added onto the sample zone.

For Ni(II) detection, dimethylglyoxime (DMG) was used as a complexing agent. Four 1.0  $\mu\text{L}$  aliquots of hydroxylamine hydrochloride (0.5 g/mL) onto eight detection zones, two 0.5  $\mu\text{L}$  aliquots of DMG (60 mM), followed by two 1.0  $\mu\text{L}$  aliquots of ammonium hydroxide (0.03 M, pH 9.5). Two 2.0  $\mu\text{L}$  aliquots of NaF (0.5 M) were added onto eight pretreatment zones, followed by two 2.0  $\mu\text{L}$  aliquots of  $\text{CH}_3\text{COOH}$  (6.3 M). 140  $\mu\text{L}$  of each metal ion solution and **All-8** were added onto the sample zone.

For V(III) detection, two 1.0  $\mu\text{L}$  aliquots of a solution of PAR (5 mM)/PDDA (5 %w/w) onto eight detection zones. Four 2.0  $\mu\text{L}$  aliquots of DCTA (0.1 M) were added onto eight pretreatment zones. 140  $\mu\text{L}$  of each metal ion solution and **All-8** were added onto the sample zone.

For Mn(II) detection, the device was added two 1.0  $\mu\text{L}$  aliquots of a PAR (5 mM)/PDDA (5 %w/w) solution onto eight detection zones. Two 2.0  $\mu\text{L}$  aliquots of a solution of triethylenetetramine (0.1 M)/DMSA (0.1 M)/en (6 M) were added onto eight pretreatment zones. 140.0  $\mu\text{L}$  of each metal ion solution and **All-8** were added onto the sample zone. The results of Mn(II) detection by using PAR as a complexing agent, the red Mn(II)-PAR complex was not obviously different from blank. Therefore, PAN was selected as a new complexing agent for Mn(II) detection. The device was added two 1.0  $\mu\text{L}$  aliquots a solution of PAN (2 mM) onto eight detection zones. Three 2.0  $\mu\text{L}$  aliquots of a solution of thiourea (1 M)/en (4 M)/KCN (0.1 M) were added onto eight pretreatment zones. 140  $\mu\text{L}$  of each metal ion solution and **All-8** were added onto the sample zone.

For Hg(II) detection, the device was added 1.0  $\mu\text{L}$  of DTZ (2 mM), followed by two 2.0  $\mu\text{L}$  aliquots of PEG 400 (80 mg/mL) onto eight detection zones. Two 2.0  $\mu\text{L}$  aliquots of en (2 M) were added onto eight pretreatment zones. 140  $\mu\text{L}$  of each metal ion solution and **All-8** were added onto the sample zone. The colored complexes of Cu(II) and Co(II) possibly interfered the red Hg(II)-DTZ complex. To improve the selectivity of Hg(II) detection by using DTZ as a complexing agent, three 1.5  $\mu\text{L}$  aliquots of PEG 400 (80 mg/mL) onto eight detection zones. Four 2.0  $\mu\text{L}$

aliquots of DCTA (0.1 M) were added onto eight pretreatment zones, two 2.5  $\mu\text{L}$  aliquots of KCN (0.1 M), followed by two 2.0  $\mu\text{L}$  aliquots of en (10 M). Masking agents on the pretreatment zone were allowed to dry and then two 1.0  $\mu\text{L}$  aliquots of DTZ (2 mM) were added onto eight detection zones. 140  $\mu\text{L}$  of each metal ion solution and **All-8** were added onto the sample zone.

For Cr(VI) detection, two 1.0  $\mu\text{L}$  aliquots of 0.2 %w/v 1,5-diphenylcarbazide (DPC) were added onto eight detection zones. 140  $\mu\text{L}$  of each metal ion solution and **All-8** were added onto the sample zone. The color complexes of Cu(II), Co(II), Ni(II), Hg(II), and V(III) possibly interfered the purple Cr(VI)-DPC complex. To improve the selectivity of Cr(VI) detection by using DPC as a complexing agent, the device was added two 1.0  $\mu\text{L}$  aliquots of DPC solution (0.2 %w/v) onto eight detection zones. Two 2.0  $\mu\text{L}$  aliquots of thiourea (1.0 M) were added onto eight pretreatment zones, followed by two 2.0  $\mu\text{L}$  aliquots NaF (0.5 M). 140  $\mu\text{L}$  of each metal ion solution and **All-8** were added onto the sample zone.

For Fe(III) detection, bathophenanthroline (Bphen) was selected as complexing agent for Fe(III) detection. Two 1.0  $\mu\text{L}$  aliquots a solution of Bphen (10 mM)/acetate buffer (20 mM, pH 5)/L-ascorbic acid (0.05 M) onto eight detection zones. Four 2.0  $\mu\text{L}$  aliquots of L-ascorbic acid (0.1 M) were added onto eight pretreatment zones. 140  $\mu\text{L}$  of each metal ion solution and **All-8** were added onto the sample zone.

For Co(II) detection, the device was added a solution of PAR (5 mM)/PDDA (5 %w/w) onto eight detection zones. Four 2.0  $\mu\text{L}$  aliquots of DCTA (0.1 M) were added onto eight pretreatment zones, three 2.0  $\mu\text{L}$  aliquots of triethylenetetramine (0.4 M), followed by two 2.0  $\mu\text{L}$  aliquots of en (4 M). 140  $\mu\text{L}$  of each metal ion solution and **All-8** were added onto the sample zone.

#### - Metal volume

Mn(II) conditions were selected to study the effect metal volume (120-160  $\mu\text{L}$ ) on the color response of metal complexes. 4-(2-Pyridylazo) resorcinol (PAR) was used as a complexing agent for Mn(II) detection. For Mn detection, two 1  $\mu\text{L}$  aliquots of a solution of PAR (5 mM)/PDDA (5%w/w) were added onto eight detection zones. Four 2.0  $\mu\text{L}$  aliquots of thiourea (1 M) was added onto eight pretreatment zones,

followed by three 2.0  $\mu\text{L}$  aliquots of en (8 M). Mn(II) solution (120-160  $\mu\text{L}$ ) was added onto the sample zone. The device was allowed to dry and then the color response on the device type E was recorded by using a scanner.

### 3.4.3 Application of simultaneous detection for eight metal ions in synthetic unknown samples

As the optimal colorimetric detection conditions of each metal ion detection, these optimal conditions were used to study the limit of detection (LOD) by naked-eye. A single metal ion detection was operated on one device by adding the same complexing agent onto eight detection zones and the same masking agent onto eight pretreatment zones. The device was allowed to dry during each reagent adding. Each metal ion solution was varied in the range of 0.05-0.4 mM. The device was allowed to dry and then the color response on the device was recorded by using a scanner. The limit of detection for each metal ion detection was observed by naked-eye.

For simultaneous Cu(II), Co(II), Hg(II), Fe(III), Ni(II), Cr(VI), V(III), and Mn(II) detection in synthetic unknown samples, the optimal conditions of each metal ion detection was combined to operate on one device. Each metal ion (0.4 mM) was mixed in the concentration ratio of 1:1 for synthetic unknown samples. Each unknown sample was prepared in 0.1 M acetate buffer at pH 5. Many types of unknown samples were possibly mixed in this work as shown **Table 3.6**. The synthetic unknown water samples were selected 46 types from 156 types. The synthetic unknown water samples No.1-46 were proceeded to detect metal ion on one device by a researcher. The device was allowed to dry and then the color response on the device was recorded by using a scanner. The color response of metal complexes on the device was compared with the color chart of the color response of metal complexes using a mixture solution of eight metal ions (**All-8**) by naked-eye.

**Table 3.6** Types of synthetic unknown samples.

Unknown samples	Metal ions
One metal ion	Cu, Co, Ni, Hg, Mn, Fe, Cr, V
Two metal ions	Cu+Co, Cu+Ni, Cu+Hg, Cu+Mn, Cu+Fe, Cu+Cr, Cu+V, Co+Ni, Co+Hg, Co+Mn, Co+Fe, Co+Cr, Co+V, Ni+Hg, Ni+Mn, Ni+Fe, Ni+Cr, Ni+V, Hg+Mn, Hg+Fe, Hg+Cr, Hg+V, Mn+Fe, Mn+Cr, Mn+Cr, Fe+Cr, Fe+V, Cr+V
Three metal ions	Cu+Co+Ni, Cu+Co+Hg, Cu+Co+Mn, Cu+Co+Fe, Cu+Co+Cr, Cu+Co+V, Co+Ni+Hg, Co+Ni+Mn, Co+Ni+Fe, Co+Ni+Cr, Co+Ni+V, Ni+Hg+Mn, Ni+Hg+Fe, Ni+Hg+Cr, Ni+Hg+V, Hg+Mn+Fe, Hg+Mn+Cr, Hg+Mn+V, Mn+Fe+Cr, Mn+Fe+V, Cu+Ni+Hg, Cu+Ni+Mn, Cu+Ni+Fe, Cu+Ni+Cr, Cu+Ni+V, Cu+Hg+Co, Cu+Hg+Ni, Cu+Hg+Mn, Cu+Hg+Fe, Cu+Hg+Cr, Cu+Hg+V, Cu+Mn+Co, Cu+Mn+Ni, Cu+Mn+Fe, Cu+Mn+Cr, Cu+Mn+V, Cu+Fe+Cr, Cu+Fe+V, Cu+Cr+V
Four metal ions	Cu+Co+Ni+Hg, Cu+Co+Ni+Mn, Cu+Co+Ni+Fe, Cu+Co+Ni+Cr, Cu+Co+Ni+V, Co+Ni+Hg+Mn, Co+Ni+Hg+Fe, Co+Ni+Hg+Cr, Co+Ni+Hg+V, Ni+Hg+Mn+Fe, Ni+Hg+Mn+Cr, Ni+Hg+Mn+V, Hg+Mn+Fe+Cr, Hg+Mn+Fe+V, Mn+Fe+Cr+V, Cu+Ni+Hg+Mn, Cu+Ni+Mn+Fe, Cu+Ni+Hg+Cr, Cu+Ni+Hg+V, Cu+Hg+Mn+Fe, Cu+Hg+Mn+Cr, Cu+Hg+Mn+V, Cu+Mn+Fe+Cr, Cu+Mn+Fe+V, Cu+Fe+Cr+V, Co+Hg+Mn+Fe, Co+Hg+Mn+Cr, Co+Hg+Mn+V, Co+Mn+Fe+Cr, Co+Mn+Fe+V, Ni+Mn+Fe+Cr, Ni+Mn+Fe+V, Hg+Fe+Cr+V

**Table 3.6** Types of synthetic unknown samples (cont.).

Unknown samples	Metal ions
Five metal ions	Cu+Co+Ni+Hg+Mn, Cu+Co+Ni+Hg+Fe, Cu+Co+Ni+Hg+Cr, Cu+Co+Ni+Hg+V, Co+Ni+Hg+Mn+Fe, Co+Ni+Hg+Mn+Cr, Co+Ni+Hg+Mn+V, Ni+Hg+Mn+Fe+Cr, Ni+Hg+Mn+Fe+V, Hg+Mn+Fe+Cr+V, Cu+Ni+Hg+Mn+Fe, Cu+Ni+Hg+Mn+Cr, Cu+Ni+Hg+Mn+V, Cu+Hg+Mn+Fe+Cr, Cu+Hg+Mn+Fe+V, Cu+Mn+Fe+Cr+V, Co+Hg+Mn+Fe+Cr, Co+Hg+Mn+Fe+V, Co+Mn+Fe+Cr+V, Ni+Mn+Fe+Cr+V, Hg+Mn+Fe+Cr+V
Six metal ions	Cu+Co+Ni+Hg+Mn+Fe, Cu+Co+Ni+Hg+Mn+Cr, Cu+Co+Ni+Hg+Mn+V, Co+Ni+Hg+Mn+Fe+Cr, Co+Ni+Hg+Mn+Fe+V, Ni+Hg+Mn+Fe+Cr+V, Cu+Ni+Hg+Mn+Fe+Cr, Cu+Ni+Hg+Mn+Fe+V, Cu+Co+Hg+Mn+Fe+Cr, Cu+Co+Hg+Mn+Fe+V, Cu+Co+Ni+Mn+Fe+Cr, Cu+Co+Ni+Mn+Fe+V, Cu+Co+Ni+Hg+Fe+Cr, Cu+Co+Ni+Hg+Fe+V, Cu+Co+Ni+Hg+Mn+Cr, Cu+Co+Ni+Hg+Mn+V, Cu+Co+Ni+Hg+Mn+Fe
Seven metal ions	Cu+Co+Ni+Hg+Mn+Fe+Cr, Cu+Co+Ni+Hg+Mn+Fe+V, Co+Ni+Hg+Mn+Fe+Cr+V, Cu+Ni+Hg+Mn+Fe+Cr+V, Cu+Co+Hg+Mn+Fe+Cr+V, Cu+Co+Ni+Mn+Fe+Cr+V, Cu+Co+Ni+Hg+Fe+Cr+V, Cu+Co+Ni+Hg+Mn+Cr+V, Cu+Co+Ni+Hg+Mn+Fe+V,
Eight metal ions (All-8)	Cu+Co+Ni+Hg+Mn+Fe+Cr+V

### 3.4.4 Metal complex study on paper-based analytical device type F

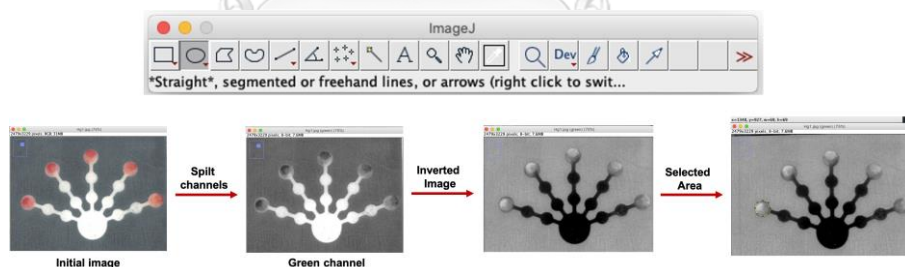
#### 3.4.4.1 Optimization conditions

For Cu(II), Co(II), Ni(II), Hg(II), and Mn(II) detection, effect of type of masking agent, color intensity, reaction time, metal ion volume, and complexing agent volume on color response were optimized. A single metal ion detection was operated on one device by adding the same complexing agent onto five detection zones and the same masking agent onto ten pretreatment zones. Each metal ion solution (0.455 mM, 300  $\mu$ L) and a mixture solution of five metal ions were added onto the sample zone. A mixture solution of five metal ions was called **All-5**. The color response of metal complexes on the device was recorded by using a scanner under the optimal reaction time.

For type of masking agent optimizations, the color response on the device of metal complexes was investigated by naked-eye. For Cu(II) detection, two 2.0  $\mu$ L aliquots of hydroxylamine hydrochloride (0.5 g/mL), 2.0  $\mu$ L of CH<sub>3</sub>COOH/NaCl buffer (10 mM, pH 4.6), and 2.0  $\mu$ L of Bc/PEG 400 solution were added onto five detection zones. Four 2.5  $\mu$ L aliquots of NaF (0.5 M) were added onto five pretreatment zones 1. For Co(II) detection, the device was added two 2.5  $\mu$ L aliquots of PAR/PDDA solution onto five detection zones. Three 2.5  $\mu$ L aliquots of en (4 M) were added onto five pretreatment zone 2. Four 2.5  $\mu$ L aliquots of EDTA (0.2 M) were added onto five pretreatment zones 1, followed by four 2.5  $\mu$ L aliquots of triethylenetetramine (0.4 M). For Ni(II) detection, two 1.5  $\mu$ L aliquots of DMG (60 mM) solution was added onto five detection zones, followed by two 2.0  $\mu$ L aliquots of ammonium hydroxide (0.03 M). Two 2.5  $\mu$ L aliquots of NaF (0.5 M) were added onto five pretreatment zones 2, followed by two 2.5  $\mu$ L aliquots of acetic acid (6.3 M). For Hg(II) detection, three 3.0  $\mu$ L aliquots of PEG 400 (80 mg/mL) was added onto five detection zones. Two 2.5  $\mu$ L aliquots of en (10 M) were added onto five pretreatment zones 2. Four 2.5  $\mu$ L aliquots of DCTA (0.1 M) were added onto five pretreatment zones 1, followed by two 2.5  $\mu$ L aliquots of KCN (0.1 M). Masking agents on all pretreatment zones were allowed to dry and then two 1.5  $\mu$ L aliquots of DTZ (2 mM) were added onto five detection zones. For Mn(II) detection, two 2.5  $\mu$ L aliquots of PAR/PDDA solution

was added onto five detection zones. Four 2.5  $\mu\text{L}$  aliquots of en (8 M) and four 2.5  $\mu\text{L}$  aliquots of thiourea (1 M) were added five the pretreatment zone 2 and zone 1, respectively. The device was allowed to dry during each reagent adding.

For color intensity optimization, all images of the color response on the device were scanned under the optimal reaction time and stored in JPEG format at 1200 dpi. An image was processed to calculate the color intensity using ImageJ software. To obtain the optimal color channel for each metal reaction, the color intensity of each reaction was studied by splitting into four color channels (gray, red, green, and blue). The average color intensity of each color channel on the detection zone was measured by creating area to define the analysis zone. An image was inverted and measured the average color intensity on the detection zone. The analysis processes are illustrated in **Figure 3.10**. The linear regression equation for each metal ion reaction was achieved by plotting between the color intensities and target metal ion concentrations. The regression equation and the correlation coefficient ( $R^2$ ) were considered to select the optimum color intensity for further study.



**Figure 3.10** ImageJ processes for image analysis.

For reaction time optimization, the reaction time (120-200 minutes) was optimized for each metal ion detection with 300  $\mu\text{L}$  of metal ion solution. The effect of reaction time of each metal ion detection on the color response was evaluated by using ImageJ software. The metal ion volume was studied in the range of 200-300  $\mu\text{L}$  by naked-eye. Mn(II) conditions were selected to study the effect metal volume on the color response of Mn(II)-PAR complexes because the viscosity of en on the pretreatment zone impacted on flowing of metal ion solution through the



pretreatment zone into the detection zone. A solution of PAR (5.0 mM)/PDDA (5%w/w) was added onto eight detection zones. Thiourea (1 M), followed by en (8 M) were added onto eight pretreatment zones. Mn(II) solution (120-160  $\mu$ L) was added onto the sample zone. Complexing agent volume of each metal ion detection was optimized in the range of 2.0-10.0  $\mu$ L by using ImageJ software.

#### **3.4.4.2 Colorimetric detection and interference study under optimal conditions**

The method performance was evaluated for Cu(II), Co(II), Ni(II), Hg(II), and Mn(II) detection under optimal conditions. A single metal ion detection was operated on one device by adding the same complexing agent onto five detection zones and the same masking agent onto ten pretreatment zones. The device was allowed to dry at room temperature during adding each reagent. Metal ion solutions (300  $\mu$ L) were added onto the sample zone. The color response of metal complexes on the device was recorded by using a scanner at optimal reaction time of 120 minutes.

For Interferences study, target metal ion (0.455 mM) was mixed with interfering ions in the concentration ratio of 1:1 and 1:2 for Cd(II), Zn(II), Pb(II), Fe(II), Fe(III), Cr(VI), and V(III) interferences. Effect of K(I), Na(I) alkali and Mg(II), Ca(II) alkaline earth groups were added 100 and 1000 times over 0.455 mM target metal ion. The color response of each metal ion detection on the device was measured using ImageJ software under the optimal reaction time of 120 minutes. The statistical data was used to evaluate interfering ions effect.

#### **3.4.4.3 Simultaneous detection of five metal ions**

For simultaneous Cu(II), Co(II), Ni(II), Hg(II), and Mn(II) detection, the optimal complexing agent and masking agent of each reaction were added onto each pretreatment zone and each detection zone. A mixture solution of five metal ions were added onto the sample zone. Each metal ion was mixed in the concentration ratio of 1:1 and 1:2. The color response of each target metal ion reaction on the device was recorded by using a scanner at the optimal reaction time of 120 minutes.

For simultaneous Cu(II), Co(II), Ni(II), Hg(II), and Mn(II) quantification, a single metal ion determination was operated on one device. The optimal complexing agent and masking agent of each metal ion determination were added onto five pretreatment zones and five detection zones. A mixture solution of five metal ions were added onto the sample zone. Each metal ion was mixed in the concentration ratio of 1:1. The color response of each target metal ion reaction on one device was recorded by using a scanner at the optimal reaction time of 120 minutes.

#### **3.4.4.4 Application of simultaneous determination of five metal ions in water samples**

The precision of the proposed method was proceeded by using a single metal ion detection on one device. The same complexing agent was added onto five detection zones and the same masking agent was added onto ten pretreatment zones. The device was allowed to dry at room temperature during adding each reagent. Each metal ion (300  $\mu$ L) was added onto the sample zone. The color response of metal complexes on the device was recorded by using a scanner under the optimal reaction time of 120 minutes. The color intensity on the device was measured with three replicate devices ( $n=3$ ) within a day to evaluate the precision.

A single metal ion detection on one device was applied for simultaneous Cu(II), Co(II), Ni(II), Hg(II), and Mn(II) determination in drinking, tap, and pond-CU waters when CU refers to Chulalongkorn University. Each target metal ion was spiked at three level concentrations in water samples. Each level concentration for each metal ion was spiked in the concentration ratio of 1:1 for Cu(II), Co(II), Hg(II), and Mn(II) determination. For Ni determination, Ni(II) was spiked of tree levels (0.800, 2.000, 4.000 mM) and other metal ions (0.910 mM Cu(II), Hg(II), Mn(II), and 0.455 mM Co(II)) were spiked for Ni(II) solution with tree level concentrations. The same complexing agent was added onto five detection zones and the same masking agent was added onto ten pretreatment zones. The device was allowed to dry at room temperature during adding each reagent. Each water sample (300  $\mu$ L) was added onto the sample zone. The color response of metal complexes on the device was recorded by using a

scanner under the optimal reaction time of 120 minutes. To quantify metal ion, ImageJ software was use calculated the color intensity.



## CHAPTER VI

### RESULTS AND DISCUSSIONS

#### 4.1 Metal complex study in solution phase

##### 4.1.1 PAN-metal complexes at pH 1-7

1-(2-Pyridylazo)-2-naphthol (PAN) formed color complexes with several metal ions<sup>28</sup>. For example, PAN was used as a chelator for preconcentration and determination of copper(II) in macroemulsion-based dispersive magnetic solid phase extraction<sup>25</sup>. Therefore, PAN was a complexing agent to detect heavy metal ions in this experiment. For preliminary study of metal complexes in solution phase, PAN was added into a vial, followed by metal ions at pH 1-7. The results in **Figure 4.1** showed that the color response of metal complexes changed from orange (PAN) to purple, green, purple, red, red, and red at pH 5-6 for Cu(II), Co(II), Zn(II), Ni(II), Cd(II), and Pb(II), respectively. Therefore, Cu(II), Co(II), Zn(II), Ni(II), Cd(II), and Pb(II) at pH 5-6 was selected for further study.

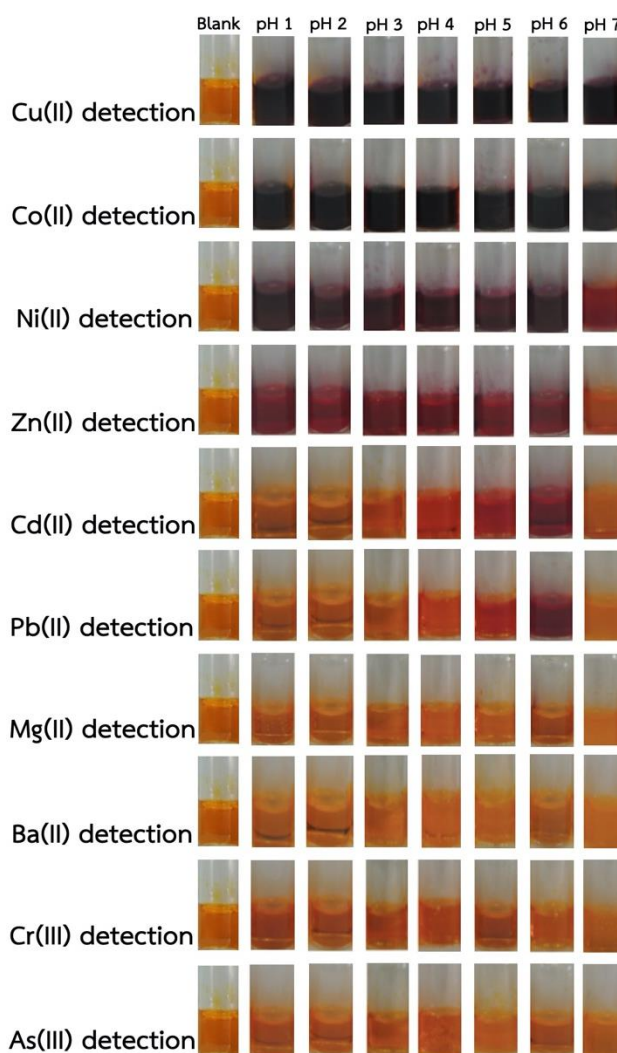
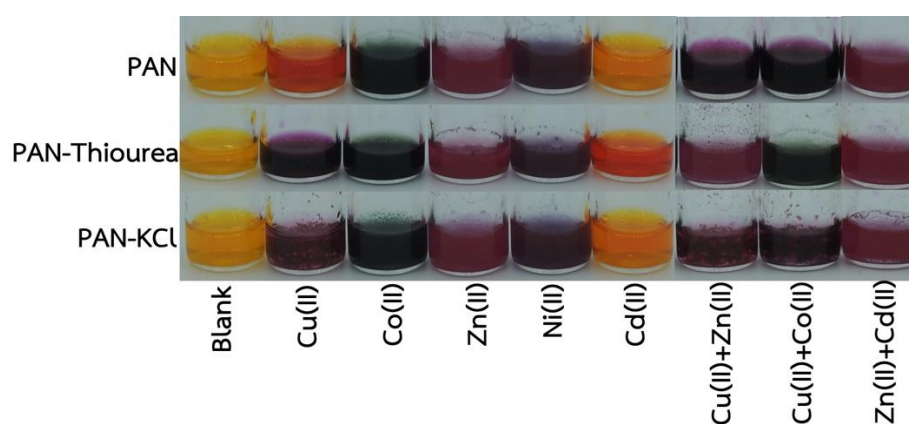


Figure 4.1 Color changes of PAN-metal complexes in solution phase at pH 1-7.

#### 4.1.2 PAN-metal complexes at pH 5

As the results in **section 4.1.1**, PAN formed colored complexes with various metal ions at pH 5-6. Therefore, masking agents were applied to mask interfering ions to obtain the selectivity for each metal ion detection. PAN was added into a vial, followed by metal ions at pH 5. Thiourea and KCl were used to mask Cu(II) and Ni(II), respectively <sup>76</sup>. The results in **Figure 4.2** demonstrated that the color response of metal complexes changed from orange (PAN) to purple, purple, and red for a mixture solution of Cu(II)+Zn(II), Cu(II)+Co(II), and Zn(II)+Cd(II), respectively. After adding thiourea as a masking agent in a vial, the color response of metal complexes

changed from purple, purple, and red to red, green, and red for a mixture solution of Cu(II)+Zn(II), Cu(II)+Co(II), and Zn(II)+Cd(II), respectively. For adding KCl, the color change of metal complexes was similar to the case without masking agent. These results indicated that thiourea efficiently masked Cu(II) while KCl was not. Thiourea forms sulphur-to-metal bonds<sup>36</sup>. Thiourea acts in a monodentate by forming 1:6 metal to ligand ratio with the Cu(thiourea)<sub>6</sub> formular<sup>36</sup>. Therefore, thiourea was selected to mask Cu(II) for further study.



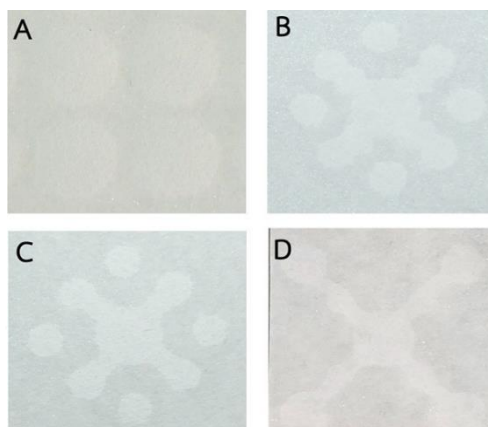
**Figure 4.2** Color changes of PAN-metal, PAN-thiourea-metal, PAN-KCl-metal complexes in solution at pH 5.

## 4.2 Metal complex study on paper-based analytical device: polymer screen printing method

### 4.2.1 Device design and fabrication method: device type A, B, C, and D

Microfluidic paper-based analytical device has been attracted attention for heavy metal ion detection in food, clinical, and environmental samples<sup>34, 54, 55</sup>. The colorimetric method on paper materials has been reported in recent years<sup>35</sup>. The device pattern was designed by using Microsoft PowerPoint. A polymer screen-printing method was used for device fabrication<sup>16</sup>. This fabrication method has attracted attention because it is simple, low cost instruments and materials<sup>16</sup>. The polystyrene solution was screened through the screen pattern and paper to generate hydrophilic zone in a single step<sup>16</sup>. The devices could bend or fold after fabrication which were used for complicated analysis<sup>16</sup>. For device type A, the spot patten was

designed for preliminary study of each metal complex. The devices type B, C, and D were designed for simultaneous detection of four metal ions. The devices after fabrication are shown in **Figure 4.3**.



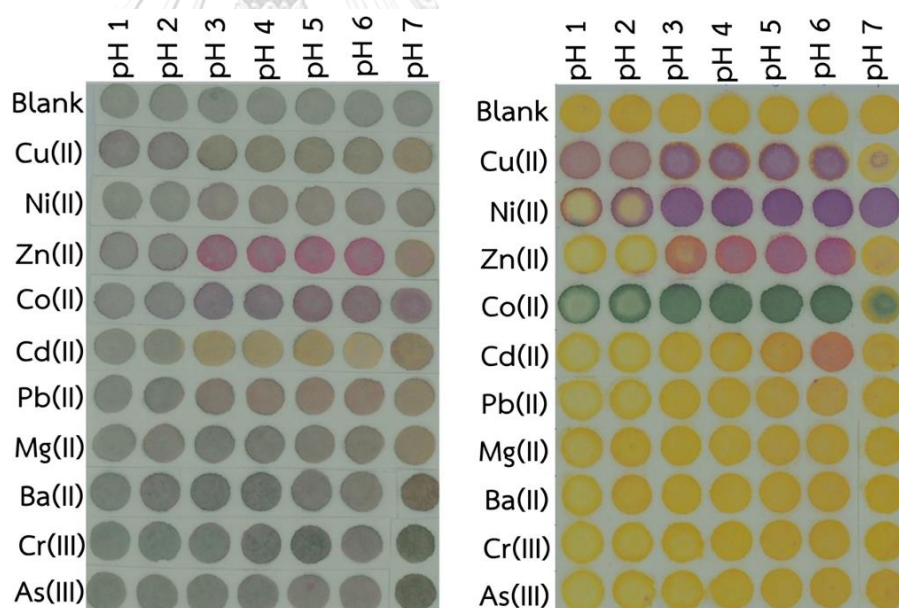
**Figure 4.3** The device type A, B, C, and D after fabrication by using polymer screen-printing method.

#### 4.2.2 Metal complex study on paper-based device type A

##### - Complexing agent and pH of metal ion solution

PAN and dithizone (DTZ) formed colored complexes with various metal ions. For example, PAN was immobilized onto polyvinyl alcohol microsphere for Cu(II) and Co(II) detection by naked-eye<sup>82</sup>. The immobilization of DTZ on agarose membrane was used for Hg(II) and Pb(II) determination<sup>80</sup>. Therefore, PAN and DTZ were attracted to use as complexing agents to detect heavy metal ions in this experiment. PAN can be dissolved in organic solvents (ethanol and methanol) and formed stable complexes with various metal ions<sup>28</sup>. Whereas, DTZ was dissolved in various solvents including chloroform, carbon tetrachloride, and sodium hydroxide<sup>61</sup>. For preliminary study on device type A, PAN or DTZ was added onto hydrophilic zones, followed by metal ions solution at pH 1-7. The results in **Figure 4.4** showed that Cu(II), Co(II), Zn(II), Ni(II), Cd(II), and Pb(II) formed various colored complexes with PAN and DTZ at pH 3-6. For PAN, the color response on device changed from yellow (PAN) to purple,

green, pink, purple, orange, and yellow for Cu(II), Co(II), Zn(II), Ni(II), Cd(II), and Pb(II), respectively. PAN formed various colored complexes with number of metal ions through the azo group and the nitrogen atom of pyridyl group<sup>28</sup>. The Cu(II), Co(II), and Zn(II)-PAN reactions are shown in **Figure 4.5**<sup>28</sup>. For DTZ, the green color appeared on the device before adding metal solution. The color response on the device were green, purple, pink, green, orange, and pink for Cu(II), Co(II), Zn(II), Ni(II), Cd(II), and Pb(II), respectively. DTZ forms colored complexes with various metals through the azo group and the nitrogen atom of pyridyl group<sup>80</sup>. The Cd(II)/Pb(II)-DTZ reaction is shown in **Figure 4.6**<sup>80</sup>. Therefore, Cu(II), Co(II), Zn(II), Ni(II), Cd(II), and Pb(II) at pH 5 were selected for naked-eye detection by using PAN and DTZ as complexing agents.



**Figure 4.4** Color changes of metal-DTZ (left) and metal-PAN (right) complexes on device type A at pH 1-7.



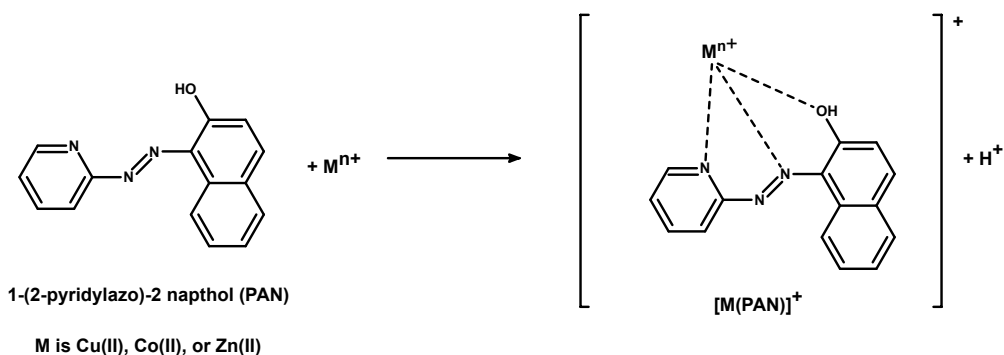


Figure 4.5 Cu(II), Co(II), and Zn(II)-PAN reaction.

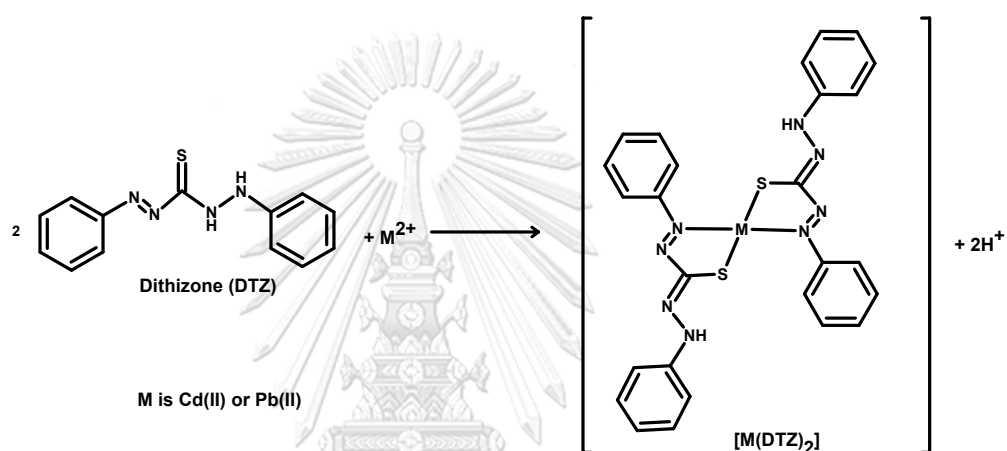


Figure 4.6 Cd(II) or Pb(II)-DTZ reaction.

#### - Paper type

The type of filter paper Grade 1 and Grade 42 was studied to evaluate the color change of metal complexes at the same conditions. PAN was added onto hydrophilic zones, followed by metal ions solution at pH 5. These results demonstrated that the color change of metal complexes on the paper Grade 1 was not significantly different from the paper Grade 42 by naked-eye as shown in **Figure 4.7**. Therefore, the paper Grade 1 was chosen for further study due to low cost.

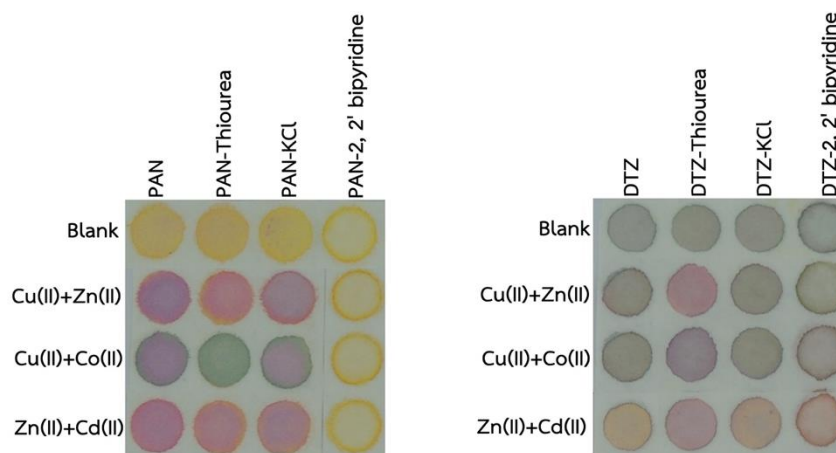


Figure 4.7 Color changes of PAN-metal complexes on device type A.

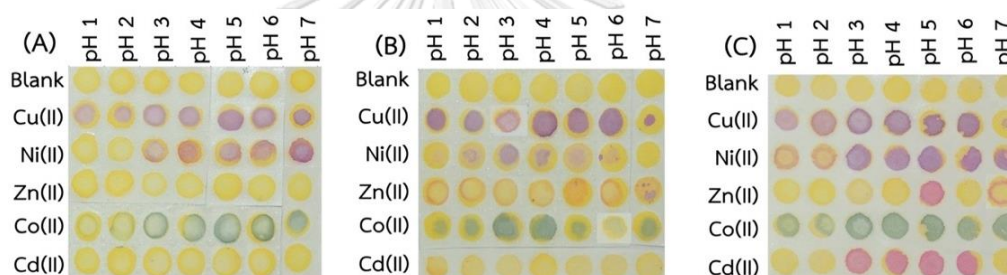
#### - Type of masking agent

As a basis concept of metal complexes formation, the most of complexing agents require the selectivity. Therefore, masking agents were used to mask interfering ions to obtain selective target metal ion detection. Thiourea, KCl, and 2, 2' bipyridine were used to mask Cu(II), Ni(II), and Zn(II), respectively<sup>76, 83</sup>. These masking agents were conducted to study interfering ions effect using a mixture of two metal ions solution (pH 5). For PAN as a complexing agent, the color response on device changed from yellow (PAN) to purple, purple, and pink for a mixture solution of Cu(II)+Zn(II), Cu(II)+Co(II), and Zn(II)+Cd(II), respectively. After adding thiourea as masking agent, the color responses on device were pink, green, and pink for a mixture of two metal ions solution of Cu(II)+Zn(II), Cu(II)+Co(II), and Zn(II)+Cd(II), respectively, indicating that thiourea efficiently masked Cu(II) under this condition as illustrated in **Figure 4.8 (left)**. After adding 2, 2' bipyridine, color response on device changed from purple, purple, and pink to yellow for all metal ions while the addition of KCl showed the same color response as the case without masking agent. These results indicated that 2, 2' bipyridine efficiently masked Cu(II), Co(II), and Zn(II) while KCl was not. For DTZ as a complexing agent in **Figure 4.8 (right)**, the color response on device was evaluated and explained similar with PAN as a complexing agent for thiourea while 2, 2' bipyridine and KCl efficiently masked Cu(II), Co(II), and Zn(II). Therefore, thiourea (1 M) was used to mask Cu(II) for further study.

In addition, tartaric acid, sodium citrate, and sodium sulphate were studied to evaluate the efficiency of masking agents at pH 1-7 by using PAN as a complexing agent. **Figure 4.9** demonstrated that tartaric acid masked Zn(II) and Cd(II) and sodium citrate masked Cd(II) at pH 1-7.



**Figure 4.8** Color changes of PAN-masking agent-metal complexes (left) and DTZ-masking agent-metal complexes (right) on device type A at pH 5.



**Figure 4.9** Color changes of (A) PAN-tartaric acid-metal complexes, (B) PAN-sodium citrate-metal complexes, and (C) PAN-sodium sulphate-metal complexes on device type A at pH 1-7.

#### - Reaction time

As the color change of metal complexes on device, this work focused on Cu(II), Co(II), Zn(II) detection by using PAN as a complexing agent and Cd(II) or Pb(II) detection by using DTZ as a complexing agent. The color responses of Zn(II) and Cd(II) complexes on the device type A were selected to study because they were representative of metal complex by using PAN and DTZ as complexing agents.

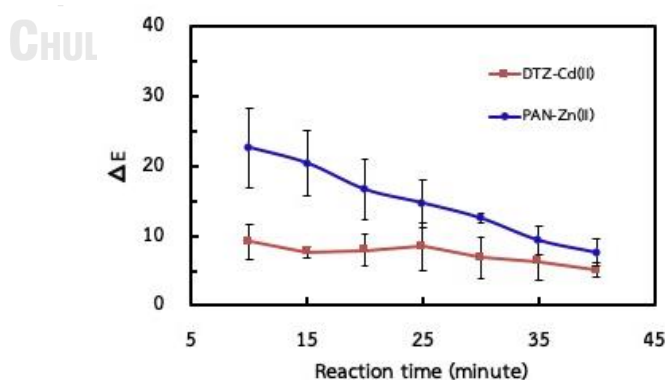
The spectrophotometer color i5 is a standard instrument used to measure the colorimetric values ( $L^*$ ,  $a^*$ ,  $b^*$ ). The  $L^*$ ,  $a^*$ , and  $b^*$  values are the lightness, red/green coordinate, and yellow/blue coordinate, respectively<sup>84</sup>. The color differences between each metal complex and blank were calculated using the

colorimetric values at 10-40 minutes. The CIE  $L^* a^* b^*$  coordinates are defined by the Commission Internationale de l'Eclairage (CIE) <sup>85</sup>. The total color difference ( $\Delta E^*$ ) is calculated following this equation <sup>85</sup>. The total color difference ( $\Delta E^*$ ) is always positive.

$$\Delta E_{ab}^* = \sqrt{(L_2^* - L_1^*)^2 + (a_2^* - a_1^*)^2 + (b_2^* - b_1^*)^2} \quad (4.1)$$

When  $L_2^*$  is  $L_{\text{metal-complex}}^*$ ,  $L_1^*$  is  $L_{\text{blank}}^*$ ,  $a_2^*$  is  $a_{\text{metal-complex}}^*$ ,  $a_1^*$  is  $a_{\text{blank}}^*$ ,  $b_2^*$  is  $b_{\text{metal-complex}}^*$ ,  $b_1^*$  is  $b_{\text{blank}}^*$ .  $L_{\text{metal-complex}(2)}^*$  minus  $L_{\text{blank}(1)}^*$  is the difference in lightness and darkness (positive is lighter and negative is darker).  $a_{\text{metal-complex}(2)}^*$  minus  $a_{\text{blank}(1)}^*$  is the difference in red and green (positive is redder and negative is greener).  $b_{\text{metal-complex}(2)}^*$  minus  $b_{\text{blank}(1)}^*$  is the difference in yellow and blue (positive is yellower and negative is bluer).

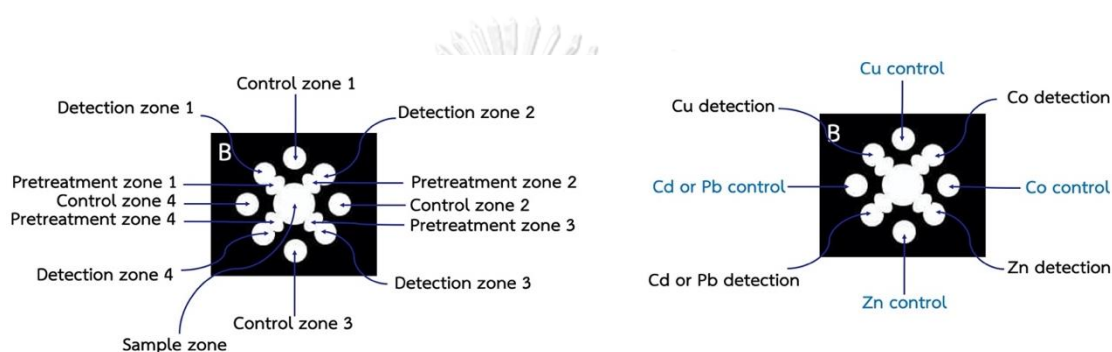
The results in **Figure 4.10** showed that total color difference ( $\Delta E^*$ ) was not significantly different at the reaction time of 10-15 minutes for Zn(II) complex and  $\Delta E^*$  of Cd(II) complex was not significantly different at the reaction time of 10-40 minutes. Therefore, the optimal reaction time of 15 minutes was used for simultaneous Cu(II), Co(II), Zn(II), Cd(II)/Pb(II) detection.



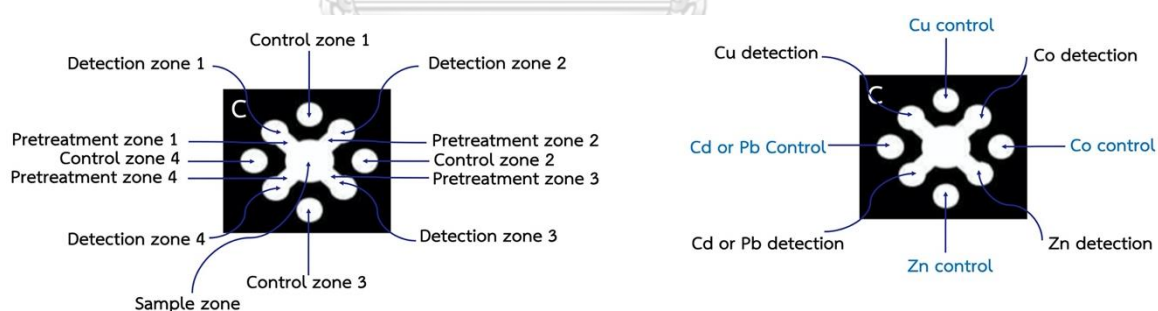
**Figure 4.10** Effect of reaction time on the color response of Zn(II) and Cd(II) complexes on device type A.

#### 4.2.3 Simultaneous detection for four metal ions by naked-eye on paper-based device type B and C

As the results for preliminary study on device type A, Cu(II), Co(II), Zn(II), Cd(II)/Pb(II) were attracted for simultaneous detection using PAN and DTZ as complexing agents. The device type B and type C are similar structure except the pattern of the pretreatment zone. The design components of device type B and C for simultaneous Cu(II), Co(II), Zn(II), Cd(II)/Pb(II) detection are shown in **Figure 4.11** and **Figure 4.12**, respectively.



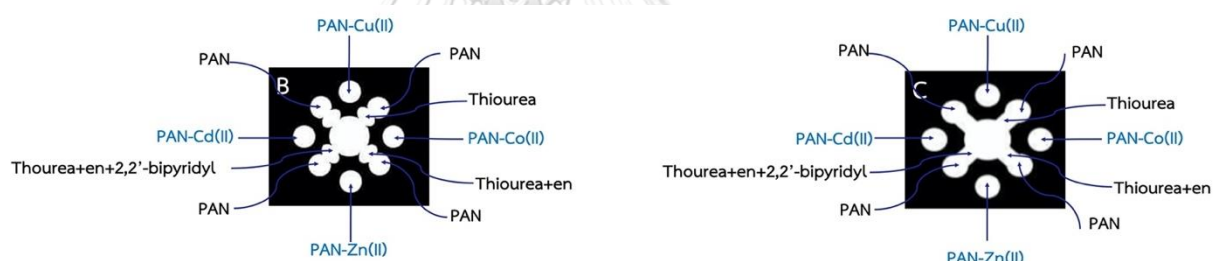
**Figure 4.11** The design components for simultaneous Cu(II), Co(II), Zn(II), Cd(II)/Pb(II) detection on device type B.



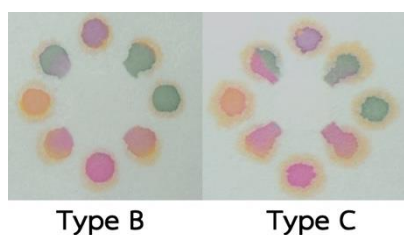
**Figure 4.12** The design components for simultaneous Cu(II), Co(II), Zn(II), Cd(II)/Pb(II) detection on device type C.

For simultaneous Cu(II), Co(II), Zn(II), Cd(II)/Pb(II) detection on device types B and C, complexing agent and masking agent for each metal ion detection were added onto the detection zones and the pretreatment zones as shown in **Figure 4.13**. A mixture solution of four metal ions (pH 5) was added onto the sample zone.

From **Figure 4.14**, PAN formed the purple complex with Cu(II) without masking agent on the detection zone 1. For Co(II) detection, thiourea was added onto the pretreatment zone to mask Cu(II) and PAN formed the green complex with Co(II) on the detection zone 2. For Zn(II) detection, a solution of thiourea/en was added onto the pretreatment zone to mask Cu(II) and Co(II)<sup>36, 86, 87</sup>. Ethylenediamine was used to mask Cu(II) and Co(II) in this condition<sup>86, 87</sup>. PAN formed the pink complex with Zn(II) on the detection zone 3. For Cd(II)/Pb(II) detection, a solution of thiourea/en were added onto the pretreatment zone to mask Cu(II), Co(II), followed by 2, 2' bipyridine to mask Cu(II), Co(II), and Zn(II). PAN formed an orange complex with Cd(II)/Pb(II) on the detection zone 4. The efficiency of 2, 2' bipyridine to mask Zn(II) was decreased by the addition of 2, 2' bipyridine and thiourea/en onto the same pretreatment zone. Therefore, the pink Zn(II)-PAN complex still appeared on the detection zone 4.



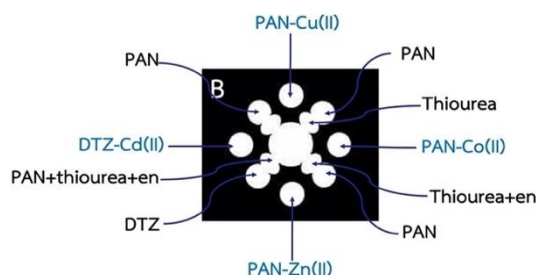
**Figure 4.13** Type of complexing agents and masking agents on device type B and C for simultaneous Cu(II), Co(II), Zn(II), Cd(II) detection.



**Figure 4.14** Color changes of metal complexes at pH 5 on device type B and C for simultaneous Cu(II), Co(II), Zn(II), Cd(II) detection.

As the previous results on device types B and C under the same conditions, the color response of Cd(II)-PAN complex was interfered with the pink Zn(II)-PAN complex the detection zone 4 (device type B and C). The color response on device type B showed higher selectivity than device type C for simultaneous Cu(II), Co(II), and Zn(II) detection 1, 2, and 3 zone, respectively. The device design type B consisted of the pretreatment zone (circle type) which could hold metal ion to react with masking agent for elimination of interfering ions more than the pretreatment zone (channel type) on device type C. Therefore, device type B was selected to optimize and improve the selectivity of Cd(II)/Pb(II) detection for further study. The complexing agent and masking agent for each metal ion detection were added onto detection zones and pretreatment zones as shown in **Figure 4.15**. DTZ was used as a complexing agent for Cd(II)/Pb(II) detection and PAN was used as a masking agent for Zn(II). A mixture solution of four metal ions (pH 5) was added onto the sample zone. As shown in **Figure 4.16**, PAN formed the purple complex with Cu(II) without masking agent on the detection zone 1. For Co(II) detection, thiourea was added onto the pretreatment zone to mask Cu(II) and PAN formed the green complex with Co(II) on the detection zone 2. For Zn(II) detection, a solution of thiourea/en was added onto the pretreatment zone to mask Cu(II) and Co(II) and PAN formed the pink color complex with Zn(II) on the detection zone 3. For Cd(II)/Pb(II) detection, a solution of thiourea/en and PAN were added onto the pretreatment zone to mask Cu(II), Co(II), and Zn(II). PAN masked Zn(II) by forming the pink complex on the pretreatment zone and DTZ formed the pink colored complex with Cd(II)/Pb(II) on the detection zone 4. The color responses on the detection zone 1, 2, and 3 were obviously observed for Cu(II), Co(II), Zn(II) detection, respectively. For Cd(II) detection, PAN masked Zn(II) by forming the pink complex on the pretreatment zone which impacted on identification the pink Cd(II) complex on the detection zone 4. The device design type B consisted of pretreatment zone (circle type) connected to the detection zone, the pretreatment zone showed small area and distance which limited time for the reaction between metal ion and masking agent. Therefore, the device type D was developed by extending the distance on pretreatment zone to increase time

consuming for the reaction between metal ion and masking agent and by increasing size of the detection zone.



**Figure 4.15** Complexing agents and masking agents on device types B for simultaneous Cu(II), Co(II), Zn(II), Cd(II) detection.

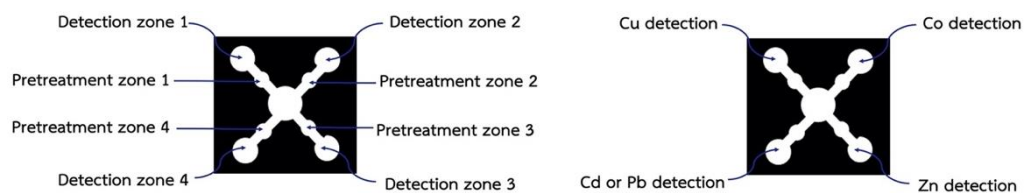


**Figure 4.16** Color changes of metal complexes at pH 5 on device type B for simultaneous Cu(II), Co(II), Zn(II), Cd(II) detection.

#### 4.2.4 Simultaneous detection for four metal ions by naked-eye on paper-based device type D

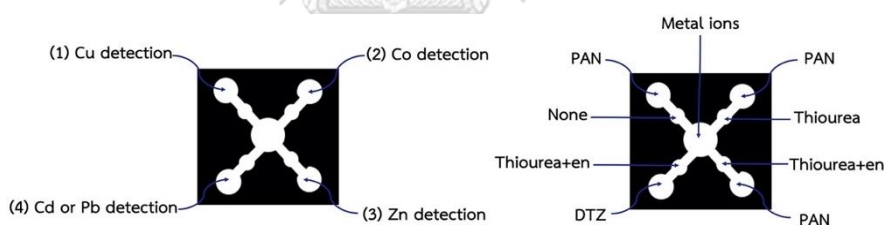
To improve the color response of metal complexes on device types B, the device type D in **Figure 4.17** was developed based on the design type B by increasing (1) distance of pretreatment zone to increasing time consuming for the reaction between metal ion and masking agent and (2) size of detection zone to easy observe the color response by naked-eye. In addition, there was no control zone on the device type D because the color response on the detection zone was developed based on the amount of metal ion flowed and reacted with complexing agent. The amount of metal ion reacted with complexing agent on the detection zone was different the control zone. Therefore, the color response on the detection zone could not compare with the control zone.





**Figure 4.17** The design components for simultaneous Cu(II), Co(II), Zn(II), Cd(II)/Pb(II) detection on device type D.

Complexing agent and masking agent for each metal ion detection were added onto the detection zones and pretreatment zones on device type D as illustrated in **Figure 4.18**. As the previous results of DTZ-thiourea-metal complexes on the device type A by adding a mixture solution of Zn(II)+Cd(II), an orange Cd(II)-DTZ complex still appeared indicating that Cd(II) formed more stable complex with DTZ than Zn(II)-DTZ ( $\log K_2$ : Cd(II)-DTZ = 15.10, Zn(II)-DTZ = 13.96<sup>76</sup>). Therefore, masking agent for Zn(II) on the pretreatment zone 4 to detect Cd(II) or Pb(II) did not need.



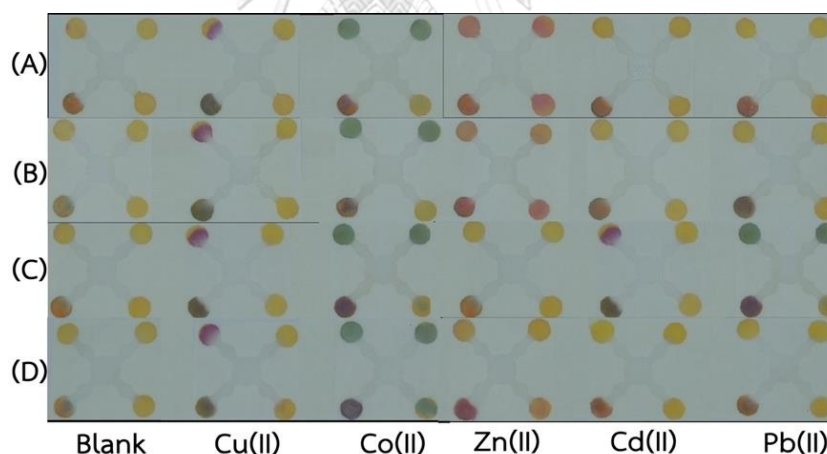
**Figure 4.18** Type of complexing agents and masking agents on device type D for simultaneous Cu(II), Co(II), Zn(II), Cd(II)/Pb(II) detection.

#### 4.2.4.1 Optimization conditions

##### - Acetate buffer concentrations (pH 5)

Acetate buffer (pH 5) was used to prepare metal ion solutions. To study the effect of acetate buffer concentrations on the color response of metal complexes, metal ion solutions (Cu(II), Co(II), Zn(II), Cd(II), or Pb(II)) were prepared in acetate buffer at various concentrations (1-5 M). As in **Figure 4.19**, PAN formed the purple complex with Cu(II) without masking agent on the detection zone 1. For Co(II) detection, thiourea was added onto the pretreatment zone to mask Cu(II) and PAN

formed the green complex with Co(II) on the detection zone 2. For Zn(II) detection, a solution of thiourea/en was added onto the pretreatment zone to mask Cu(II) and Co(II) and PAN formed the pink complex with Zn(II) on the detection zone 3. For Cd(II)/Pb(II) detection, a solution of thiourea/en was added onto the pretreatment zone to mask Cu(II), and Co(II). DTZ formed an orange Cd(II) complex or the purple Pb(II) complex on the detection zone 4. The color responses of all metal complexes on the device showed similar results for 1-5 M acetate buffer but the color responses of Cd(II)-DTZ was obviously different from Pb(II)-DTZ for 2 M acetate buffer. 1 M acetate buffer, the color response between Cd(II) and Pb(II) complexes on the detection zone 4 was not different. 3-5 M of acetate buffer, the green Co(II) complex still appeared on the detection zone 3 because en in acidic buffer was probably protonated resulting in incomplete mask Co(II). Therefore, acetate buffer (2 M, pH 5) was used as the optimal buffer concentration to prepare metal ion solution for the further study.

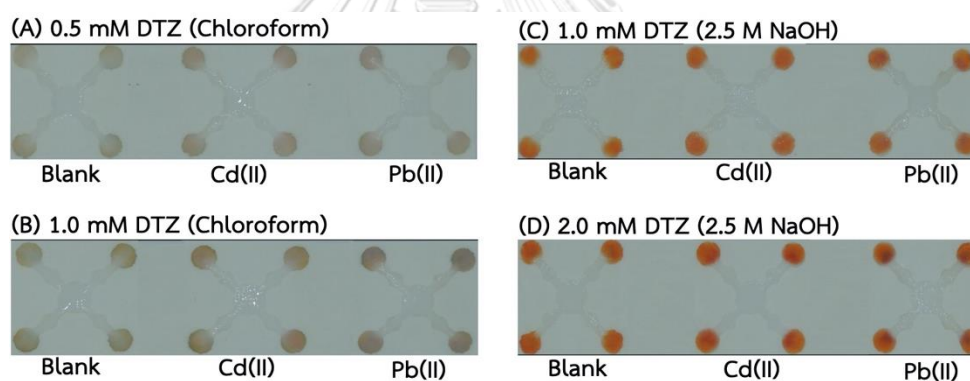


**Figure 4.19** Effect of acetate buffer concentrations (A) 1 M, (B) 2 M, (C) 3 M, (D) 5 M at pH 5 on color response of Cu(II), Co(II), Zn(II), Cd(II), and Pb(II) complexes on device type D.

#### - Solvent and concentration of complexing agent

As the results from the effect of acetate buffer concentration, the purple Cu(II)-PA, green Co(II), and pink Zn(II) complexes with PAN dissolved in ethanol were obvious observed by naked-eye. The color response of Cd(II) and Pb(II) complexes

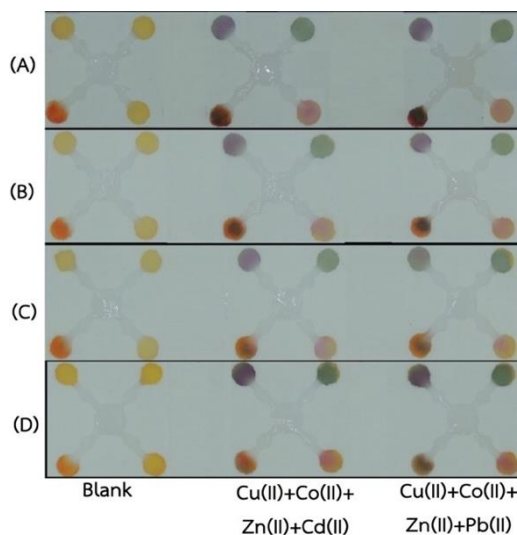
was not clearly different by using DTZ dissolved in chloroform. To improve the color response of Cd(II) and Pb(II) complexes, 0.5-2 mM DTZ dissolved in chloroform and 2.5 M NaOH were studied<sup>61</sup>. DTZ can be dissolved in chloroform given green solution<sup>88</sup> and 2.5 M NaOH given orange solution<sup>61</sup>. For Cd(II)/Pb(II) detection, DTZ (0.5-2 M) was added onto four detection zones, followed by a solution of thiourea/en onto four pretreatment zones. Cd(II) or Pb(II) solution was added onto the sample zone. The results indicated that the color response between Cd(II) and Pb(II) complexes was not clearly different from blank by dissolving DTZ in chloroform (**Figure 4.20A** and **Figure 4.20B**). Whereas, the color response between red Cd(II) and Pb(II) complexes was slightly different from blank by dissolving 2 mM DTZ in 2.5 M NaOH as shown in **Figure 4.20D**. Therefore, NaOH solution was selected solvent as DTZ for the further study.



**Figure 4.20** Effect of DTZ solvent and concentration on the color responses of Cd(II) and Pb(II) complexes on device type D.

As the previous results, NaOH was selected as DTZ solvent. DTZ formed red complex with Cd(II) and Pb(II) while blank showed an orange color on the device. At high concentration of NaOH, the color response of blank (orange) was also high which impacted on the red complex with Cd(II) and Pb(II). Therefore, the effect of NaOH concentration (0.1-2.5 M) on the color response of Cd(II) and Pb(II) complexes was studied. For Cu(II), Co(II), and Zn(II) detection, the optimal reagents for each metal ion detection were added on detection zone and pretreatment zone 1, 2, and 3, respectively. For Cd(II)/Pb(II) detection, a solution of thiourea/en was added onto

the pretreatment zone to mask Cu(II), and Co(II). DTZ formed the red Cd(II) complex or the purple Pb(II) complex on the detection zone 4 by using 0.1 M NaOH as DTZ solvent. The results indicated that the color response of the red Cd(II) complex was clearly different from the purple Pb(II) complex as shown in **Figure 4.21**.



**Figure 4.21** Effect of NaOH concentration as DTZ solvent (A) 2.5 M, (B) 2 M, (C) 1 M, (D) 0.1 M on the color response of Cd(II) and Pb(II) complexes on the detection zone 4 for simultaneous Cu(II), Co(II), Zn(II), Cd(II)/Pb(II) detection on device type D.

The complexing and masking agent preparations for metal ion detection on the device type D are concluded in **Table 4.1**.

**Table 4.1** The complexing and masking agent preparations for metal ion detection (50 mg/L) on the device type D.

Complexing and masking agents	Concentration	Solvent	Volume ( $\mu\text{L}$ )	
			Detection zone	Pretreatment zone
PAN	2 mM	Ethanol	1.0	-
DTZ	2 mM	NaOH (0.1 M)	5.0	-
Thiourea	1 M	Acetate buffer (2 M, pH 5)	-	3.0+3.0
Thiourea/en	1 M/3 M	Acetate buffer (2 M, pH 5)	-	3.0+3.0

The optimal conditions for simultaneous Cu(II), Co(II), Zn(II), Cd(II)/Pb(II) detection on the device type D are summarized in **Table 4.2**.

**Table 4.2** The optimal conditions for simultaneous Cu(II), Co(II), Zn(II), Cd(II)/Pb(II) detection on the device type D.

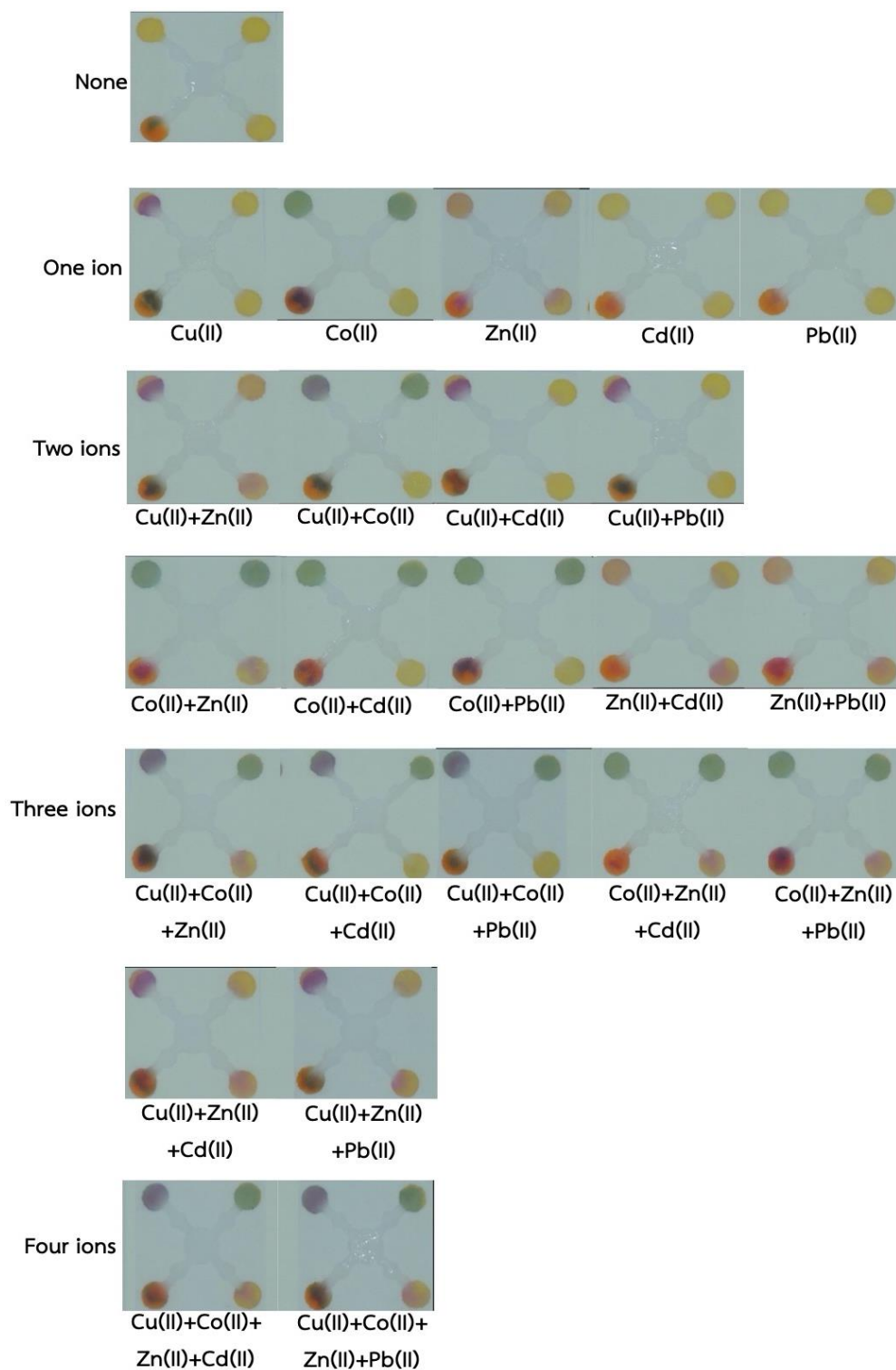
Metal ion detection	Detection zone	Pretreatment zone	
		Masking agent	Masked ion
Cu(II)	PAN	-	-
Co(II)	PAN	Thiourea	Cu(II)
Zn(II)	PAN	Thiourea/en	Cu(II), Co(II)
Cd(II)/Pb(II)	DTZ	Thiourea/en	Cu(II), Co(II)

#### 4.2.4.2 Application of simultaneous detection of four metal ions in synthetic unknown samples

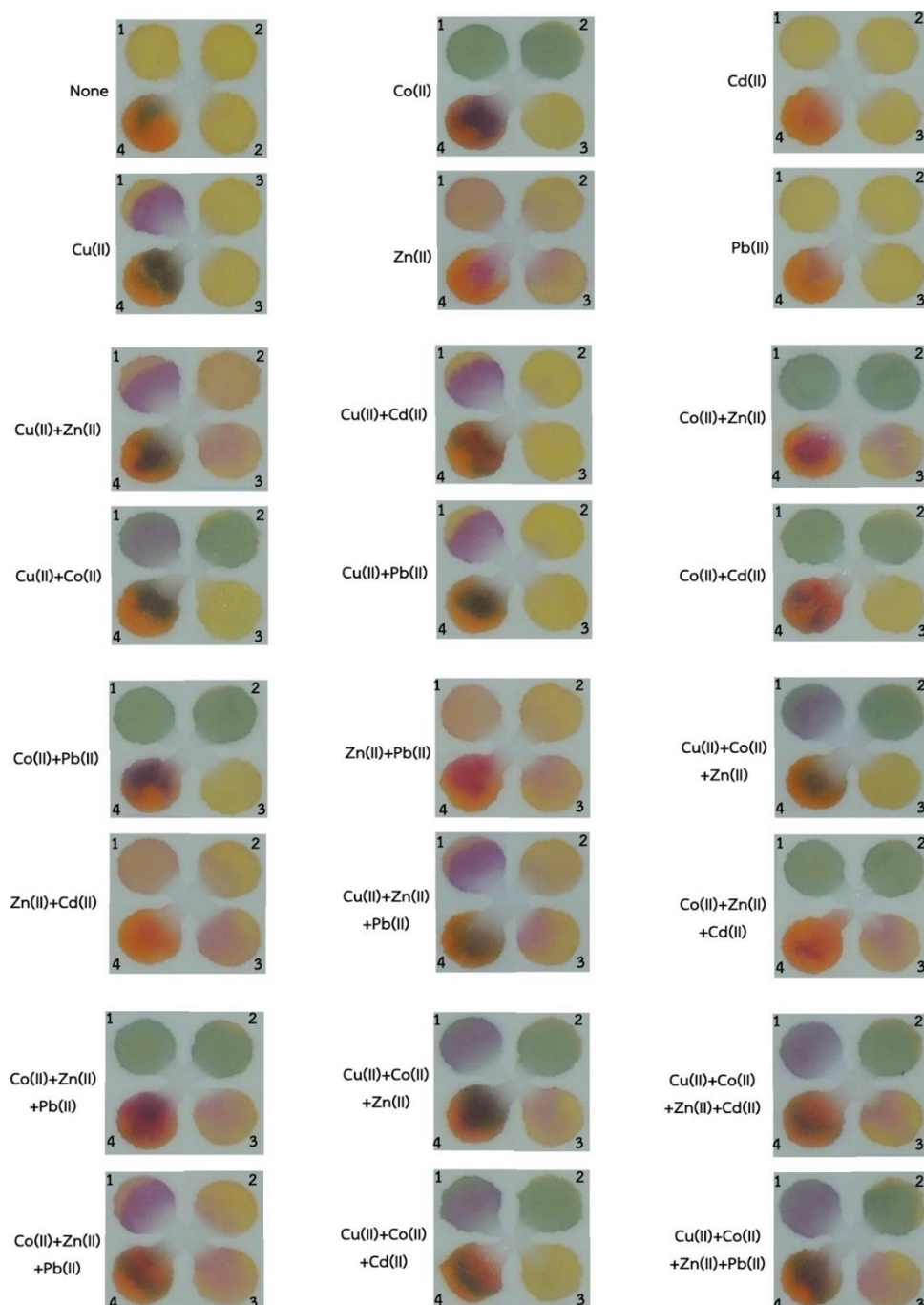
For simultaneous Cu(II), Co(II), Zn(II), Cd(II)/Pb(II) detection on one device, a solution of metal ions (pH 5) consisted of 24 types which was possibly mixed in this study. A solution of unknown sample was added onto the sample zone for simultaneous detection on one device. The color response of metal complexes is shown in **Figure 4.22**. The color response of metal complexes on the device was

recorded by using digital camera at the reaction time of 15 minutes. All images of the color response on the device were proceeded to generate the color chart by cropping each detection zone as illustrated in **Figure 4.23**. The pathway for simultaneous Cu(II), Co(II), Zn(II), Cd(II)/Pb(II) identification is shown in **Figure 4.24**.



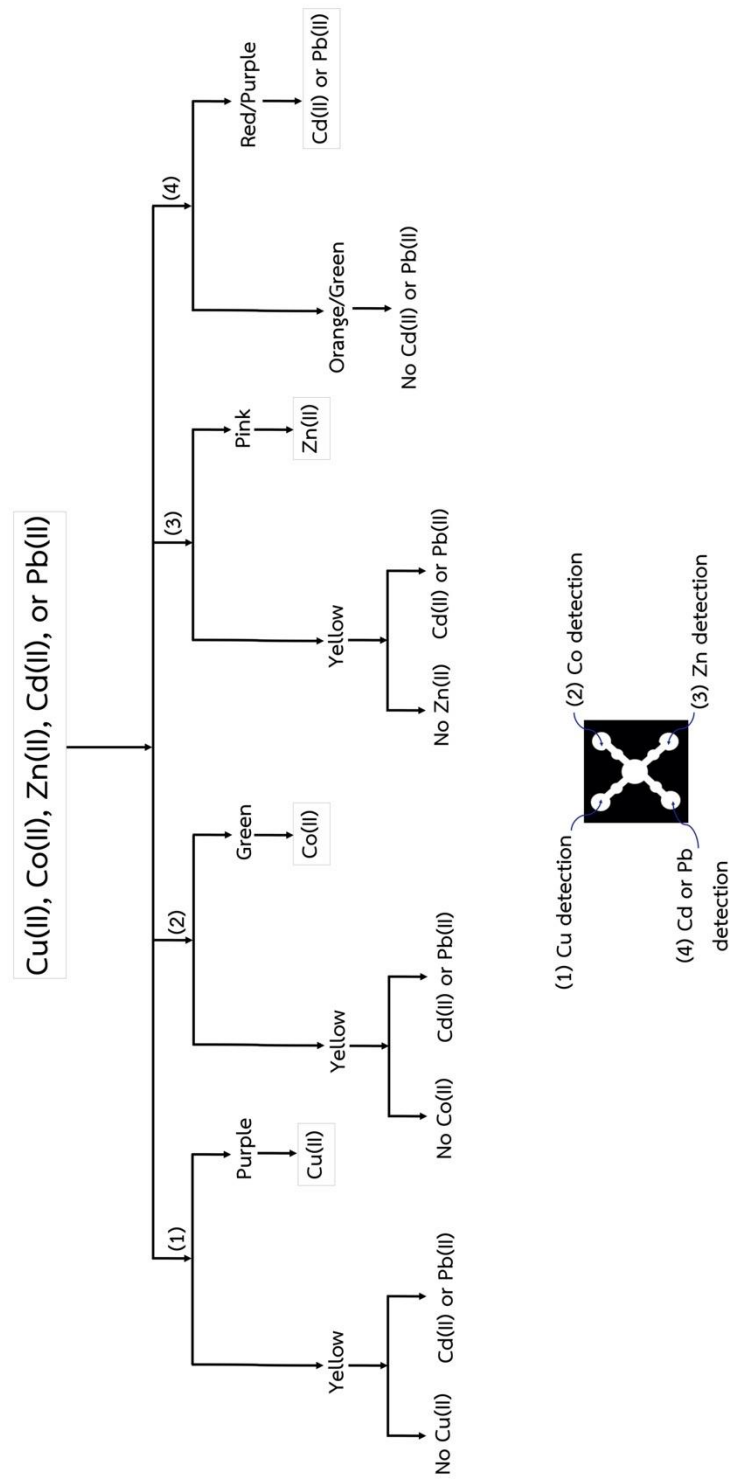


**Figure 4.22** Color changes of metal complexes (24 types) for simultaneous Cu(II), Co(II), Zn(II), Cd(II)/Pb(II) detection on device type D.



**Figure 4.23** Color chart of metal complexes (24 types) for simultaneous Cu(II), Co(II), Zn(II), Cd(II)/Pb(II) detection on device type D.





**Figure 4.24** Pathway for simultaneous Cu(II), Co(II), Zn(II), Cd(II)/Pb(II) identification on device type D.

To evaluate the accuracy of the proposed method by a researcher under optimal conditions, 24 types of the synthetic unknown water samples were prepared in 2 M acetate buffer at pH 5. The optimal reagents for each metal ion detection were added on 24 devices. Synthetic unknown water sample was added onto the sample zone. Each unknown sample was repeated detection with four replicate devices ( $n=4$ ,  $n$  was defined as the number of device) by a researcher. An image of the color response on the device was recorded using digital camera at the reaction time of 15 minutes. The identification of each metal ion in unknown samples was performed as follows: (1) the color response on the device was compared to the photograph of the color chart of metal complexes by naked-eye and (2) the color response of metal complexes on the device was compared to the color chart of metal complexes in computer display by naked-eye. For the comparison between the color response on the device and the photograph of the color chart, the process could be applied for on-site analysis. In addition, the comparison between the color response on the device and the color chart in computer display was observed because the color response of metal complex could fade over time. Briefly, the colors were purple (Cu(II)), green (Co(II)), or pink (Zn(II)) on the detection zone 1, 2, or 3, respectively. The color was the red Cd(II) or purple Pb(II) complex on the detection zone 4. The color response on the detection zone 4 depended on metal ion in unknown samples. The results showed that the accuracy and relative standard deviations (RSDs) were found in the range of 79.6-87.5% and 4.5% ( $n=4$ ) in comparison with photograph of the color chart. The accuracy and RSDs were evaluated in the range of 91.7-95.8% and 2.6% ( $n=4$ ) in comparison with the color chart in computer display. The accuracy was calculated following this equation, where  $X$  was the number of correct identifications.

$$\% \text{ Accuracy} = \frac{X}{24} \times 100 \quad (4.2)$$

The accuracy of the proposed method was also evaluated by ten students. 24 Types of the synthetic unknown water samples were prepared in 2 M acetate

buffer at pH 5 and labeled No.1-24 by a researcher. The students were briefly suggested about the experimental procedures and they performed to identify each unknown sample under optimal conditions. Each unknown sample was evaluated on one device. For metal ion identification, the results in **Table 4.3** show that the accuracy was found in the range of 41.7-87.5% (n=10) in comparison with photograph of the color chart. The accuracy was demonstrated in the range of 20.8-83.3% (n=10) in comparison with the color chart in computer display. The accuracy results from a researcher and students were different, the accuracy of students was lower than a researcher both in comparison with photograph of the color chart and with the color chart in computer display because some skill of the experimental procedures such as micropipette use was required.

**Table 4.3** The accuracy (student's results, n=10) for metal ion identification in 24 types of unknown samples.

Student number	%Accuracy	
	Photograph	Photograph via computer display
1	58.3	62.5
2	41.7	33.3
3	70.8	58.3
4	45.8	41.7
5	41.7	20.8
6	54.2	41.7
7	62.5	54.2
8	62.5	58.3
9	45.8	45.8
10	87.5	83.3

As the accuracies from ten students for metal ions identification (24 unknown samples), these results could be divided into three groups of unknown samples based on the accuracy. The accuracies were more than 70% (group 1), 50-69% (group 2), and less than 50% (group 3) in comparison with photograph of the color chart as shown in **Table 4.4** and in comparison with the color chart in computer display as shown **Table 4.5**. These results indicated that the color response was randomly error identified by naked-eye based on each observer. Therefore, metal ion identification of each group was different both in comparison with photograph of the color chart and in comparison with the color chart in computer display.

**Table 4.4** The summary of the accuracy for metal ion identification in comparison with photograph of the color chart.

Group	Metal ions identification	%Accuracy
1	Cu(II), Cd(II), Pb(II) Cu(II)+Cd(II), Co(II)+Cd(II) Cu(II)+Zn(II)+Pb(II), Cu(II)+Zn(II)+Cd(II) Co(II)+Co(II)+Cd(II), Cu(II)+Co(II)+Zn(II)+Cd(III)	$\geq 70$
2	None Cu(II)+Co(II), Cu(II)+Pb(II), Zn(II)+Cd(II), Zn(II)+Pb(II), Co(II)+Pb(II) Co(II)+Zn(II)+Pb(II), Co(II)+Zn(II)+Cd(II), Cu(II)+Co(II)+Zn(II)+Pb(II)	50-69
3	Co(II), Zn(II) Cu(II)+Zn(II), Co(II)+Zn(II) Cu(II)+Co(II)+Zn(II), Cu(II)+Co(II)+Pb(II)	$< 50$

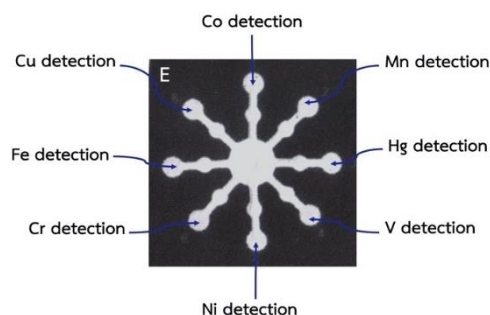
**Table 4.5** The summary of the accuracy for metal ion identification in comparison with the color chart in computer display.

Group	Metal ions identification	%Accuracy
1	None Cu(II)+Co(II), Cu(II)+Cd(II), Zn(II)+Cd(II), Zn(II)+Pb(II)	$\geq 70$
2	Cu(II), Pb(II) Co(II)+Zn(II), Co(II)+Cd(II), Co(II)+Pb(II), Cu(II)+Pb(II) Cu(II)+Co(II)+Zn(II), Cu(II)+Co(II)+Cd(II), Cu(II)+Co(II)+Zn(II)+Pb(II)	50-69
3	Co(II), Zn(II) Cu(II)+Pb(II), Cu(II)+Zn(II) Co(II)+Zn(II)+Cd(II), Co(II)+Zn(II)+Pb(II), Cu(II)+Zn(II)+Cd(II) Cu(II)+Co(II)+Zn(II)+Cd(II)	$< 50$

### 4.3 Metal complex study on paper-based analytical device: wax printing method

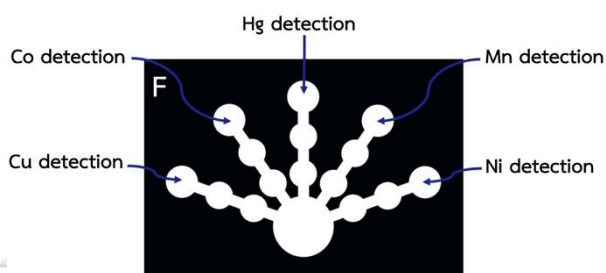
#### 4.3.1 Device design and fabrication method: device type E and F

The device type E was designed and fabricated based on device type D by increasing the number of detection zone and pretreatment zone for simultaneous Cu(II), Co(II), Hg(II), Ni(II), Fe(III), Cr(VI), V(III), and Mn(II) detection. The design components of device type E are shown in **Figure 4.25**.



**Figure 4.25** The design components of device type E for simultaneous detection of eight metal ions.

The device type F was designed to improve the selectivity for simultaneous Cu(II), Co(II), Hg(II), Ni(II), and Mn(II) detection by adding area of the pretreatment zone which was used to (1) increase the area for loading masking agents to eliminate interfering ions, (2) decrease strongly basic effect of ethylenediamine at pH 12.2 (WHO, 1991) as a masking agent by loading en separated zone from other masking agent. The design components of device type F are illustrated in **Figure 4.26**.



**Figure 4.26** The design components of device type F for simultaneous detection of five metal ions.

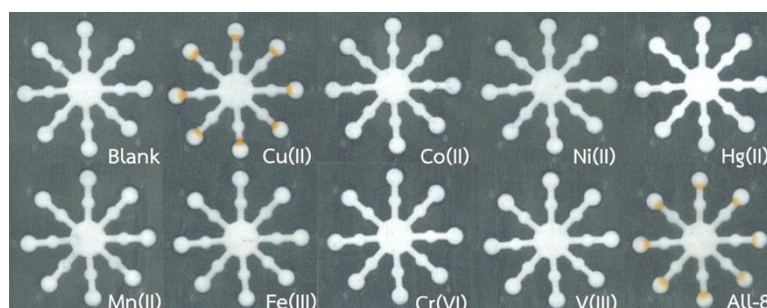
### 4.3.2 Metal complexes study on paper-based analytical device type E

#### 4.3.2.1 Optimization conditions

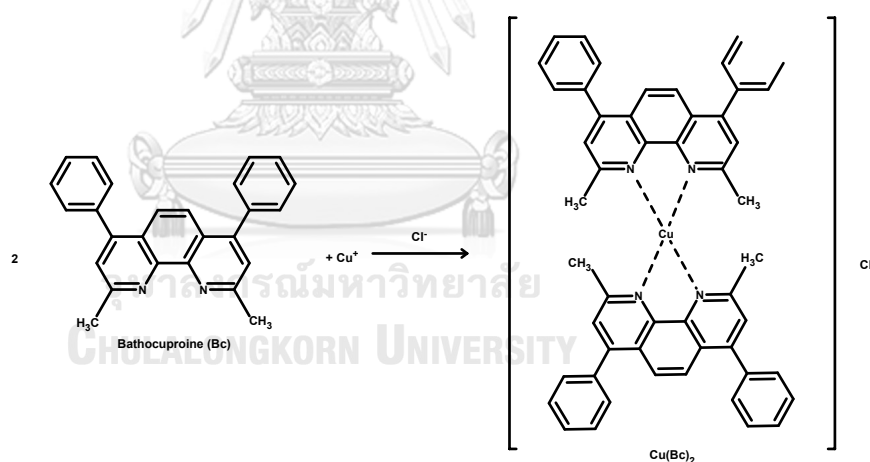
##### - Types of complexing agent and masking agent

As the color response of the purple Cu(II)-PAN and Ni(II)-PAN complexes on the device type A, the purple Ni(II)-PAN complex interfered with the Cu(II) detection by using PAN as a complexing agent. Therefore, bathocuproine (Bc) is attracted to use as a complexing agent because Bc is applied for colorimetric detection of Cu(II) in the standard method<sup>62</sup>. Hydroxylamine hydrochloride (0.5 g/mL) was added onto the detection zone to (1) reduce Cu(II) to Cu(I), and (2) mask Zn(II), Co(II), Cd(II) interferences<sup>62</sup>, followed by CH<sub>3</sub>COOH/NaCl buffer (10 mM, pH 4.6) to adjust the pH. Cu(Bc)<sub>2</sub> Complex was stabilized with the Cl<sup>-</sup> anion<sup>62</sup>. Bc (10 mM/PEG 400 (80 mg/mL) solution was added on the detection zone. As the hydrophobicity of Bc, it obstructed aqueous solution flowing into the detection zone. To solve this problem, PEG 400 (80 mg/mL) as a hydrophilic substance was mixed into Bc solution to improve this property. NaF (0.5 M) was added onto the pretreatment zone to mask Fe(III) and

Co(II) <sup>89</sup>. Each metal ion solution and **All-8** were added onto the sample zone. Bc reacted with Cu(I) to form an orange  $\text{Cu}(\text{Bc})_2$  complex <sup>62</sup>. The results demonstrated that the an orange **(All-8)-Bc** complex was similar to an orange  $\text{Cu}(\text{Bc})_2$  complex as shown in **Figure 4.27**. The Cu(II)-Bc reaction is shown in **Figure 4.28**. Therefore, Bc was selected as a complexing agent for Cu(II) detection.



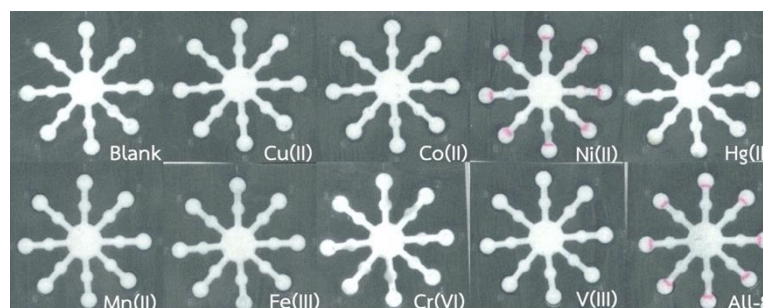
**Figure 4.27** Color changes of metal-BC complexes on the device type E for Cu(II) detection.



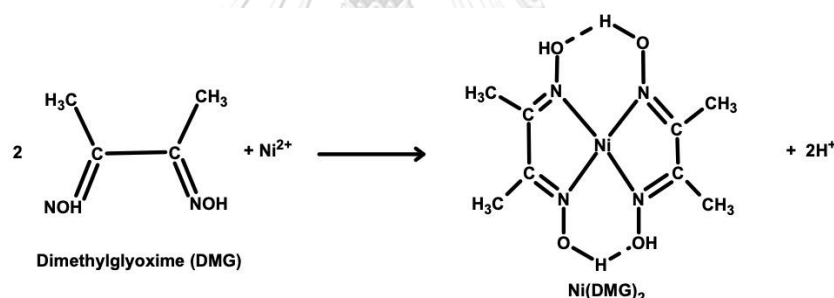
**Figure 4.28** Cu-Bathocuproine reaction.

Dimethylglyoxime (DMG) is a selective complexing agent which is applied for Ni(II) colorimetric detection in the standard method. Hydroxylamine hydrochloride (0.5 g/mL) was added onto eight detection zones to mask Co(II), Zn(II), Cd(II) <sup>62</sup>. DMG (60 mM) was added onto eight detection zones followed by ammonium hydroxide (0.03 M, pH 9.5) to adjust the pH. NaF (0.5 M) and  $\text{CH}_3\text{COOH}$  (6.3 M) were added onto eight pretreatment zones to mask Fe(III) and Co(II) <sup>62</sup>. Each metal ion solution and

**All-8** were added onto the sample zone. The pink (**All-8**)-DMG complex was similar to the pink Ni(II)-DMG complex as shown in **Figure 4.29**. The Ni(II)-DMG reaction is shown in **Figure 4.30** <sup>62</sup>. Therefore, DMG was used as a complexing agent to detect Ni(II).



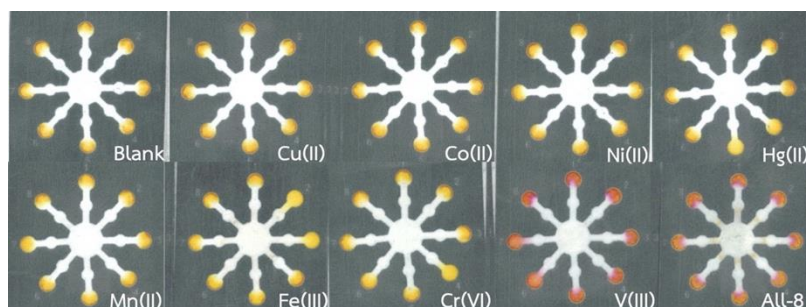
**Figure 4.29** Color changes of metal-DMG complexes on the device type E for Ni(II) detection.



**Figure 4.30** Ni-Dimethylglyoxime reaction.

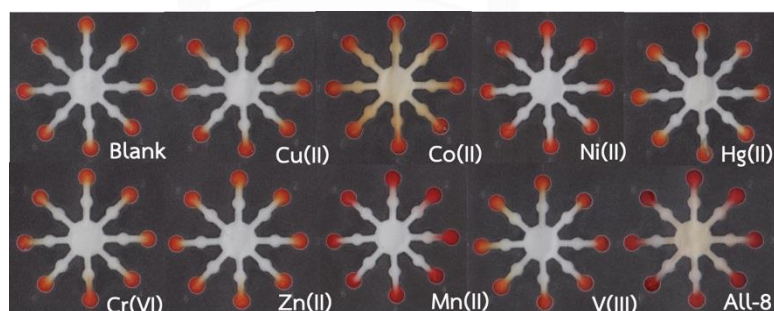
4-(2-Pyridylazo) resorcinol (PAR) formed color complexes with numerous metal ions. A solution of PAR (5 mM)/PDDA (5 %w/w) was added onto eight detection zones. PDDA was mixed into PAR solution to stabilize the metal PAR complexes and to prevent the reaction products flow into the edges of the detection zone <sup>39</sup>. DCTA (0.1 M) was added onto eight pretreatment zones to mask Cu(II), Co(II), Ni(II), Cr(VI), Mn(II), Pb(II), and Zn(II) <sup>78</sup>. Each metal ion solution and **All-8** were added onto the sample zone. An orange (**All-8**)-PAR complex was similar to an orange V(III)-PAR complex by naked-eye as shown in **Figure 4.31**. Therefore, PAR was selected for V(III) detection.





**Figure 4.31** Color changes of metal-PAR complexes on the device type E for V(III) detection.

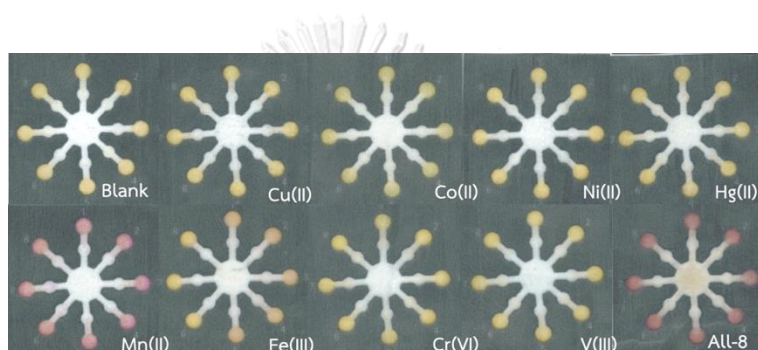
For Mn(II) detection, A solution of PAR (5 mM)/PDDA (5 %w/w) also added onto eight detection zones. Triethylenetetramine (0.1 M)/DMSA (0.1 M)/en (6 M) were added onto eight pretreatment zones. Triethylenetetramine was expected to mask Cu(II), Zn(II), Cd(II), Pb(II)<sup>81</sup> and en mask Cu(II), Ni(II), Zn(II), Cd(II), Pb(II)<sup>86, 87</sup>. DMSA was used to mask Co(II), Ni(II), Zn(II), Cd(II), Pb(II)<sup>39</sup>. Each metal ion solution and **All-8** were added onto the sample zone. These results showed that the red (**All-8**)-PAR complex was similar to the red Mn(II)-PAR complex shown in **Figure 4.32**. In addition, the red Mn(II)-PAR complex was not obviously different from blank by naked-eye.



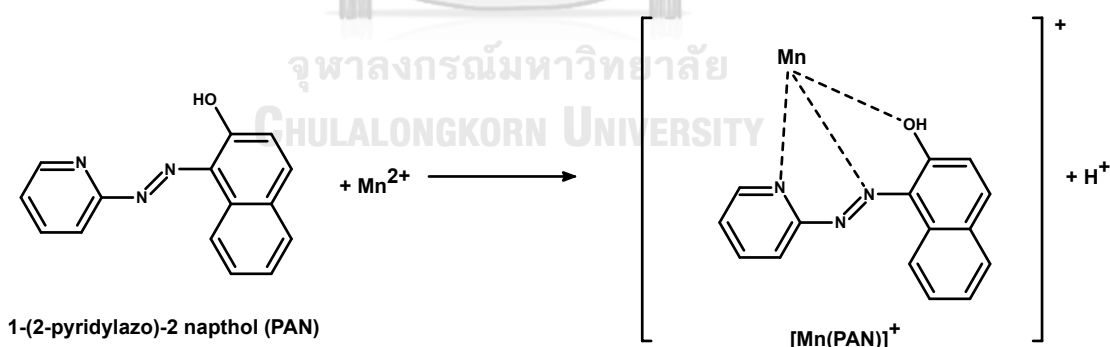
**Figure 4.32** Color changes of metal-PAR complexes on the device type E for Mn(II) detection.

As the previous results of Mn(II) detection by using PAR as a complexing agent, the red (**All-8**)-PAR complex was similar the red Mn(II)-PAR complex but the red Mn(II)-PAR complex was not obviously different from blank. Therefore, PAN as a

new complexing was selected to detect Mn(II). PAN (2 mM) was added onto eight detection zones. A solution of thiourea (1 M)/en (4 M)/KCN (0.1 M) were added onto eight pretreatment zones. Thiourea masked Cu(II), en masked Cu(II), Ni(II), Zn(II), Cd(II), Pb(II)<sup>86, 87</sup> and KCN masked Cu(II), Zn(II), Cd(II), Ni(II), Co(II) in this condition<sup>90</sup>. Each metal ion solution and **All-8** were added onto the sample zone. The pink (**All-8**)-PAN complex was similar to the pink Mn(II)-PAN complex as shown in **Figure 4.33**. The Mn(II)-PAN reaction is shown in **Figure 4.34**. Therefore, PAN was used to detect Mn(II).



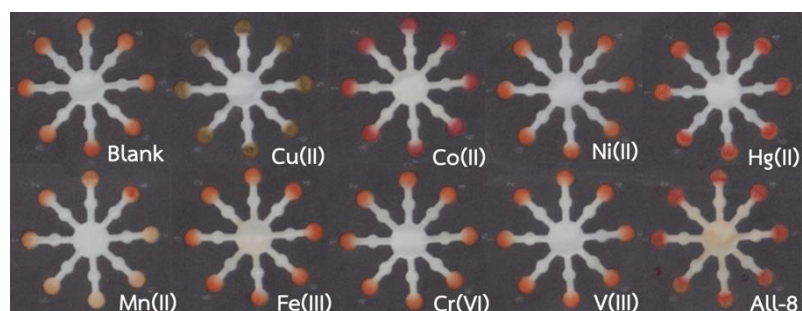
**Figure 4.33** Color changes of metal-PAN complexes on the device type E for Mn(II) detection.



**Figure 4.34** Mn-PAN reaction<sup>28</sup>.

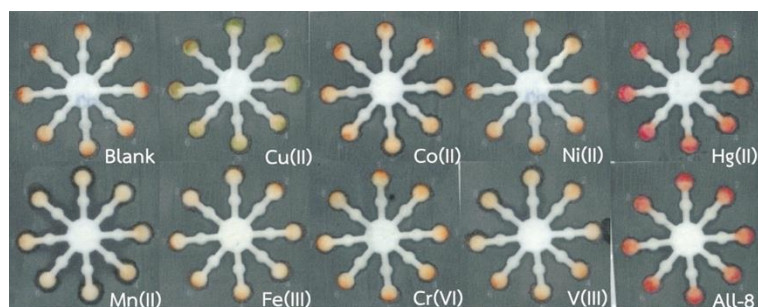
For Hg(II) detection, PEG 400 (80 mg/mL) was added onto eight detection zones to decrease the hydrophobicity of DTZ on the detection zone<sup>62</sup>. Ethylenediamine (2 M) was added onto eight pretreatment zones to mask Cu(II), Ni(II), Zn(II), Cd(II), Pb(II)<sup>86, 87</sup>. Masking agents on the pretreatment zone were allowed to dry

and then DTZ (2 mM) were added onto eight detection zones. Each metal ion solution and **All-8** were added onto the sample zone. The color response of **(All-8)**-DTZ complex was slightly similar to the red Hg(II)-DTZ complex as shown in **Figure 4.35**. In addition, Cu(II) and Co(II) also formed complexes with DTZ. For this assumption, the colored complexes of Cu(II) and Co(II) possibly interfered the red Hg(II)-DTZ complex.

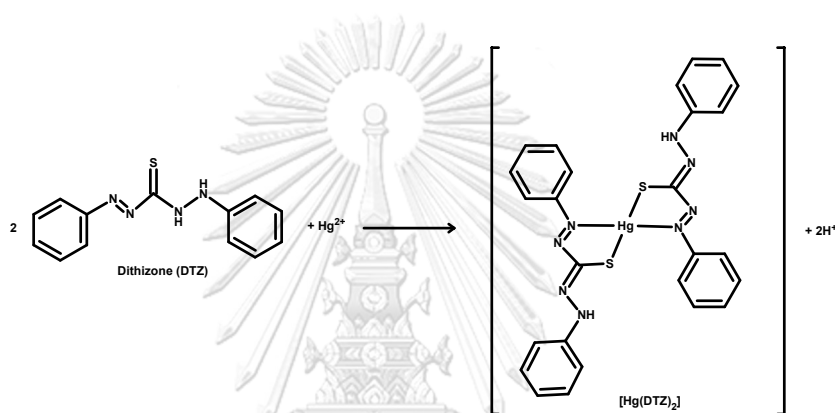


**Figure 4.35** Color changes of metal-DTZ complexes by using en as a making agent on the device type E for Hg(II) detection.

To improve the selectivity for Hg(II) detection by using DTZ as a complexing agent, PEG 400 (80 mg/mL) was added onto eight detection zones. DCTA (0.1 M) was added onto eight pretreatment zones to mask Cu(II), Co(II), Ni(II), Cr(VI), Mn(II), Pb(II), Zn(II) [49], KCN (0.1 M) to mask Cu(II), Zn(II), Cd(II), Ni(II), Co(II) <sup>78, 90</sup>, followed by en (10 M) to mask Cu(II), Ni(II), Zn(II), Cd(II), Pb(II) <sup>86, 87</sup>. Masking agents on the pretreatment zone were allowed to dry and then DTZ (2 mM) were added onto eight detection zones. Each metal ion solution and **All-8** were added onto the sample zone. The red **(All-8)**-DTZ complex was similar to the red Hg(II)-DTZ complex as shown in **Figure 4.36**. Therefore, DCTA, KCN, and en were selected as masking agents for Hg(II) detection. The Hg(II)-DTZ reaction is shown in **Figure 4.37**.

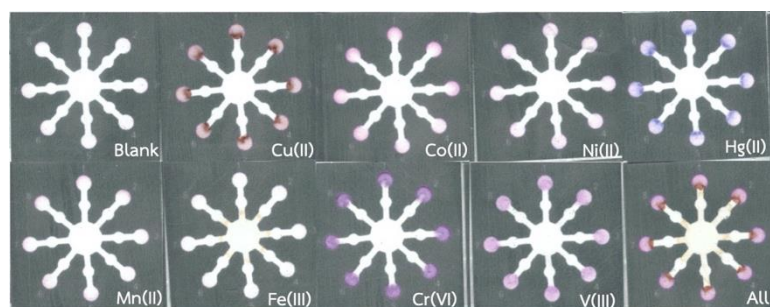


**Figure 4.36** Color changes of metal-DTZ complexes by using DCTA, KCN, and en as making agents on the device type E for Hg(II) detection.



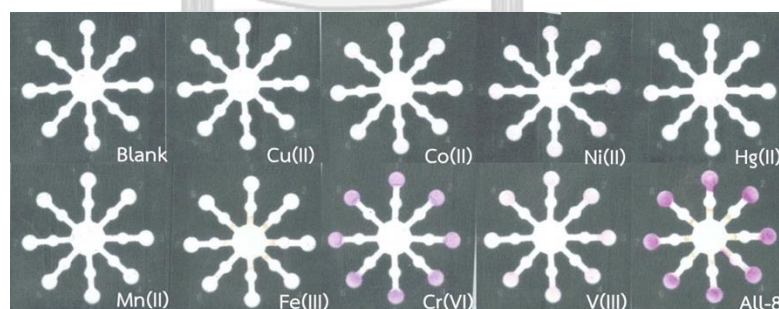
**Figure 4.37** Hg-Dithizone reaction <sup>80</sup>.

1,5-Diphenylcarbazide (DPC) is a sensitive complexing agent which is used to detect Cr(VI) in the standard method. DPC (0.2 %w/v) was added onto eight detection zones. Metal ion solutions were added onto the sample zone. Each metal ion solution and **All-8** were added onto the sample zone. The purple (**All-8**)-DPC complex was different from the purple complex of Cr(VI)-DPC as shown in **Figure 4.38**. In addition, Cu(II), Co(II), Ni(II), Hg(II), and V(III) also formed the pink or purple complexes with DPC. For this assumption, the color complexes of Cu(II), Co(II), Ni(II), Hg(II), and V(III) possibly interfered the purple Cr(VI)-DPC complex.

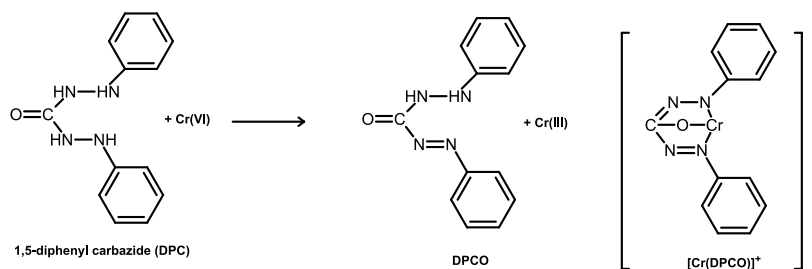


**Figure 4.38** Color changes of metal-DPC complexes on the device type E for Cr(VI) detection.

To improve the selectivity for Cr(VI) detection by using DPC as a complexing agent, DPC solution (0.2 %w/v) was added onto eight detection zones. Thiourea (1 M) was added onto eight pretreatment zones to mask Cu(II), followed by NaF (0.5 M) to mask Co(II) and Fe(III) interferences<sup>89</sup>. Each metal ion solution and **All-8** were added onto the sample zone. DPC formed the violet Cr(VI) complex under acidic conditions. The purple (**All-8**)-DPC complex was similar to the purple Cr(VI) complex as shown in **Figure 4.39**. Although V(III) also formed the pink color with DPC, the color response of (**All-8**)-DPC complex could be identified as the purple complex of Cr(VI). Therefore, DPC was used to detect Cr(VI). The Cr(VI)-DPC reaction is shown in **Figure 4.40**.

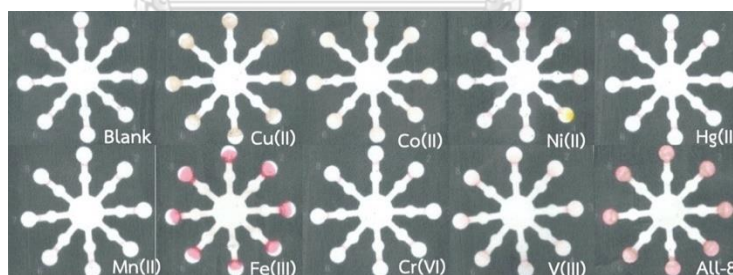


**Figure 4.39** Color changes of metal-DPC complexes by using thiourea and NaF as masking agents on the device type E for Cr(VI) detection.



**Figure 4.40** Cr-DPC reaction <sup>91</sup>.

Bathophenanthroline (Bphen) is a sensitive and selective complexing agent for Fe complex <sup>34</sup>. A solution of Bphen (10 mM)/acetate buffer (20 mM, pH 5.0)/L-ascorbic acid (0.05 M) was added onto eight detection zones. L-ascorbic acid (0.1 M) was added onto eight pretreatment zones to reduce Fe(III) to Fe(II) <sup>34</sup>. Each metal ion solution and **All-8** were added onto the sample zone. The color response of (**All-8**)-Bphen complex was similar to the pink Fe(II)-Bphen complex as shown in **Figure 4.41**. Although the brown Cu(II) complex were also appeared, the color response of (**All-8**)-Bphen complex could identified as the pink complex of Fe(II). Therefore, Bphen was selected for Fe(III) detection. The Fe(II)-Bphen reaction is shown in **Figure 4.42**.



**Figure 4.41** Color changes of metal-Bphen complexes on the device type E for Fe(III) detection.

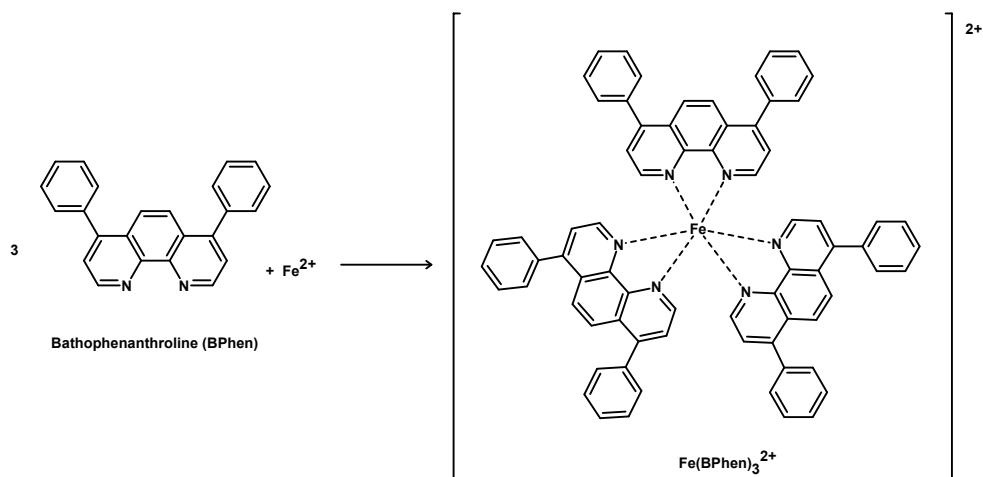
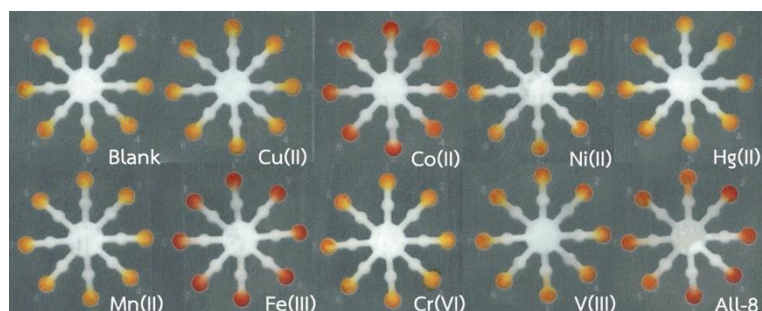
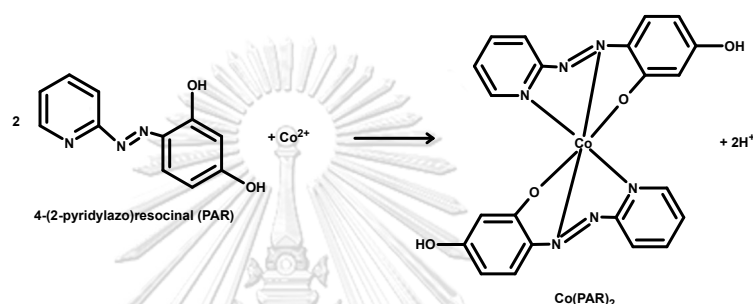


Figure 4.42 Fe-Bphen reaction <sup>34</sup>.

For Co(II) detection, PAR was selected as a complexing agent for Co(II) detection. The molar absorption coefficient for Co(II)-PAR is very high which could present lower detectable concentration of Co(II) <sup>74</sup>. A solution of PAR (5 mM)/PDDA (5 %w/w) onto eight detection zones. EDTA (0.2 M) were added onto eight pretreatment zones to mask Mn(II), Ni(II), Zn(II), Cd(II), Pb(II), Fe(III) <sup>39</sup>, triethylenetetramine (0.4 M) to mask Cu(II), Zn(II), Cd(II), Pb(II) <sup>39</sup>, followed by en (4.0 M) to mask Cu(II), Ni(II), Zn(II), Cd(II), Pb(II) <sup>86, 87</sup>. Each metal ion solution and **All-8** were added onto the sample zone. The red (**All-8**)-PAR complex was similar with the red Co(II)-PAR and Fe(III)-PAR complexes as shown in **Figure 4.43**. Although PAR formed both the red Co(II)-PAR and Fe(III)-PAR complexes, Co(II) formed colorless complex with Bphen for Fe(III) detection conditions. These results could be applied for simultaneous eight metal ions identification by using the red Co(II)-PAR and Fe(III)-PAR complexes compared to the color responses of Fe(III) detection conditions to identify red Co(II)-PAR or Fe(III)-PAR complex in Co(II) detection conditions. These conditions were successfully used in synthetic unknown water samples which consisted of Co(II) or Fe(III). Therefore, PAR was selected for Co(II) detection. The Co(II)-PAR reaction is shown in **Figure 4.44**.



**Figure 4.43** Color changes of metal-PAR complexes on the device type E for Co(II) detection.

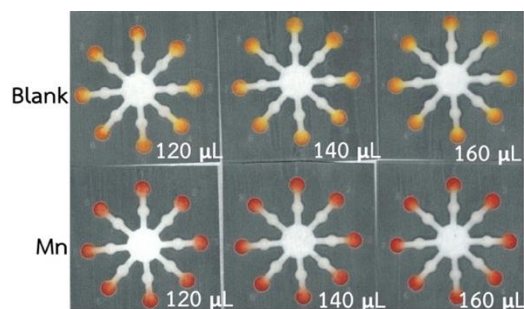


**Figure 4.44** Co-4-(2-Pyridylazo) resorcinol reaction <sup>39</sup>.

#### - Metal volume

Mn(II) conditions were chosen to study the effect metal volume (120.0-160.0  $\mu\text{L}$ ) on the color response of metal complexes because the viscosity of ethylenediamine on the pretreatment zone impacted on flowing of metal ion solution through the pretreatment zone into the detection zone. A solution of PAR (5.0 mM)/PDDA (5%w/w) was added onto eight detection zones. Thiourea (1 M), followed by en (8 M) were added onto eight pretreatment zones. Mn(II) solution (120.0-160.0  $\mu\text{L}$ ) was added onto the sample zone. The red complex of Mn(II)-PAR on the device at various volumes (120.0-160.0  $\mu\text{L}$ ) was slightly different as shown in **Figure 4.45**. Therefore, metal volume (140.0  $\mu\text{L}$ ) was used as optimum volume for further study. Moreover, the device was allowed to dry as soon as possible after the reaction time of 50 minutes. Then the color response on the device type E was recorded by using a scanner.





**Figure 4.45** Effect of metal ion volume (120.0-160.0  $\mu\text{L}$ ) on the color response for Mn(II) detection on the device type E.

The reagent preparations and optimal conditions for metal ion detection on the device type E are concluded in **Table 4.6**.



**Table 4.6** The reagent preparations and optimal conditions for metal ion detection on the device type E.

Detection	Reagents	Concentration	Solvent	Volume ( $\mu\text{L}$ )	
				Detection zone	Pretreatment zone
Cu(II)	Bc/PEG 400	10 mM/ 80 mg/L	Chloroform	1.0	-
	Hydroxylamine hydrochloride	0.5 g/mL	Milli-Q water	1.0+1.0+1.0	-
	CH <sub>3</sub> COOH/ NaCl buffer	10 mM, pH 4.6	Milli-Q water	1.0	-
	NaF	0.5 M	Milli-Q water	-	2.0+2.0+2.0+2.0
N(II)	DMG	60 mM	Methanol	0.5+0.5	-
	Hydroxylamine hydrochloride	0.5 g/mL	Milli-Q water	1.0+1.0+1.0+1.0	-
	NH <sub>4</sub> OH	0.03 M, pH 9.5	Milli-Q water	1.0+1.0	-
	NaF	0.5 M	Milli-Q water	-	2.0+2.0
	CH <sub>3</sub> COOH	6.3 M	Milli-Q water	-	2.0+2.0
V(III)	PAR/PDDA	5 mM/5 %w/w	0.1 M Borate buffer (pH 10)	1.0+1.0	-
	DCTA	0.1 M	NaOH (0.4 M)	-	2.0+2.0+2.0+2.0
Mn(II)	PAN	2 mM	Ethanol	1.0+1.0	-
	Thiourea/KCN/en	1 M/0.1 M/4 M	Milli-Q water	-	2.0+2.0+2.0

**Table 4.6** The reagent preparations and optimal conditions for metal ion detection on the device type E (cont.).

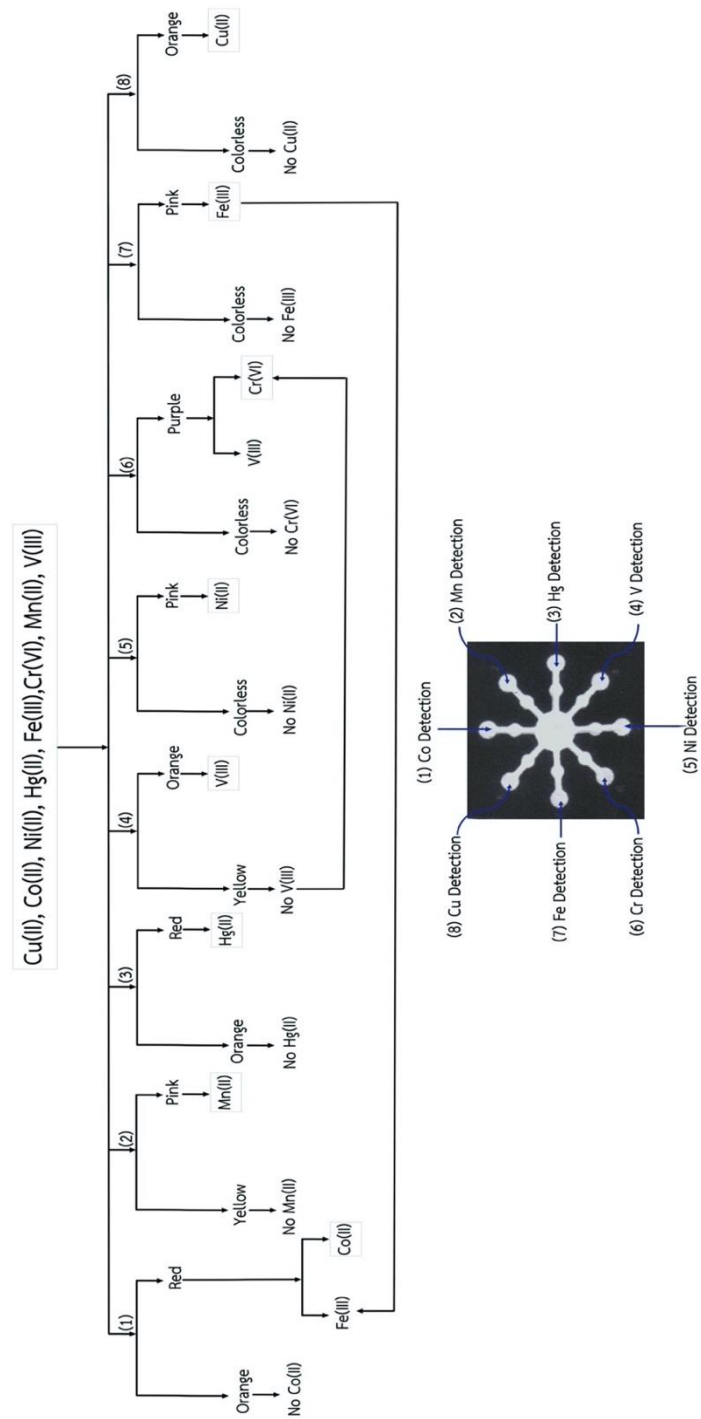
Detection	Reagents	Concentration	Solvent	Volume ( $\mu\text{L}$ )	
				Detection zone	Pretreatment zone
Hg(II)	DTZ	2 mM	Chloroform	1.0+1.0	-
	PEG 400	80 mg/L	Milli-Q water	1.5+1.5+1.5	-
	DCTA	0.1 M	NaOH (0.4 M)	-	2.0+2.0+2.0+2.0
	KCN	0.1 M	Milli-Q water	-	2.0+2.0
	en	10 M	Acetate buffer (2 M, pH 5)	-	2.0+2.0
Cr(VI)	DPC	0.2 %w/v	Acetone:0.4 M HNO <sub>3</sub> (1:1)	1.0+1.0	-
	Thiourea	1 M	Milli-Q water	-	2.0+2.0
	NaF	0.5 M	Milli-Q water	-	2.0+2.0
Fe(III)	Bphen/acetate buffer pH 5/ L-ascorbic acid	10 mM/ 20 mM/0.05 M	95/5 %w/v isopropanol/H <sub>2</sub> O	1.0+1.0	-
	L-ascorbic acid	0.1 M	Milli-Q water	-	2.0+2.0+2.0+2.0
Co(II)	PAR/PDDA	5 mM/5 %w/w	0.1 M Borate buffer (pH 9.3)	-	-
	EDTA	0.2 M	NaOH (0.4 M)	-	2.0+2.0+2.0+2.0
	TETA	0.4 M	Phosphate buffer (0.1 M, pH 10)	-	2.0+2.0+2.0
	en	4 M	Acetate buffer (2 M, pH 5)	-	2.0+2.0

The masking agents for metal ion detection on the device type E are summarized in **Table 4.7**.

**Table 4.7** The masking agents for metal ion detection (0.40 mM) on the device type E.

Detection	Detection zone	Pretreatment zone	
		Masking agent	Masked ion
Cu(II)	Bc	NaF	-Co(II), Fe(III)
Co(II)	PAR	-EDTA	-Mn(II), Ni(II), Zn(II), Cd(II), Pb(II), Fe(III)
		-TETA	-Cu(II), Zn(II), Cd(II), Pb(II)
		-en	-Cu(II), Ni(II), Zn(II), Cd(II), Pb(II)
Ni(II)	DMG	NaF	-Co(II), Fe(III)
Hg(II)	DTZ	-DCTA	-Cu(II), Co(II), Ni(II), Cr(VI), Mn(II), Pb(II), Zn(II)
		-KCN	-Cu(II), Zn(II), Cd(II), Ni(II), Co(II)
		-en	-Cu(II), Ni(II), Zn(II), Cd(II), Pb(II)
Fe(III)	Bphen	-None	-
Cr(VI)	DPC	-Thiourea	-Cu(II)
		-NaF	-Co(II), Fe(III)
V(III)	PAR	DCTA	-Cu(II), Co(II), Ni(II), Cr(VI), Mn(II), Pb(II), Zn(II)
Mn(II)	PAN	-Thiourea	-Cu(II)
		-en	-Cu(II), Ni(II), Zn(II), Cd(II), Pb(II)
		-KCN	-Cu(II), Co(II), Ni(II), Zn(II), Cd(II)

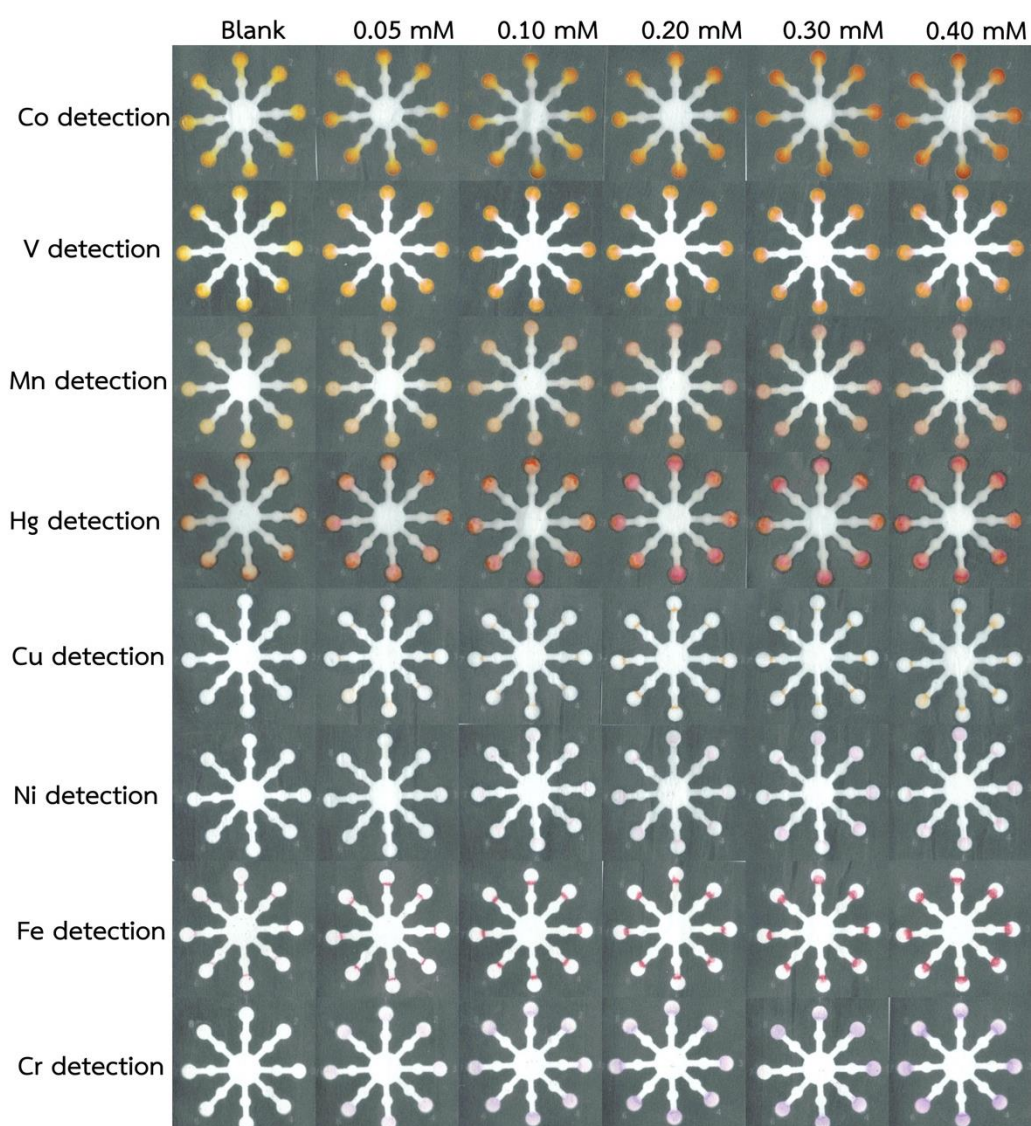
The pathway for metal ion identification in unknown samples on the device type E is illustrated in **Figure 4.46**.



**Figure 4.46** Pathway for simultaneous Cu(II), Co(II), Hg(II), Ni(II), Fe(III), Cr(VI), V(III), and Mn(II) identification on the device type E.

#### 4.3.2.2 Application of simultaneous detection for eight metal ions in synthetic unknown samples

As the optimal conditions for each metal ion detection, these conditions were used to study the limit of detection (LOD) by naked-eye. For each condition, metal ion concentration was varied in the range of 0.05-0.40 mM. The color responses on the device of each metal ion detection are illustrated in **Figure 4.47**. The limit of detection by naked-eye is shown in **Table 4.8**.

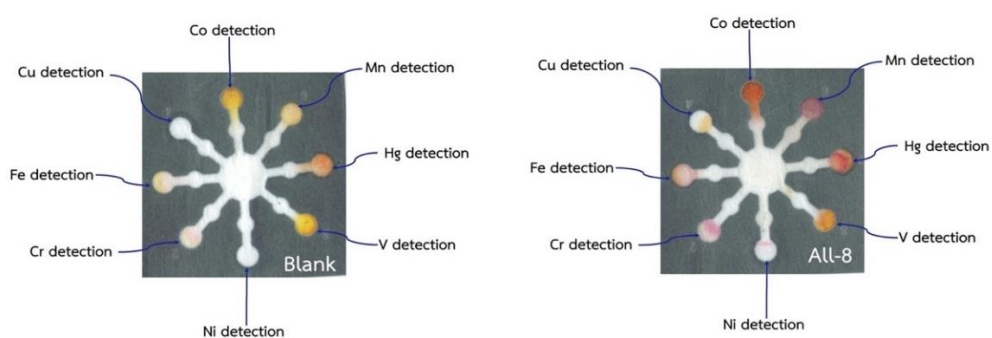


**Figure 4.47** Color changes for limit of detection study of each metal ion detection on the device type E.

**Table 4.8** The limit of detection (LOD) by naked-eye on device type E.

Metal ion detection	LOD (mM)	LOD (mg/L)
Co(II)	0.10	5.89
V(III)	0.05	2.55
Mn(II)	0.10	5.49
Hg(II)	0.20	40.12
Cu(II)	0.05	3.18
Ni(II)	0.20	11.74
Fe(III)	0.10	5.58
Cr(VI)	0.10	5.20

The accuracy of the proposed method was evaluated in synthetic unknown water samples under optimal conditions. As the result of LOD by naked-eye, the highest of limit of detection by naked-eye for eight metal ions detection was 0.20 mM (Hg(II) and Ni(II)). Therefore, 0.4 mM each metal ion was selected to mix into the synthetic unknown samples. The synthetic unknown water samples (46 samples) were prepared by another researcher under the optimum conditions. The synthetic unknown water samples were proceeded to detect metal ion on one device by a researcher. The color response of metal complexes on the device was compared with color chart in **Figure 4.48**. The color responses on the device for 46 samples analysis are shown **Figure 4.49**. The accuracy was 73.91% by a researcher for metal ion identification in 46 unknown samples.

**Figure 4.48** Color chart for simultaneous detection of eight metal ions on the device type E.



**Figure 4.49** Color changes of metal complexes on the device type E from 46 unknown samples.



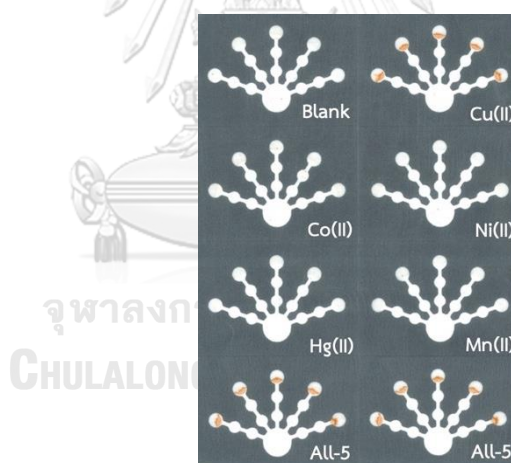
### 4.3.3 Metal complex study on paper-based analytical device type F

#### 4.3.3.1 Optimization conditions

For metal complex study on the device type F, the optimal complexing agents and masking agents were selected from the device type E. A new design of device type F was focused to applied for quantitative analysis. Therefore, type of masking agent, color intensity, reaction time, metal ion volume, and complexing agent volume were optimized.

#### - Type of masking agents

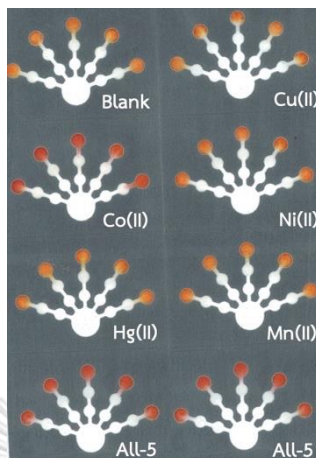
For Cu(II) detection, Hydroxylamine hydrochloride (0.5 g/mL), CH<sub>3</sub>COOH/NaCl buffer (10 mM, pH 4.5), and Bc (10 mM/PEG 400 (80 mg/mL) solution were added onto the detection zone. NaF (0.5 M) was added onto the pretreatment zone 1. 300.0 μL of each metal ion solution and **All-5** were added onto the sample zone. An orange (**All-5**)-Bc complex was similar to an orange Cu(Bc)<sub>2</sub> complex as shown in Figure 4.50.



**Figure 4.50** Color changes of metal-Bc complexes on the device type F for Cu(II) detection.

For Co(II) detection, a PAR (5 mM) /PDDA (5% w/w) solution was added onto the detection zone. Ethylenediamine (4 M) was added on the pretreatment zone 2. Ethylenediamine was separately added from other masking agents to decrease the strongly basic effect which could impact on the efficiency of other masking agents. Triethylenetetramine (0.4 M) and EDTA (0.2 M) was added onto the pretreatment zone 1. 300.0 μL of each metal ion solution and **All-5** were added onto the sample

zone. The red **(All-5)-PAR** complex was similar to the red  $\text{Co(PAR)}_2$  complex as shown in **Figure 4.51**.



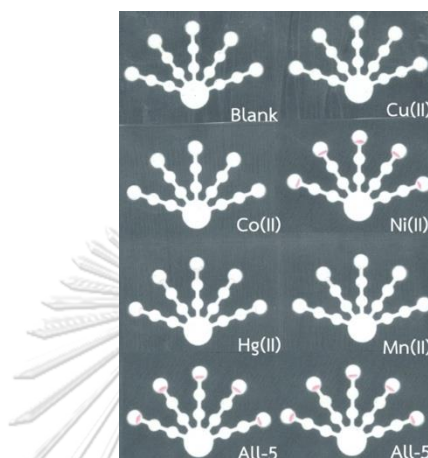
**Figure 4.51** Color changes of metal-PAR complexes on the device type F for Co(II) detection.

For Ni(II) detection, DMG (60 mM) solution, ammonium hydroxide (0.03 M) were added onto the detection zone. NaF (0.5 M) and acetic acid (6.3 M) were added onto the pretreatment zone 2. 300.0  $\mu\text{L}$  of each metal ion solution and **All-5** were added onto the sample zone. The pink **(All-5)-DMG** complex was similar to the pink  $\text{Ni(DMG)}_2$  complex. Co(II) also formed yellow complex with DMG which interfered with pink **(All-5)-DMG** as shown in **Figure 4.52**.



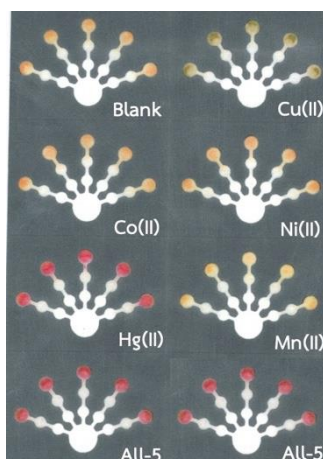
**Figure 4.52** Color changes of metal-DMG complexes on the device type F for Ni(II) detection.

To improve the selectivity of Ni(II) detection by using DMG as a complexing agent, hydroxylamine hydrochloride (0.5 g/mL) was also added onto the detection zone to mask Co(II), Zn(II), Cd(II). The pink **All-5**-DMG complex was similar to the pink Ni(DMG)<sub>2</sub> complex as shown in **Figure 4.53**.



**Figure 4.53** Color changes of metal-DMG complexes by using hydroxylamine hydrochloride as a masking agent on the device type F for Ni(II) detection.

For Hg(II) detection, en (10 M) was separately added onto the pretreatment zone 2. DCTA (0.1 M) and KCN (0.1 M) were added onto the pretreatment zone. PEG 400 (80 mg/mL) was added onto the detection zone, followed by DTZ. 300.0  $\mu$ L of each metal ion solution and **All-5** were added onto the sample zone. The red **All-5**-DTZ complex was similar to the red Hg(DTZ)<sub>2</sub> complex as shown in **Figure 4.54**.



**Figure 4.54** Color changes of metal-DTZ complexes on the device type F for Hg(II) detection.

For Mn(II) detection, a PAR (5.0 mM)/PDDA (5 %w/w) solution was added onto the detection zone. Ethylenediamine (8 M) and thiourea (1 M) were added onto the pretreatment zone 2 and 1, respectively. PAR was applied for Mn(II) detection on the device type F, the device design based on two pretreatment zones was separately added masking agents which improved the selectivity for Mn(II) detection. 300.0  $\mu$ L of each metal ion solution and **All-5** were added onto the sample zone. The red (**All-5**)-PAR complex was similar to the red Mn(PAR)<sub>2</sub> complex as shown in **Figure 4.55**.



**Figure 4.55** Color change of metal-PAR complexes on the device type F for Mn(II) detection.

- Color intensity

The optimal regression equation and correlation coefficient ( $R^2$ ) results evaluated that the gray for Cu(II) and green for Ni(II), Co(II), Hg(II), and Mn(II) intensities were selected as optimal color intensities as shown in **Figure 4.56-4.60**.

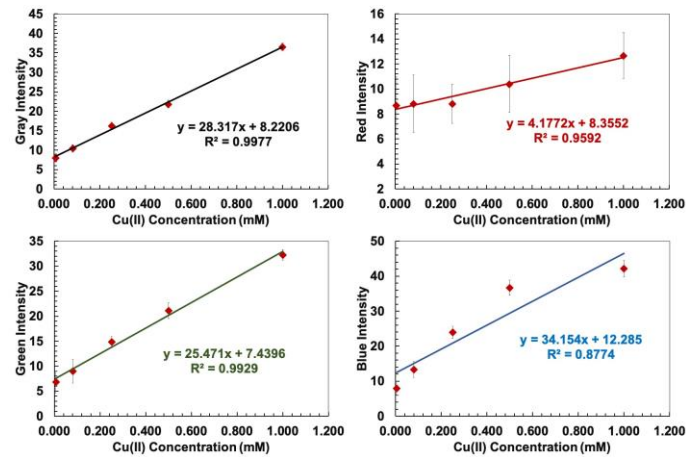


Figure 4.56 The color intensity optimization for Cu(II) calibration on the device type

F.

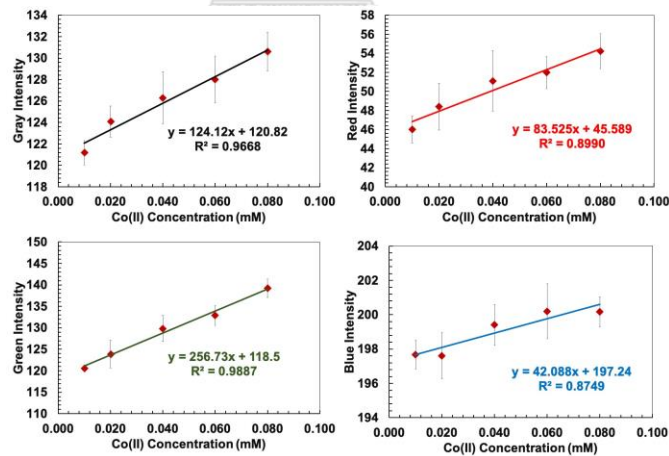


Figure 4.57 The color intensity optimization for Co(II) calibration on the device type

F.

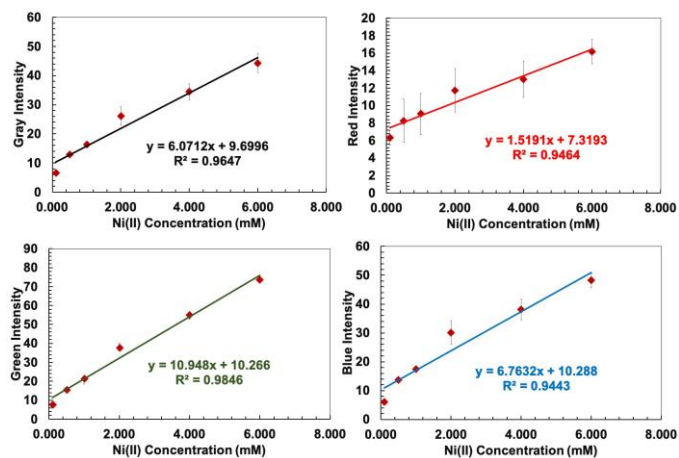


Figure 4.58 The color intensity optimization for Ni(II) calibration on the device type F.

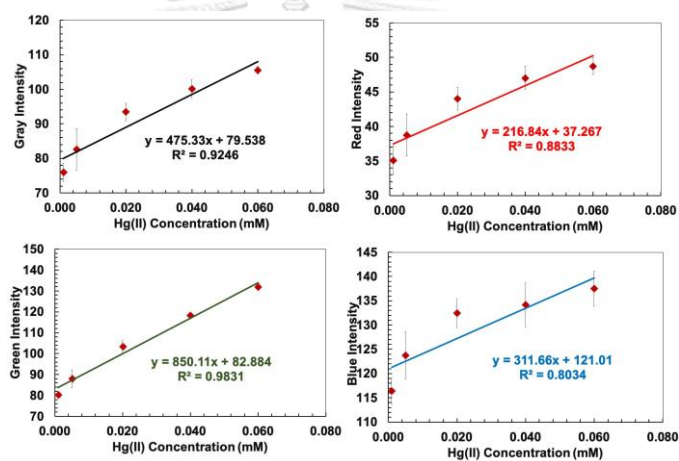
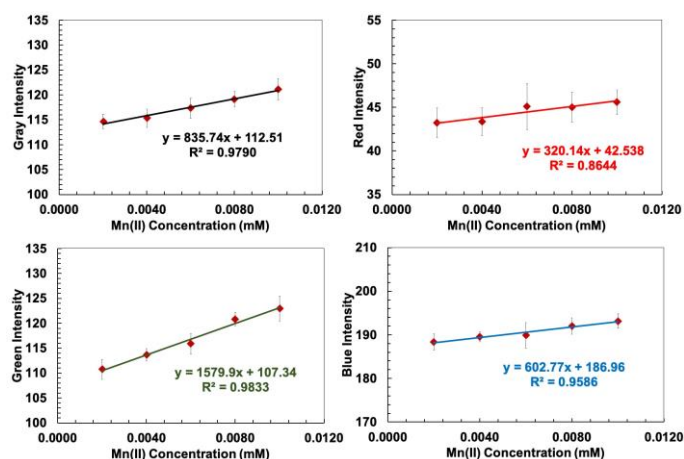


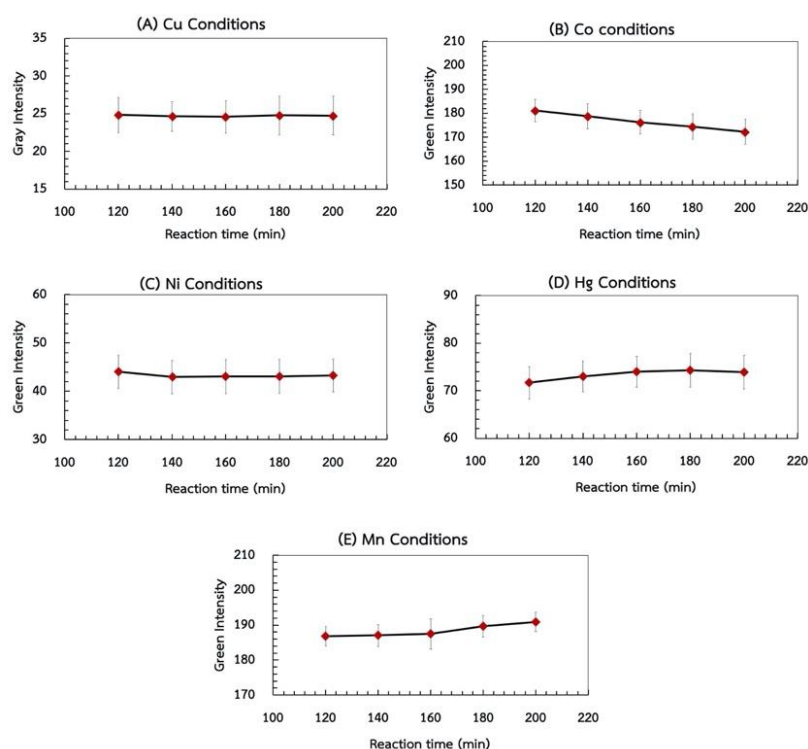
Figure 4.59 The color intensity optimization by for Hg(II) calibration on the device type F.



**Figure 4.60** The color intensity optimization for Mn(II) calibration on the device type F.

#### - Reaction time

The reaction time was optimized in the range of 120-200 minutes with metal ion volume of 300.0  $\mu\text{L}$ . The results indicated that the color intensities were not significantly different with increasing time for Cu(II), Co(II), Ni(II), Hg(II), and Mn(II) detections as shown in **Figure 4.61**. Therefore, 120 minutes were selected for further study because the paper was allowed to dry as soon as possible.

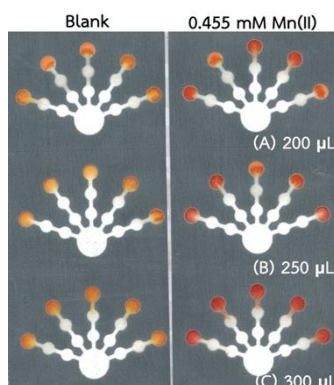


**Figure 4.61** Effect of reaction time on the color response for (A) Cu(II), (B) Co(II), (C) Ni(II), (D) Hg(II), (E) Mn(II) detections on the device type F.

#### - Metal ion volume

As the optimal reaction time of 120 minutes, this reaction time was slightly long analysis time. Metal ion solution based on Mn(II) detection was decreased in the range of 200.0-250.0  $\mu\text{L}$  to improve the reaction time but metal ion solution (200.0-250.0  $\mu\text{L}$ ) did not completely flow into the detection zone within 120 minutes by naked-eye as illustrated in **Figure 4.62**. The viscosity of en on the pretreatment zone impacted on flowing of metal ion solution into the detection zone. Therefore, 300.0  $\mu\text{L}$  of metal ion solution was chosen for further study. Although the metal ion volume optimization did not assist to improve the reaction time (decrease analysis time), the presence of en as a masking agent showed efficiently mask interfering ions for Hg(II), Co(II), and Mn(II) detections.

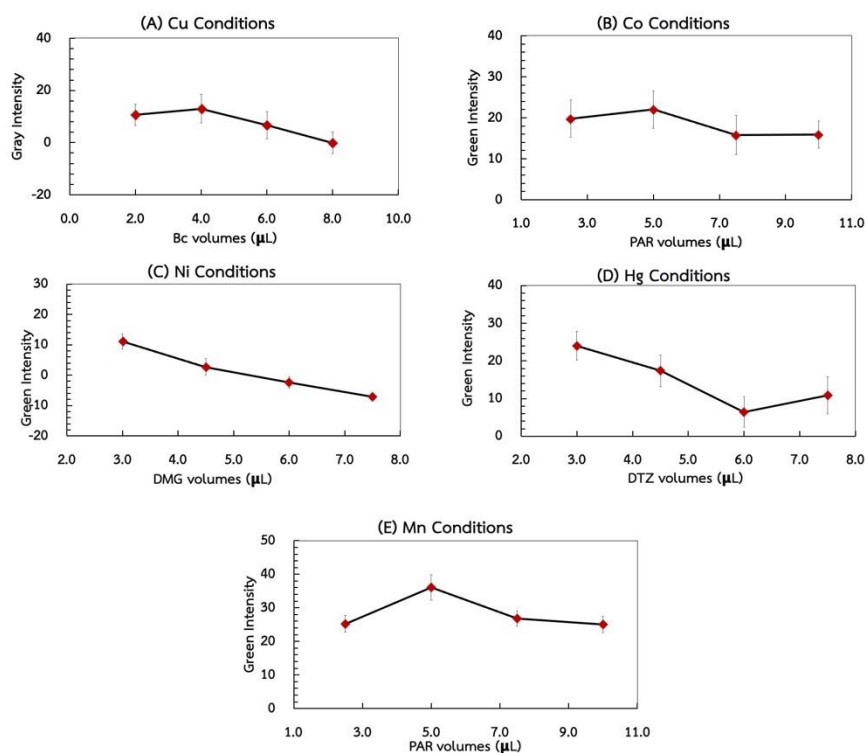




**Figure 4.62** Effect of metal ion volume for (A) 200.0  $\mu\text{L}$ , (B) 250.0  $\mu\text{L}$ , (C) 300.0  $\mu\text{L}$  Mn(II) on the color response for Mn(II) detection on the device type F.

#### - Complexing agent volume

The complexing agent volume was studied to achieve the optimal complexing agent volume reacted with metal ion on the detection zone which presented the maximum color intensity. The complexing agent volume was optimized using 300.0  $\mu\text{L}$  of metal ion volume and reaction time (120 minutes). From the results in **Figure 4.63**, the optimal complexing agent volume evaluated the maximum color intensity of each metal ion detection with Bc (2.0  $\mu\text{L}$ ), PAR (5.0  $\mu\text{L}$ ), DMG (3.0  $\mu\text{L}$ ), DTZ (3.0  $\mu\text{L}$ ), and PAR (5.0  $\mu\text{L}$ ) for Cu(II), Co(II), Ni(II), Hg(II), and Mn(II) detection, respectively as shown. At lower volume of complexing agent for PAR (<5.0  $\mu\text{L}$ ), the color intensity decreased because the complexing agent did not efficiently react with metal ion. At the higher volume for PAR (>5.0  $\mu\text{L}$ ), the color intensity also decreased with complexing agent increasing due to high background color intensity. At the higher volume for DMG (>3.0  $\mu\text{L}$ ), DTZ (>3.0  $\mu\text{L}$ ), and Bc (>2.0  $\mu\text{L}$ ), the color intensity also decreased with complexing agent increasing because of high hydrophobicity of complexing agent on the detection zone.



**Figure 4.63** Effect of complexing agent volume on the color response for (A) Cu(II), (B) Co(II), (C) Ni(II), (D) Hg(II), (E) Mn(II) detections on the device type F.

The optimal parameters for metal ion detection are summarized in **Table 4.9**.

**Table 4.9** The optimal parameters for metal ion detection on device type F.

Parameters	Optimal conditions
Color Intensity	Gray for Cu(II) Green for Ni(II), Co(II), Hg(II), Mn(II)
Reaction Time	120 minutes
Metal Ion Volume	300.0 μL
Complexing Agent Volume	Bc (2.0 μL) for Cu(II) DMG (3.0 μL) for Ni(II) DTZ (3.0 μL) for Hg(II) PAR (5.0 μL) for Co(II) PAR (5.0 μL) for Mn(II)

#### 4.3.3.2 Colorimetric detection and interference study under optimal conditions

As the results of optimization conditions for metal ion detection, the reagent preparations and optimal conditions are summarized in **Table 4.10**.

**Table 4.10** The reagent preparations and optimal conditions for metal ion detection on device type F.

Detection	Reagents	Concentration	Solvent	Volume ( $\mu\text{L}$ )		
				Detection zone	Pretreatment zone	
					1	2
Cu(II)	Bc/PEG 400	10 mM/ 80 mg/L	Chloroform	2.0	-	-
	Hydroxylamine hydrochloride	0.5 g/mL	Milli-Q water	2.0+2.0	-	-
	CH <sub>3</sub> COOH/ NaCl buffer	10 mM, pH 4.6	Milli-Q water	2.0	-	-
	NaF	0.5 M	Milli-Q water	-	2.5+2.5+ 2.5+2.5	-
Co(II)	PAR/PDDA	5 mM/ 5 %w/w	0.1 M Borate buffer (pH 9.3)	2.5+2.5	-	-
	EDTA	0.2 M	NaOH (0.4 M)	-	2.5+2.5+ 2.5+2.5	-
	TETA	0.4 M	Phosphate buffer (0.1 M, pH 10)	-	2.5+2.5+ 2.5+2.5	-
	en	4 M	Acetate buffer (2 M, pH 5)	-	-	2.5+2.5+ 2.5

**Table 4.10.** The reagent preparations and optimal conditions for metal ion detection on device type F (cont.).

Detection	Reagents	Concentration	Solvent	Volume ( $\mu\text{L}$ )		
				Detection zone	Pretreatment zone	
					1	2
N(II)	DMG	60 mM	Methanol	1.5+1.5	-	-
	Hydroxylamine hydrochloride	0.5 g/mL	Milli-Q water	2.0+2.0+ 2.0+2.0	-	-
	NH <sub>4</sub> OH	0.03 M, pH 9.5	Milli-Q water	2.0+2.0	-	-
	NaF	0.5 M	Milli-Q water	-	2.5+2.5+ 2.5+2.5	-
Hg(II)	DTZ	2 mM	Chloroform	1.5+1.5	-	-
	PEG 400	80 mg/L	Milli-Q water	3.0+3.0+ 3.0	-	-
	DCTA	0.1 M	NaOH (0.4 M)	-	2.5+2.5+ 2.5+2.5	-
	KCN	0.1 M	Milli-Q water	-	2.5+2.5	-
	en	10 M	Acetate buffer (2 M, pH 5)	-	-	2.5+2.5
Mn(II)	PAR/PDDA	5 mM/5 %w/w	0.1 M Borate buffer (pH 9.3)	2.5+2.5	-	-
	Thiourea	1 M	Milli-Q water	-	2.5+2.5+ 2.5+2.5	-
	en	10 M	Acetate buffer (2 M, pH 5)	-	-	2.5+2.5+ 2.5+2.5

The masking agents for metal ion detection on the device type F are summarized in **Table 4.11**.

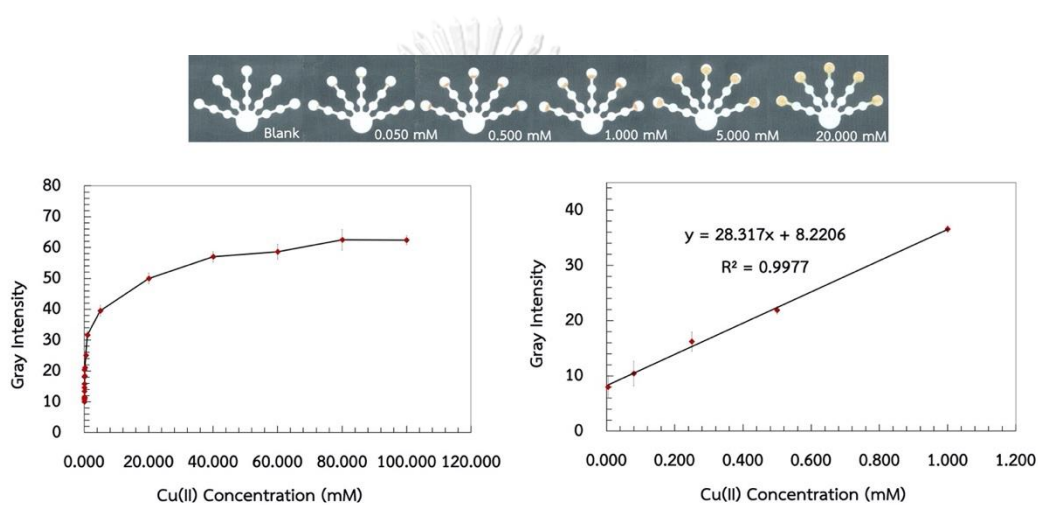
**Table 4.11** The masking agents for metal ion detection on detection on the device type F.

Detection	Detection zone	Pretreatment zone 1	Masked ions	Pretreatment zone 2	Masked ions
Cu(II)	Bc	-NaF	-Fe(III), Co(II)	-None	-
Co(II)	PAR	-EDTA -TETA	-Fe(III), Ni(II), Mn(II) Zn(II), Cd(II), Pb(II) -Cu(II), Zn(II), Cd(II), Pb(II)	-en	-Cu(II), Ni(II), Zn(II), Cd(II), Pb(II)
Ni(II)	DMG	-None	-	-NaF	-Fe(III), Co(II)
Hg(II)	DTZ	-DCTA -KCN	-Cu(II), Co(II), Ni(II), Cr(VI), Mn(II), Pb(II), Zn(II) -Cu(II), Co(II), Ni(II), Zn(II), Cd(II)	-en	-Cu(II), Ni(II), Zn(II), Cd(II), Pb(II)
Mn(II)	PAR	-Thiourea	-Cu(II)	-en	-Cu(II), Ni(II), Zn(II), Cd(II), Pb(II)

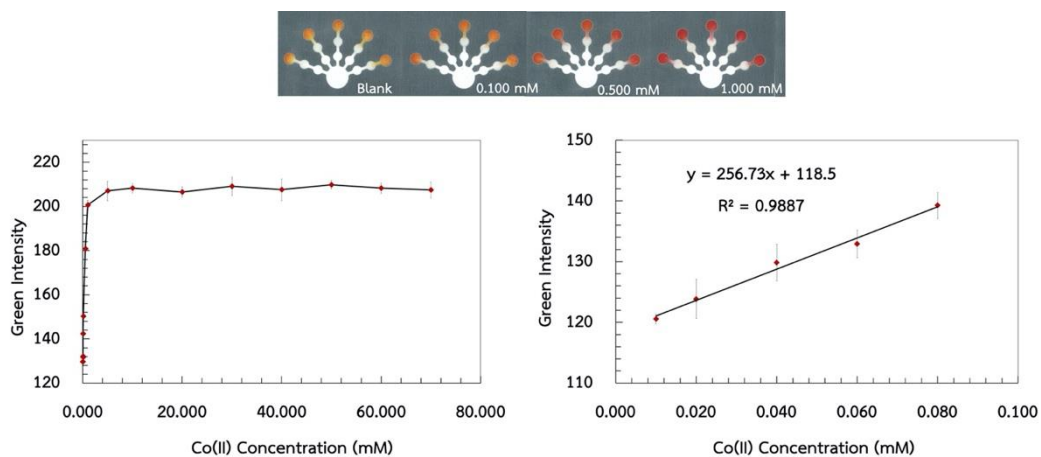
These optimal conditions were used to evaluate the proposed method performance. The proposed method performance was evaluated with the lowest detectable concentration, linear range, and saturated concentration. The lowest detectable concentration is defined as the lowest amount of metal ion which was reproducibly detected on the device <sup>34</sup>. A single metal ion detection was operated on one device by adding a set of reagents of each metal ion detection onto five detection zones and ten pretreatment zones. The device was allowed to dry at room temperature during adding each reagent. 300.0  $\mu$ L of metal ion solution was

added onto the sample zone. The color response on the device was recorded by using a scanner at optimal reaction time of 120 minutes.

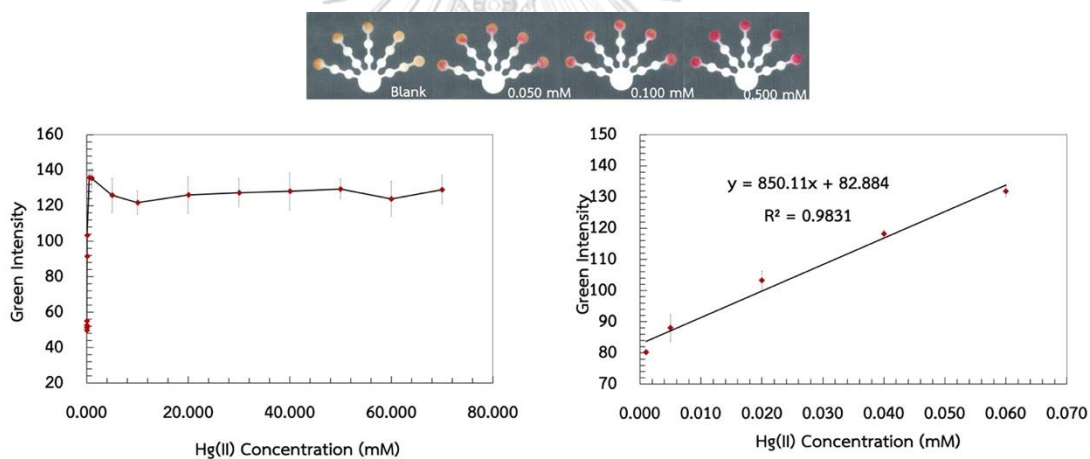
The lowest detectable concentration of Cu(II), Co(II), Ni(II), Hg(II), and Mn(II) detection were 0.005, 0.010, 0.100, 0.001, and 0.0020 mM, respectively. The linear range was 0.005-1.000 mM (Cu(II)), 0.010-0.080 mM (Co(II)), 0.100-6.000 mM (Ni(II)), 0.001-0.060 mM (Hg(II)), and 0.0020-0.0100 mM (Mn(II)). The calibration curve and visual calibration for Cu(II), Co(II), Ni(II), Hg(II), and Mn(II) detections are illustrated in **Figure 4.64-4.68**.



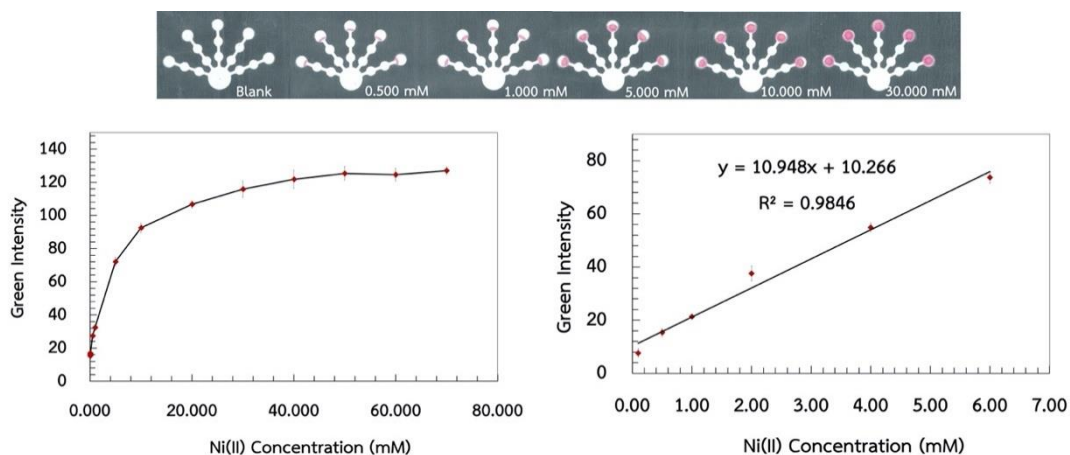
**Figure 4.64** Visual calibration for semi-quantitative Cu(II) determination (top). Cu(II) Calibration curve (0.005-1.000 mM) by analyzing the gray intensity of the color response on the detection zone (bottom).



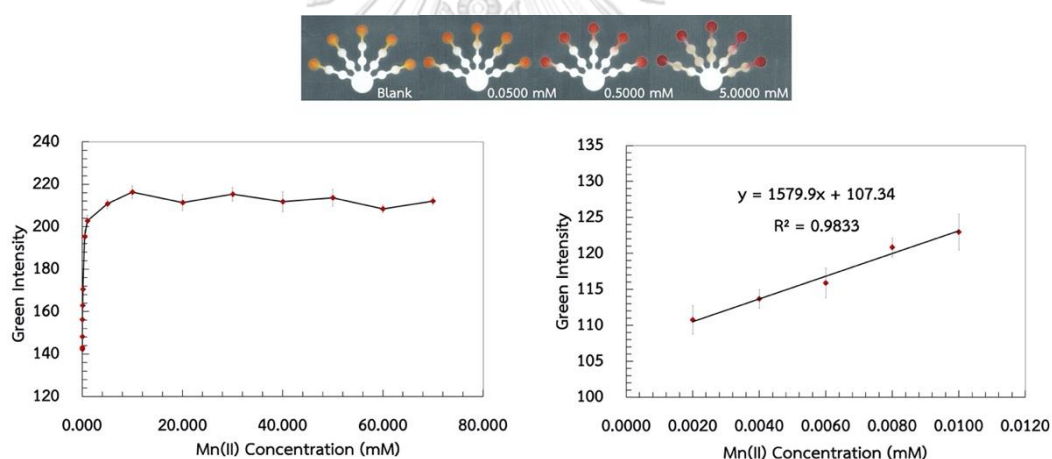
**Figure 4.65** Visual calibration for semi-quantitative Co(II) determination (top). Co(II) Calibration curve (0.010-0.080 mM) by analyzing the green intensity of the color response on the detection zone (bottom).



**Figure 4.66** Visual calibration for semi-quantitative Hg(II) determination (top). Hg(II) Calibration curve (0.001-0.060 mM) by analyzing the green intensity of the color response on the detection zone (bottom).



**Figure 4.67** Visual calibration for semi-quantitative Ni(II) determination (top). Ni(II) Calibration curve (0.100-6.000 mM) by analyzing the green intensity of the color response on the detection zone (bottom).



**Figure 4.68** Visual calibration for semi-quantitative Mn(II) determination (top). Mn(II) Calibration curve (0.0020-0.0100 mM) by analyzing the green intensity of the color response on the detection zone (bottom).

The proposed method performance demonstrated that the linear regression equation of each target metal ion reaction was achieved by plot the optimum color intensity versus metal ion concentrations with  $y = 28.317x + 8.2206$  ( $R^2 = 0.9977$ ),  $y = 256.73x + 118.5$  ( $R^2 = 0.9887$ ),  $y = 10.948x + 10.266$  ( $R^2 = 0.9846$ ),  $y = 850.11x + 82.884$  ( $R^2 = 0.9831$ ), and  $y = 1579.9x + 107.34$  ( $R^2 = 0.9833$ ) for Cu(II), Co(II), Ni(II), Hg(II), and Mn(II) detections, respectively. The lowest detectable concentration, linear

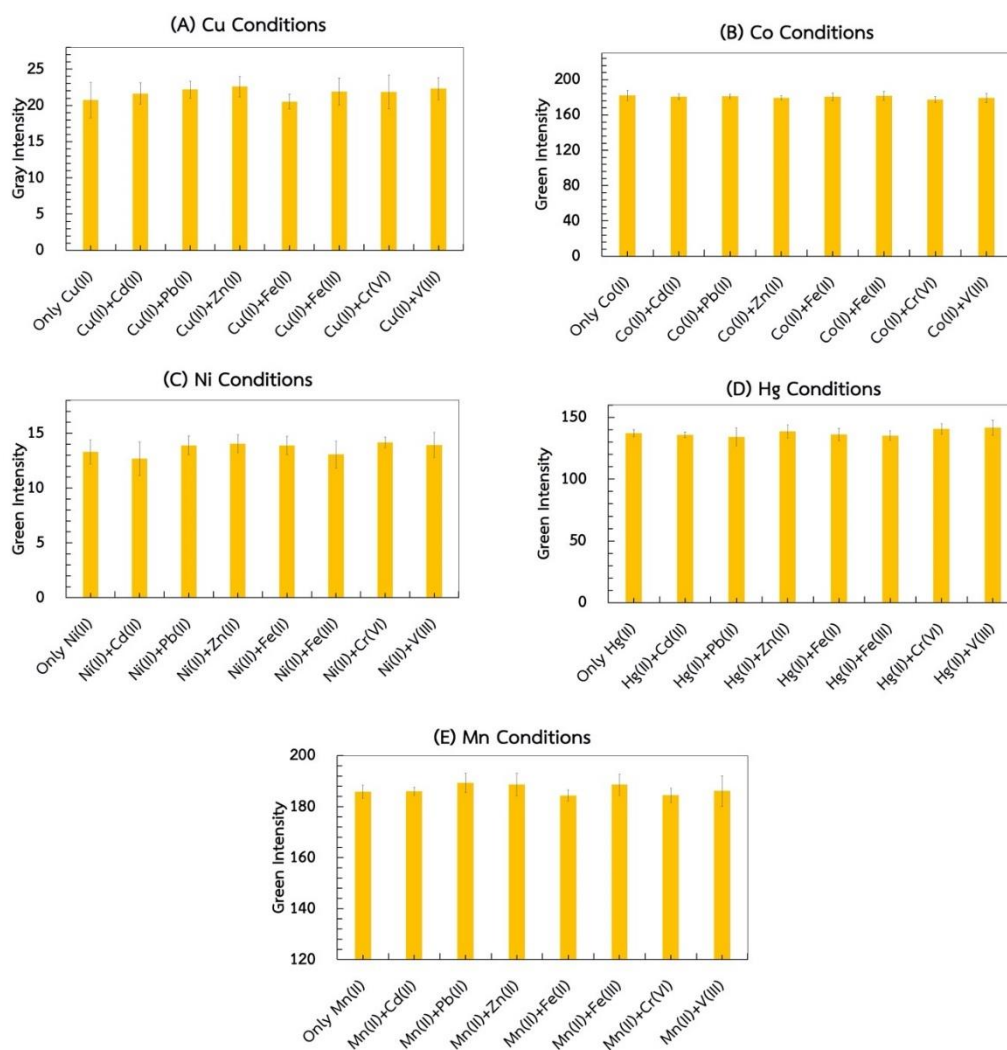


range, and saturated concentration for each metal ion detection are shown in **Table 4.12**. The saturated concentration was useful for simultaneous semi-quantitative analysis which was could be applied for on-site detection.

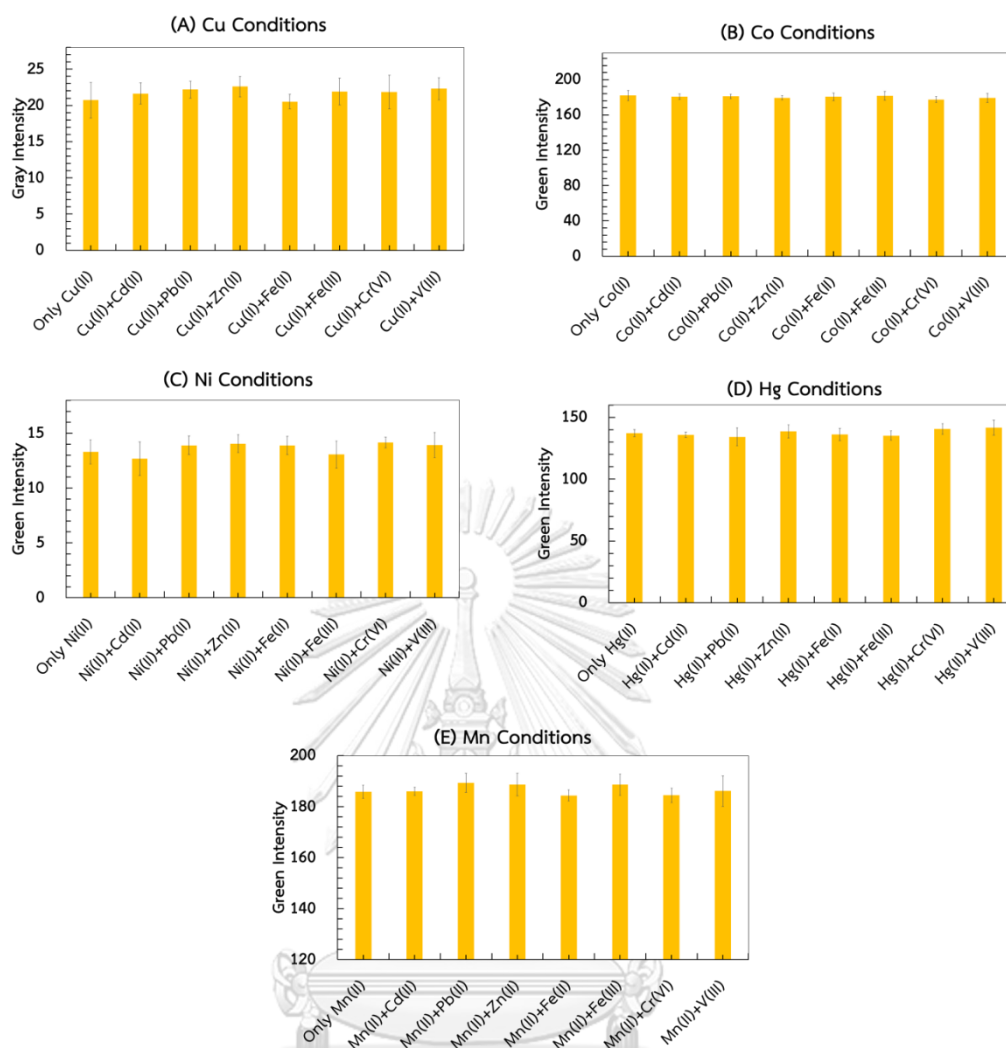
**Table 4.12** Summary of the analytical performance of the proposed method for Cu(II), Co(II), Ni(II), Hg(II), and Mn(II) detection (n=5).

Detection	LOD (naked-eye)		Color intensity					
			Lowest detectable concentration		Linear range		Saturated concentration	
	mM	mg/L	mM	mg/L	mM	mg/L	mM	mg/L
Cu(II)	0.050	3.18	0.005	0.32	0.005-1.000	0.32-63.55	40.0	2542
Co(II)	0.050	2.95	0.010	0.59	0.010-0.080	0.59-4.71	10.0	589
Ni(II)	0.500	29.35	0.100	5.87	0.100-6.000	5.87-352.16	40.0	2348
Hg(II)	0.050	10.03	0.001	0.20	0.001-0.060	0.20-12.04	1.0	201
Mn(II)	0.0500	2.75	0.0020	0.11	0.0020-0.0100	0.11-0.55	10.0	549

Effect of interfering ions on a target metal ion detection was proceeded under the optimum conditions. Interfering ions in target group (Cu(II), Co(II), Ni(II), Hg(II), Mn(II), **All-5**) and other interferences (Cd(II), Zn(II), Pb(II), Fe(III), Fe(II), Cr(VI), and V(III)) were studied for each target metal ion detection by varying the concentration ratio of 1:1 and 1:2. Alkali and alkaline earth group were evaluated at the same conditions by varying the concentration ratio of 1:100 and 1:1000. The tolerance limit is defined as ion concentration which cause a relative error of target ion detection smaller than  $\pm 10\%$  [15]. The results showed no interferences at the ratio of 1:1 as shown in **Figure 4.69** and **Figure 4.70**. The error bars were obtained from the standard deviation (n=5) on one device.

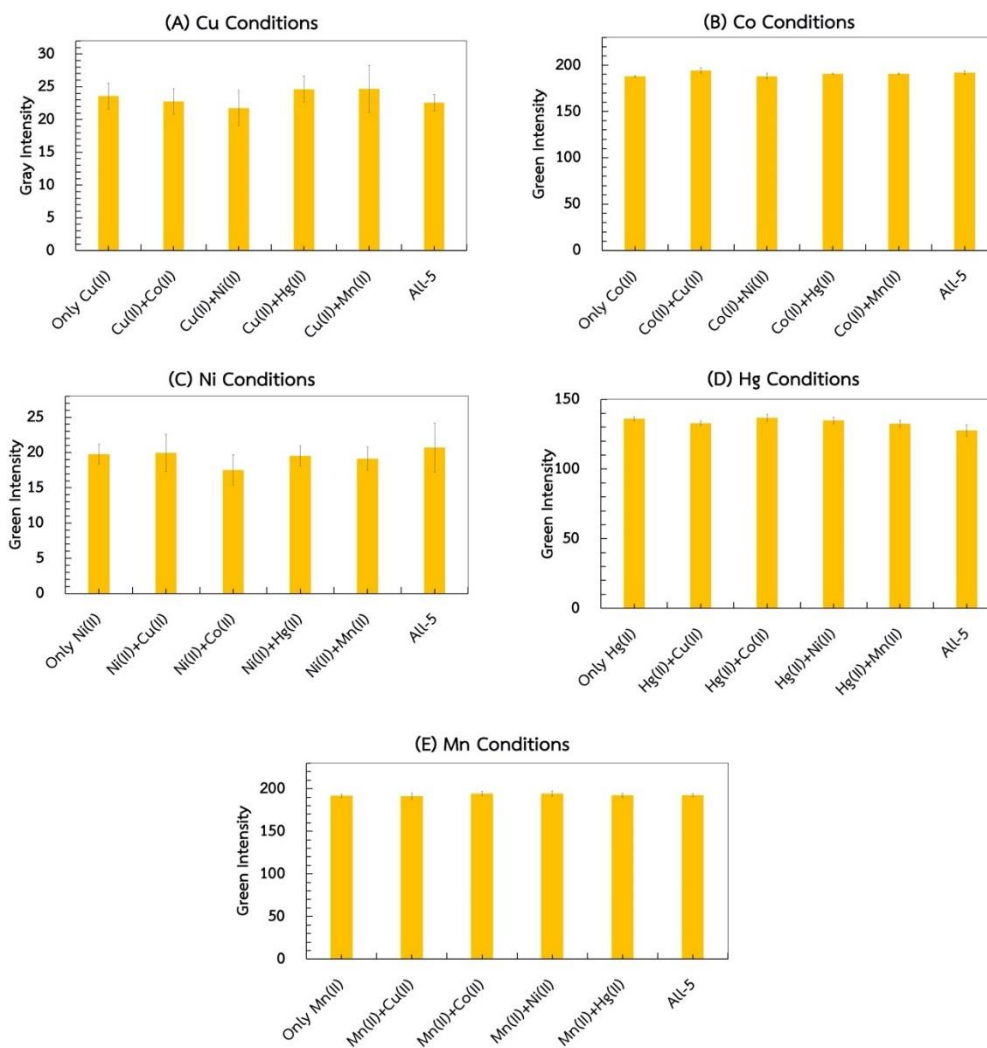


**Figure 4.69** The color intensities of 0.455 mM (A) Cu(II), (B) Co(II), (C) Ni(II), (D) Hg(II), (E) Mn(II) in the presence of 0.455 mM Cu(II), Co(II), Ni(II), Hg(II), Mn(II), and All-5 for Cu(II), Co(II), Ni(II), Hg(II), and Mn(II) detection, respectively.

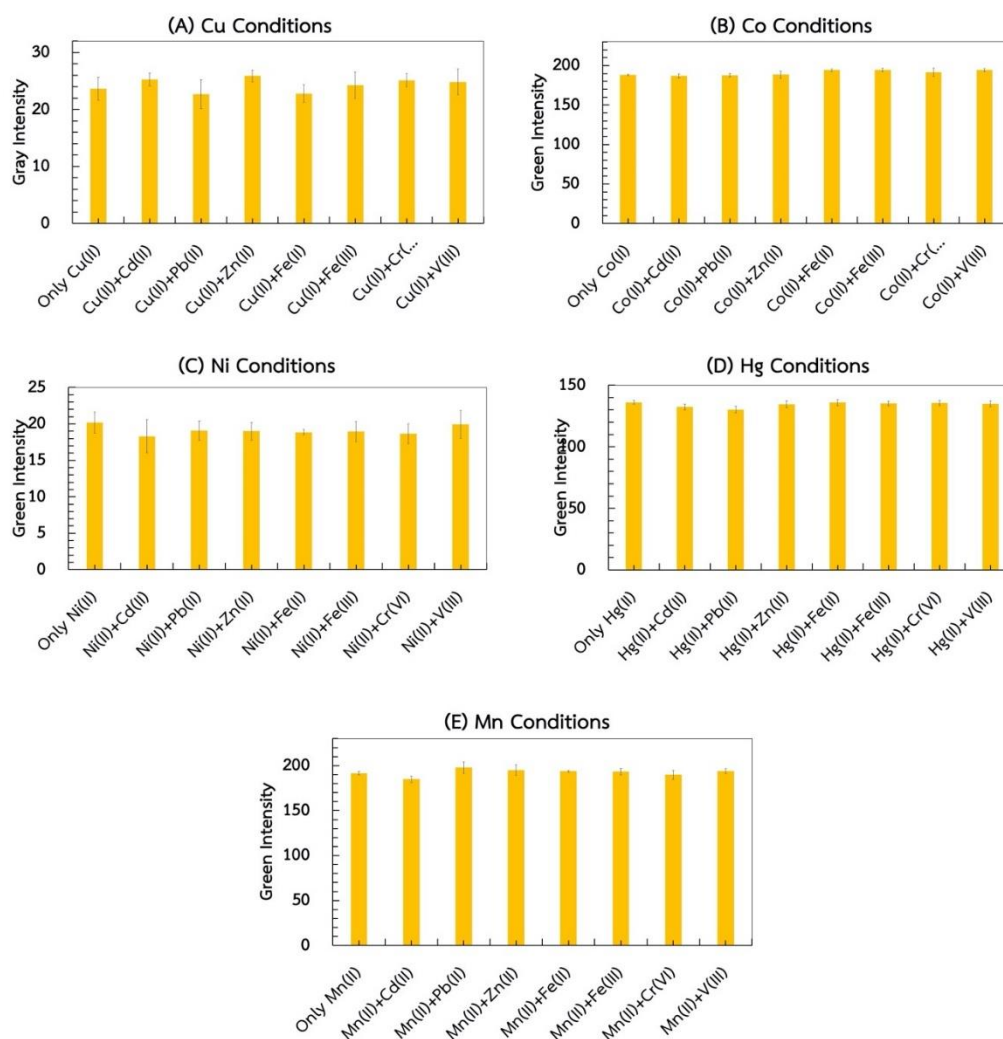


**Figure 4.70** The color intensities of 0.455 mM (A) Cu(II), (B) Co(II), (C) Ni(II), (D) Hg(II), (E) Mn(II) in the presence of 0.455 mM Cd(II), Zn(II), Pb(II), Fe(II), Fe(III), Cr(VI), and V(III) for Cu(II), Co(II), Ni(II), Hg(II), and Mn(II) detection, respectively.

For Ni(II) determination, the examined interferences (1:2) showed 0.910 mM Co(II) interferes with Ni(II) detection. For Cu(II), Co(II), Hg(II), and Mn(II) determination, the examined interferences (1:2) showed no interferences as shown in **Figure 4.71** and **Figure 4.72**.

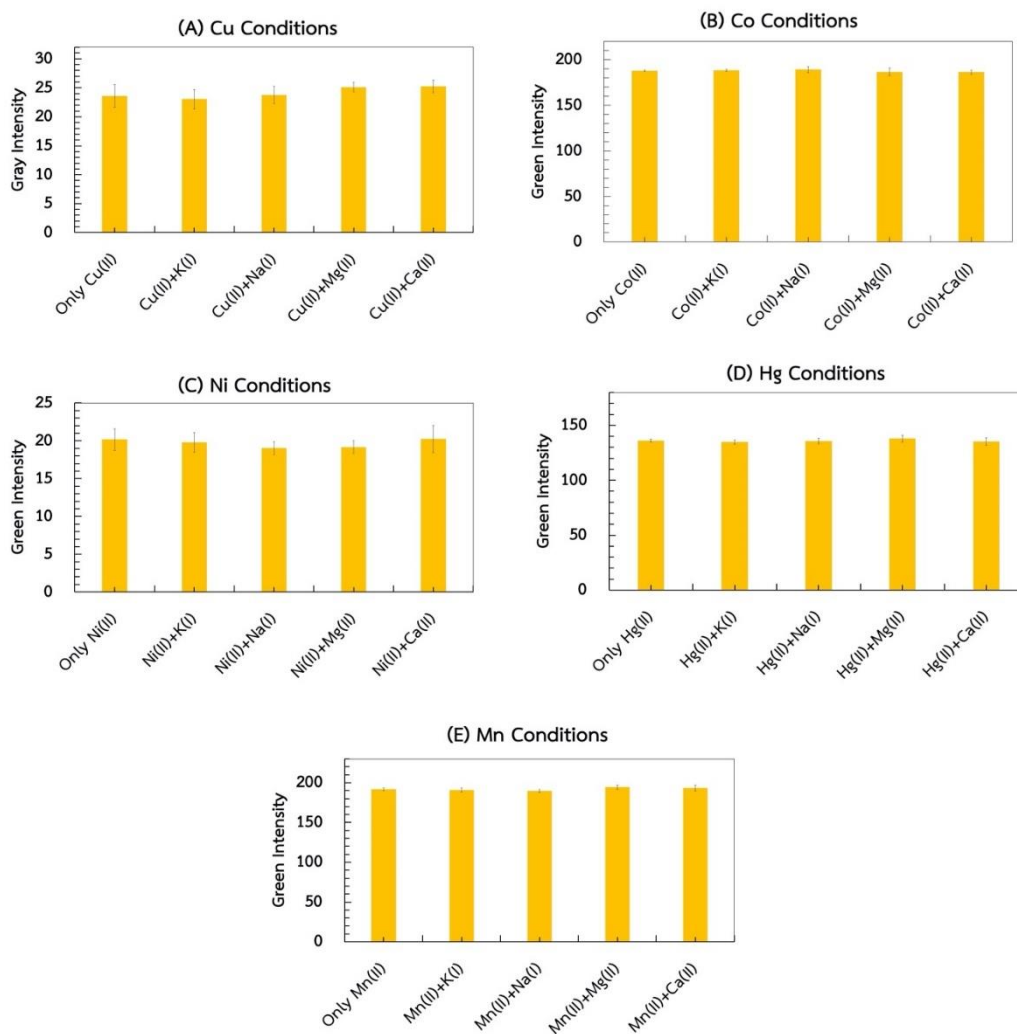


**Figure 4.71** The color intensities of 0.455 mM (A) Cu(II), (B) Co(II), (C) Ni(II), (D) Hg(II), (E) Mn(II) in the presence of 0.910 mM Cu(II), Co(II), Ni(II), Hg(II), Mn(II), and All-5 for Cu(II), Co(II), Ni(II), Hg(II), and Mn(II) detection, respectively.

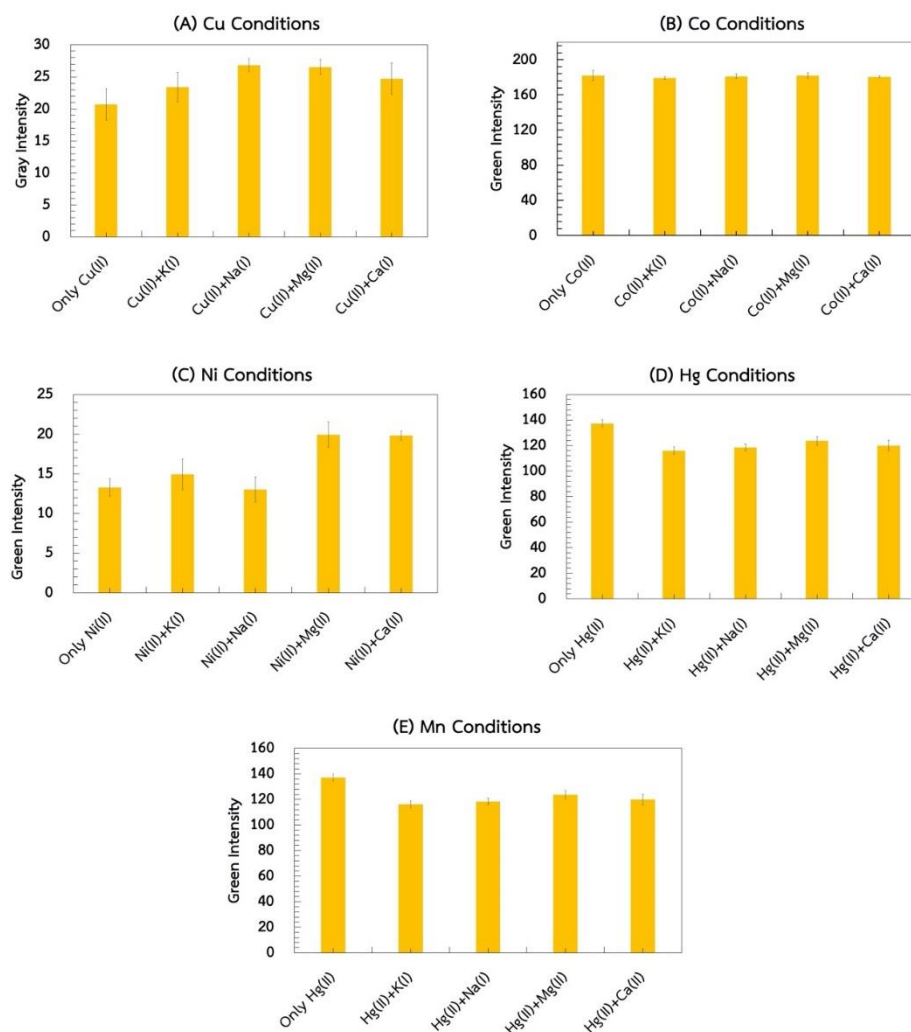


**Figure 4.72** The color intensities of 0.455 mM (A) Cu(II), (B) Co(II), (C) Ni(II), (D) Hg(II), (E) Mn(II) in the presence of 0.910 mM Cd(II), Zn(II), Pb(II), Fe(II), Fe(III), Cr(VI), and V(III) for Cu(II), Co(II), Ni(II), Hg(II), and Mn(II) detection, respectively.

From the results in **Figure 4.73**, at 100 times of K(I), Na(I), Mg(II), and Ca(II) were not interfered for Cu(II), Co(II), Ni(II), Hg(II), and Mn(II) determinations. At 1000 times of K(I), Na(I), Mg(II), and Ca(II) were not interfered for Co(II) determination as illustrated in **Figure 4.74**. Moreover, 1000 times of Na(I) was not interfered for Ni(II) determination.



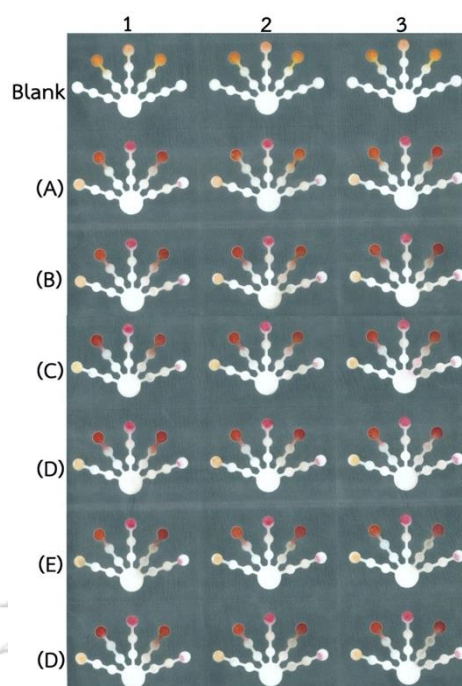
**Figure 4.73** The color intensities of 0.455 mM (A) Cu(II), (B) Co(II), (C) Ni(II), (D) Hg(II), (E) Mn(II) in the presence of 45.5 mM Na(I), K(I), Mg(II), Ca(II) for Co(II) detection.



**Figure 4.74** The color intensities of 0.455 mM (A) Cu(II), (B) Co(II), (C) Ni(II), (D) Hg(II), (E) Mn(II) in the presence of 455 mM Na(I), K(I), Mg(II), Ca(II) for Co(II) detection.

#### 4.3.3.3 Simultaneous detection of five metal ions

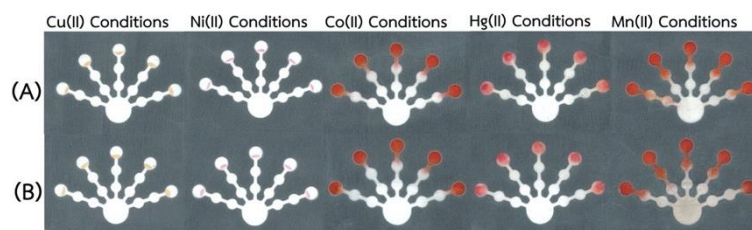
For simultaneous Cu(II), Co(II), Ni(II), Hg(II), and Mn(II) detection, the optimized reagents of each metal ion detection were added onto each pretreatment zone and detection zone. A mixture solution of five metal ions was added onto the sample zone. Orange  $\text{Cu}(\text{BC})_2$ , pink  $\text{Ni}(\text{DMG})_2$ , red  $\text{Hg}(\text{DTZ})_2$ , red  $\text{Co}(\text{PAR})_2$ , and red  $\text{Mn}(\text{PAR})_2$  complexes on the devices. The color changes of metal complexes for simultaneous five metal ions detection on the one device ( $n=3$  devices) are illustrated in **Figure 4.75**. The proposed method provided highly selective for simultaneous Cu(II), Co(II), Ni(II), Hg(II), and Mn(II) detection by naked-eye.



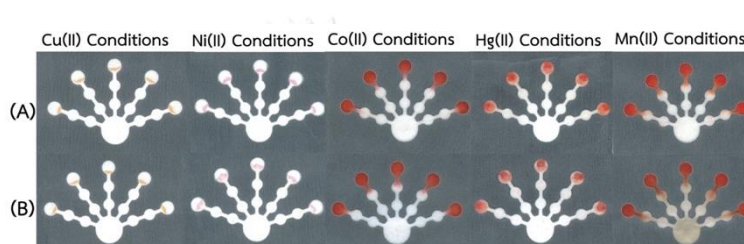
**Figure 4.75** Color changes of metal complexes (A) 1:1 ratio for All-5, (B) 1:2 for Cu(II):other metal ions, (C) 1:2 for Co(II):other metal ions, (D) 1:2 for Ni(II):other metal ions, (E) 1:2 for Hg(II):other metal ions, (F) 1:2 for Mn(II):other metal ions.

For simultaneous Cu(II), Co(II), Ni(II), Hg(II), and Mn(II) quantification using a single metal ion detection on one device, the optimized reagent of each metal ion was added onto ten pretreatment zones and five detection zones on one device. A mixture solution of five metal ions (mixing in the concentration ratio of 1:1) was added onto the sample zone. Orange  $\text{Cu}(\text{Bc})_2$ , pink  $\text{Ni}(\text{DMG})_2$ , red  $\text{Hg}(\text{DTZ})_2$ , red  $\text{Co}(\text{PAR})_2$ , and red  $\text{Mn}(\text{PAR})_2$  complexes on the devices are illustrated in **Figure 4.76**. Moreover, a mixture solution of five metal ions (mixing in the concentration ratio of 1:2) was added onto the sample zone. Orange  $\text{Cu}(\text{Bc})_2$ , pink  $\text{Ni}(\text{DMG})_2$ , red  $\text{Hg}(\text{DTZ})_2$ , red  $\text{Co}(\text{PAR})_2$ , and red  $\text{Mn}(\text{PAR})_2$  complexes on the devices are illustrated in **Figure 4.77**. The proposed method provided efficient simultaneous Cu(II), Co(II), Ni(II), Hg(II), and Mn(II) determination.






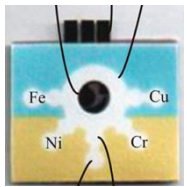
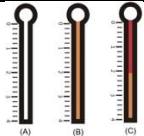
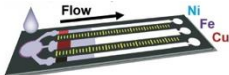
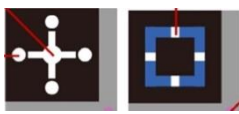
**Figure 4.76** Color changes of metal complexes using (A) 0.455 mM target metal ion (B) a mixture solution of five metal ions (mixing in the concentration ratio of 1:1) for each metal ion detection.



**Figure 4.77** Color changes of metal complexes using (A) 0.455 mM target metal ion (B) a mixture solution of five metal ions (mixing in the concentration ratio of 1:2) for each metal ion detection.

The comparison between the performance of this proposed paper-based and other paper-based sensor for heavy metals analysis by colorimetric methods are shown in **Table 4.13**. The proposed sensor showed effectively simultaneous five metal ions analysis. For example, the number of metal ions assay is higher than previous conditions, the lowest detectable concentrations of Cu(II), Ni (II), and Hg(II) are lower than the previous works, the linear range is wider for Cu(II) assay as well as Ni(II). The proposed  $\mu$ PAD provides a simple fabrication method and is easy to use and analyze.

**Table 4.13** Comparison of the performance between the proposed  $\mu$ PAD and other  $\mu$ PADs based on wax printing fabrication method for heavy metals detection by colorimetric methods.

Metal ion	Lowest detectable concentration (mg/L)	Complexing agent	Linear range (mg/L)	Device design	Ref.
Cu(II)	0.32	bathocuproine	0.32-63.55		This work
Co(II)	0.59	4-(2-pyridylazo) resorcinol	0.59-4.71		
Ni(II)	5.87	dimethylglyoxime	5.87-352.16		
Hg(II)	0.20	dithizone	0.20-12.04		
Mn(II)	0.11	4-(2-pyridylazo) resorcinol	0.11-0.55		
Cu(II)	15	bathocuproine	60-300		23
Ni(II)	15	dimethylglyoxime	30-300		
Cr(VI)	2.4	1,5-diphenylcarbazide	7.6-120		
Fe(III)	15	1,10-phenanthroline	30-300		
Hg(II)	0.93	dithizone	1-30		61
Fe(II)	20	4,7-diphenyl-1,10-phenanthroline	100-1100		34
Ni(II)	100	dimethylglyoxime	20-1300		
Cu(II)	100	dithiooxamide	100-1300		
Cu(II)	1.60	bathocuproine	5-80		92
Ni(II)	4.80	dimethylglyoxime	15-60		
Cr(VI)	0.18	1,5-diphenylcarbazide	0.50-10		

#### 4.3.3.4 Application of simultaneous determination of five metal ions in water samples

To evaluate the precision of the proposed method, the proposed method was performed using a single metal ion detection on one device by measurement the color intensity of each target metal ion with three replicate devices ( $n=3$ ). The relative standard deviations (RSDs) were found in the range of 3.98-5.77%, 1.69-

3.21%, 1.46-4.79%, 2.08-4.66%, and 1.39-2.29% for Cu(II), Co(II), Ni(II), Hg(II), and Mn(II) detection, respectively. The proposed method showed good acceptable precision with Association of Official Analytical Chemists (AOAC) <sup>93</sup>.

For simultaneous Cu(II), Co(II), Ni(II), Hg(II), and Mn(II) determination in real water samples, the application was performed using a single metal ion detection on one device. Each target metal ion was spiked at three level concentrations in drinking, tap, and pond-CU water samples. The optimized reagent for each metal ion detection were added onto the device and water samples were added onto the sample zone. The recoveries and %RSDs were evaluated in the range of 91-109% and 1.98-8.28% (Cu(II)), 100-120% and 0.80-3.48% (Co(II)), 101-107% and 2.58-5.49% (Ni(II)), 100-113% and 0.58-4.63% (Hg(II)), 112-125% and 0.68-2.92% (Mn(II)) for drinking, tap, and pond-Cu waters as shown in **Table 4.14**, **Table 4.15**, and **Table 4.16**, respectively. The accuracy of the proposed method showed good agreement with ICP-OES as the standard method. The statistical data was used to compare the difference between the proposed method and the standard method. These results demonstrated that the proposed method was not significantly different from ICP-OES (paired t-test, 95 % confidence interval). The proposed method showed good acceptable accuracy with Association of Official Analytical Chemists (AOAC) <sup>93</sup>. The recovery of Mn(II) determination in Pond-Cu water was slightly high because of matrix effect, lowest spiked concentration and narrow linearity. While the recovery of Mn(II) determination in drinking water was also high due to lowest spiked concentration.

**Table 4.14** Summary of the recovery and RSD of the proposed sensor and the standard method (ICP-OES) for simultaneous Cu(II), Co(II), Ni(II), Hg(II), and Mn(II) determination in drinking water.

Metal ion	Added (mM)	Proposed sensor (n=5)			ICP-OES (n=3)		
		Found (mM)	%Recovery	%RSD	Found (mM)	%Recovery	%RSD
Cu(II)	-	N.D.			N.D.		
	0.080	0.086 ± 0.031	108	8.28	0.094 ± 0.001	118	0.35
	0.400	0.415 ± 0.034	104	4.82	0.434 ± 0.003	109	0.63
	0.800	0.834 ± 0.064	104	5.70	0.825 ± 0.008	103	0.99
Co(II)	-	N.D.			N.D.		
	0.020	0.020 ± 0.013	100	2.65	0.021 ± 0.001	105	1.36
	0.040	0.041 ± 0.016	103	3.19	0.042 ± 0.002	105	3.07
	0.060	0.063 ± 0.004	105	0.80	0.076 ± 0.001	127	1.81
Ni(II)	-	N.D.			N.D.		
	0.800	0.835 ± 0.077	104	4.34	0.786 ± 0.001	98	0.05
	2.000	2.145 ± 0.083	107	2.70	2.168 ± 0.003	108	0.14
	4.000	4.179 ± 0.186	104	3.63	4.092 ± 0.009	102	0.21
Hg(II)	-	N.D.			N.D.		
	0.008	0.008 ± 0.003	100	2.91	0.008 ± 0.001	100	1.57
	0.020	0.022 ± 0.003	110	2.49	0.020 ± 0.001	100	0.59
	0.040	0.044 ± 0.001	110	0.58	0.040 ± 0.001	100	0.19
Mn(II)	-	N.D.			N.D.		
	0.0040	0.0047 ± 0.0005	118	0.68	0.0049 ± 0.0003	123	2.90
	0.0060	0.0072 ± 0.0013	120	1.78	0.0071 ± 0.0001	118	2.29
	0.0080	0.0096 ± 0.0010	120	1.27	0.0087 ± 0.0001	109	0.69

**Table 4.15** Summary of the recovery and RSD of the proposed sensor and the standard method (ICP-OES) for simultaneous Cu(II), Co(II), Ni(II), Hg(II), and Mn(II) determination in tap water.

Metal ion	Added (mM)	Proposed sensor (n=5)			ICP-OES (n=3)		
		Found (mM)	%Recovery	%RSD	Found (mM)	%Recovery	%RSD
Cu(II)	-	N.D.			N.D.		
	0.080	0.073 ± 0.021	91	5.69	0.093 ± 0.002	116	0.83
	0.400	0.410 ± 0.037	103	5.24	0.427 ± 0.002	107	1.45
	0.800	0.756 ± 0.021	95	1.98	0.805 ± 0.009	101	0.60
Co(II)	-	N.D.			N.D.		
	0.020	0.024 ± 0.004	120	0.83	0.021 ± 0.001	105	4.16
	0.040	0.047 ± 0.011	118	2.25	0.040 ± 0.001	100	5.61
	0.060	0.067 ± 0.018	112	3.48	0.058 ± 0.001	97	2.82
Ni(II)	-	N.D.			N.D.		
	0.800	0.856 ± 0.057	107	3.19	0.778 ± 0.002	97	0.10
	2.000	2.135 ± 0.082	107	2.68	2.145 ± 0.006	107	0.29
	4.000	4.056 ± 0.129	101	2.58	4.033 ± 0.016	101	0.29
Hg(II)	-	N.D.			N.D.		
	0.008	0.009 ± 0.001	113	1.86	0.008 ± 0.001	100	0.08
	0.020	0.022 ± 0.003	110	1.19	0.019 ± 0.001	95	0.30
	0.040	0.044 ± 0.003	110	2.25	0.040 ± 0.002	100	0.22
Mn(II)	-	0.0047 ± 0.0026			0.0014 ± 0.0002		
	0.0040	0.0092 ± 0.0012	113	1.61	0.0061 ± 0.0001	117	1.13
	0.0060	0.0114 ± 0.0023	112	2.92	0.0078 ± 0.0001	107	1.30
	0.0080	0.0139 ± 0.0013	115	1.55	0.0098 ± 0.0002	105	1.04

**Table 4.16** Summary of the recovery and RSD of the proposed sensor and the standard method (ICP-OES) for simultaneous Cu(II), Co(II), Ni(II), Hg(II), and Mn(II) determination in pond-CU water.

Metal ion	Added (mM)	Proposed sensor (n=5)			ICP-OES (n=3)		
		Found (mM)	%Recovery	%RSD	Found (mM)	%Recovery	%RSD
Cu(II)	-	N.D.			N.D.		
	0.080	0.081 ± 0.023	101	6.30	0.090 ± 0.001	113	0.46
	0.400	0.434 ± 0.035	109	4.87	0.417 ± 0.004	104	0.87
	0.800	0.748 ± 0.024	94	2.36	0.792 ± 0.006	99	0.81
Co(II)	-	N.D.			N.D.		
	0.020	0.022 ± 0.015	110	3.03	0.022 ± 0.001	110	4.16
	0.040	0.044 ± 0.012	110	2.31	0.039 ± 0.001	98	5.61
	0.060	0.066 ± 0.013	110	2.46	0.058 ± 0.001	97	2.82
Ni(II)	-	N.D.			N.D.		
	0.800	0.839 ± 0.098	105	5.49	0.786 ± 0.001	98	0.00
	2.000	2.128 ± 0.121	106	3.94	2.154 ± 0.004	108	0.27
	4.000	4.218 ± 0.157	105	3.05	4.087 ± 0.018	102	0.50
Hg(II)	-	N.D.			N.D.		
	0.008	0.008 ± 0.005	100	3.45	0.008 ± 0.001	100	1.68
	0.020	0.022 ± 0.006	110	4.46	0.022 ± 0.001	110	1.79
	0.040	0.044 ± 0.003	110	4.63	0.043 ± 0.001	108	0.91
Mn(II)	-	N.D.			N.D.		
	0.0040	0.0050 ± 0.0007	125	1.02	0.0045 ± 0.0001	113	2.15
	0.0060	0.0074 ± 0.0022	123	2.89	0.0067 ± 0.0003	112	2.80
	0.0080	0.0099 ± 0.0017	124	2.22	0.0084 ± 0.0004	105	3.13

CU refers to Chulalongkorn University.

## CHAPTER V

### CONCLUSIONS

A polymer screen printing method was successfully used to fabricate the device types A, B, C, D. The device type A was applied for preliminary study of each metal complex. The device types B, C, and D were designed to use for simultaneous detection of four metal ions. The device type D was successfully applied for simultaneous detection of four metal ions by naked-eye. A wax printing method was also applied to fabricate the device types E and F. The device type E was designed for simultaneous detection of eight metal ions by naked-eye and the device type E was used to determine for simultaneous detection of five metal ions.

For simultaneous Cu(II), Co(II), Zn(II), Cd(II)/Pb(II) detection on device type D, the device was fabricated by using a polymer screen-printing method. The colorimetric reaction between the metal ions and complexing agents in each detection zone was used to identify each metal ion. The proposed method was successfully applied in synthetic unknown water samples by naked-eye. The accuracies of the proposed method were evaluated by a researcher and 10 students under optimal conditions. The accuracies by a researcher were found in the range of 79.6-87.5% in comparison with real photograph of the color chart. The accuracies were evaluated in the range of 91.7-95.8% in comparison with the color chart in computer display. The accuracies by 10 students (n=10) were established in the range of 41.7-87.5% in comparison with real photograph of the color chart. The accuracies were demonstrated in the range of 20.8-83.3% in comparison with the color chart in computer display.

For simultaneous Cu(II), Co(II), Ni(II), Hg(II), Fe(III), Cr(VI), V(III), and Mn(II) detection on device type E, the device was fabricated by using a wax printing method. The colorimetric reaction between the metal ions and complexing agents in each detection zone was used to identify each metal ion. The proposed method was effectively applied in synthetic unknown water samples by naked-eye. The accuracies

of the proposed method were evaluated by a researcher under optimal reaction. The synthetic unknown water samples (46 types) were selected to study the accuracy form 156 types. The accuracy was 73.91% for metal ion identification by a researcher. The proposed sensor was effectively for simultaneous an anion (Cr(VI)) and seven cations (Cu(II), Co(II), Ni(II), Hg(II), Fe(III), V(III), and Mn(II)) detection.

For simultaneous Cu(II), Co(II), Ni(II), Hg(II), and Mn(II) determination on device type F couple with a scanner, the device was fabricated by using a wax printing method. For simultaneous Cu(II), Co(II), Ni(II), Co(II), and Mn(II) analysis in real water samples, the device was prepared with a set of reagents for a single metal ion ( $n=5$ ) on one device for simultaneous five metal ions quantification and the device was prepared with the five optimized reagent conditions on one device for simultaneous five metal ions identification by naked-eye. The colorimetric reaction between the metal ions and complexing agents in each detection zone was used to analyze each metal ion. In addition, a device design consisted of two pretreatment zones with various masking agents to increase specificity for removing interfering ions. The orange  $\text{Cu}(\text{BC})_2$ , pink red  $\text{Ni}(\text{DMG})_2$ , pink red  $\text{Hg}(\text{DTZ})_2$ , red  $\text{Co}(\text{PAR})_2$ , and red  $\text{Mn}(\text{PAR})_2$  complexes showed highly selective for simultaneous Cu(II), Co(II), Ni(II), Hg(II), and Mn(II) detection. The optimal conditions were determined to obtain the lowest detectable concentration of 0.005 mM (0.32 mg/L), 0.010 mM (0.59 mg/L), 0.100 mM (5.87 mg/L), 0.001 mM (0.20 mg/L), and 0.0020 mM (0.11 mg/L) for Cu(II), Co(II), Ni(II), Hg(II), and Mn(II) determination, respectively. The lowest detectable concentration of Cu(II) was lower than regulation levels and Mn(II) was close to regulation levels for heavy metal ions in in drinking water [4]. The method performance was evaluated in three types of water samples. The results from the proposed method were compared to results from the standard ICP-OES method with good accuracy and precision. This proposed method demonstrated utility in real water samples with highly selective, sensitive, low cost, and simultaneous detection of Cu(II), Co(II), Ni(II), Hg(II), and Mn(II) by naked-eye.



## REFERENCES

1. Qu, X.; Xu, W.; Ren, J.; Zhao, X.; Li, Y.; Gu, X., A field study to predict Cd bioaccumulation in a soil-wheat system: Application of a geochemical model. *J. Hazard. Mater.* **2020**, *400*, 123135.
2. Lin, Y.; Gritsenko, D.; Feng, S.; Teh, Y. C.; Lu, X.; Xu, J., Detection of heavy metal by paper-based microfluidics. *Biosens Bioelectron* **2016**, *83*, 256-66.
3. Hamida, S.; Ouabdeslam, L.; Ladjel, A. F.; Escudero, M.; Anzano, J., Determination of cadmium, copper, lead, and zinc in pilchard sardines from the bay of boumerdés by atomic absorption spectrometry. *Anal. Lett* **2018**, *51*, 2501-2508.
4. Endah, S. R. N., Surantaatmadja, S. I., The determination of heavy metals level lead in cosmetic soap preparation by atomic absorption spectrophotometer (AAS). *J. Phys. Conf. Ser.* **2019**, *1179*, 12178.
5. Lo, M.; Diaw, A. K. D.; Gningue-Sall, D.; Oturan, M. A.; Chehimi, M. M.; Aaron, J. J., A novel fluorescent sensor based on electrosynthesized benzene sulfonic acid-doped polypyrrole for Pb(II) and Cu(II). *J. Lumin* **2019**, *34*, 489-499.
6. Smirnova, S. V.; Ilin, D. V.; Pletnev, I. V., Extraction and ICP-OES determination of heavy metals using tetrabutylammonium bromide aqueous biphasic system and oleophilic collector. *Talanta* **2021**, *221*, 121485.
7. Huang, W.; Zhang, Y.; Li, Y.; Zeng, T.; Wan, Q.; Yang, N., Morphology-controlled electrochemical sensing of environmental Cd(II) and Pb(II) ions on expanded graphite supported CeO<sub>2</sub> nanomaterials. *Anal. Chim. Acta* **2020**, *1126*, 63-71.
8. Xin, X.; Hu, N.; Ma, Y.; Wang, Y.; Hou, L.; Zhang, H.; Han, Z., Polyoxometalate-based crystalline materials as a highly sensitive electrochemical sensor for detecting trace Cr(VI). *Dalton Trans.* **2020**, *49*, 4570-4577.
9. Thanh, N. M.; Van Hop, N.; Luyen, N. D.; Phong, N. H.; Tam, T.; Tran, T.,

- Simultaneous determination of Zn(II), Cd(II), Pb(II), and Cu(II) using differential pulse anodic stripping voltammetry at a bismuth film-modified electrode. *ADV MATER SCI EN* **2019**, *2019*, 1-11.
10. Martinez, A. W., Microfluidic paper-based analytical devices: from POCKET to daper-based ELISA. *Bioanalysis* **2011**, *3*, 2589-2592.
  11. Martinez, A. W.; Phillips, S. T.; Wiley, B. J.; Gupta, M.; Whitesides, G. M., FLASH: A rapid method for prototyping paper-based microfluidic devices. *LAB CHIP* **2008**, *8*, 2146-2150.
  12. Lu, Y.; Shi, W.; Jiang, L.; Qin, J.; Lin, B., Rapid prototyping of paper-based microfluidics with wax for low-cost, portable bioassay. *Electrophoresis* **2009**, *30* (9), 1497-500.
  13. Dungchai, W.; Chailapakul, O.; Henry, C. S., Use of multiple colorimetric indicators for paper-based microfluidic devices. *Anal. Chim. Acta* **2010**, *674*, 227-33.
  14. Yu, L.; Shi, Z. Z., Microfluidic paper-based analytical devices fabricated by low-cost photolithography and embossing of parafilm(R). *LAB CHIP* **2015**, *15* (7), 1642-5.
  15. Abe, K.; Koji Suzuki, K.; Citterio, D., Inkjet-printed microfluidic multianalyte chemical sensing paper. *Anal. Chem.* **2008**, *80*, 6928-6934.
  16. Sameenoi, Y.; Nongkai, P. N.; Nouanthavong, S.; Henry, C. S.; Nacapricha, D., One-step polymer screen-printing for microfluidic paper-based analytical device (uPAD) fabrication. *Analyst* **2014**, *139*, 6580-6588.
  17. Teengam, P.; Siangproh, W.; Tuantranont, A.; Vilaivan, T.; Chailapakul, O.; Henry, C. S., Multiplex paper-based colorimetric DNA sensor using pyrrolidinyl peptide nucleic acid-induced AgNPs aggregation for detecting MERS-CoV, MTB, and HPV oligonucleotides. *Anal. Chem.* **2017**, *89*, 5428-5435.
  18. Bracher, P. J.; Gupta, M.; Mack, E. T.; Whitesides, G. M., Heterogeneous films of ionotropic hydrogels fabricated from delivery templates of patterned paper. *ACS Appl. Mater. Interfaces* **2009**, *1*, 1807-12.
  19. Carrilho, E.; Andres, W. M.; A. W; Whitesides., G. M., Understanding wax printing: A simple micropatterning process for paper-based microfluidics. *Anal.*

- Chem.* **2009**, *81*, 7091–7095.
20. Sharifi, H.; Tashkhourian, J.; Hemmateenejad, B., A 3D origami paper-based analytical device combined with PVC membrane for colorimetric assay of heavy metal ions: Application to determination of Cu(II) in water samples. *Anal. Chim. Acta* **2020**, *1126*, 114-123.
  21. Muhammad-Aree, S.; Teepoo, S., On-site detection of Heavy metals in wastewater using a single paper strip integrated with a smartphone. *Anal. Bioanal. Chem.* **2020**, *412*, 1395-1405.
  22. Dong, R. E. K., Ping; Xu, X.-L. C., Liu-Xin; Guo, Z., Cation-exchange strategy for a colorimetric paper sensor: belt-like ZnSe nanoframes toward visual determination of heavy metal ions. *Sensors and Actuators B: Chemical* **2020**, *312*.
  23. Rattanarat, P.; Dungchai, W.; Cate, D.; Volckens, J.; Chailapakul, O.; Henry, C. S., Multilayer paper-based device for colorimetric and electrochemical quantification of metals. *Anal. Chem.* **2014**, *86*, 3555-62.
  24. Wang, H.; Yang, L.; Chu, S.; Liu, B.; Zhang, Q.; Zou, L., Semiquantitative visual detection of lead ions with a smartphone via a colorimetric paper-based analytical device. *Anal. Chem.* **2019**, *91*, 9292-9299.
  25. Cunha, F. A. S.; Ferreira, D. T. S.; Andrade, W. C. R.; Fernandes, J. P. A.; Lyra, W. S.; Pessoa, A. G. G.; de Araujo, M. C. U., Macroemulsion-based dispersive magnetic solid phase extraction for preconcentration and determination of copper(II) in gasoline. *Mikrochim Acta* **2018**, *185*, 99.
  26. Ebrahimi, B.; Bahar, S.; Moedi, S. E., Cold-induced aggregation microextraction technique based on ionic liquid for preconcentration and determination of nickel in food samples. *J. Braz. Chem. Soc.* **2013**.
  27. Saleviter, S.; Fen, Y. W.; Omar, N. A. S.; Zainudin, A. A.; Daniyal; Mohd, W. M. E. M., Optical and structural characterization of immobilized 4-(2-pyridylazo)resorcinol in chitosan-graphene oxide composite thin film and its potential for Co<sup>2+</sup> sensing using surface plasmon resonance technique. *Results Phys.* **2018**, *11*, 118-122.
  28. K., C. L.; Brey, H. R., 1-(2-Pyridylazo)-2-naphthol as a possible analytical

- reagent. *Anal. Chem.* **1995**, *27*, 782-785.
29. Shahat, A.; Hassan, H. M.; Azzazy, H. M., Optical metal-organic framework sensor for selective discrimination of some toxic metal ions in water. *Anal. Chim. Acta* **2013**, *793*, 90-8.
  30. P. Paradkar; R., P.; Williams, R. R., Micellar colorimetric determination of dithizone metal chelates. *Anal. Chem.* **1994**, *66*, 2752-2756.
  31. Soares, S. A. R.; Costa, S. S. L.; Araujo, R. G. O.; Teixeira, L. S. G.; Dantas, A. F., Comparison of spectrophotometric methods for the determination of copper in sugar cane spirit. *J. AOAC Int.* **2018**, *101*, 876-882.
  32. Najarzadegan, H.; Sereshti, H., Development of a colorimetric sensor for nickel ion based on transparent electrospun composite nanofibers of polycaprolactam-dimethylglyoxime/polyvinyl alcohol. *J. Mater. Sci.* **2016**, *51*, 8645-8654.
  33. Zhou, X.; Nie, J.; Du, B., 4-(2-Pyridylazo)-resorcinol functionalized thermosensitive ionic microgels for optical detection of heavy metal ions at nanomolar level. *ACS Appl. Mater. Interfaces* **2015**, *7*, 21966-21974.
  34. Cate, D. M.; Noblitt, S. D.; Volckens, J.; Henry, C. S., Multiplexed paper analytical device for quantification of metals using distance-based detection. *LAB CHIP* **2015**, *15*, 2808-2818.
  35. Alamad, W.; Tungkijanansin, N.; Kanate, T.; Varanusupakul, P., A colorimetric paper-based analytical device coupled with hollow fiber membrane liquid phase microextraction (HF-LPME) for highly sensitive detection of hexavalent chromium in water samples *Talanta* **2018**, *190*, 78-84.
  36. Raoot, N., Raoot, S, Selective complexometric determination of palladium, with thiourea as masking agent. *Talanta* **1981**, *28*, 327-328.
  37. Chakrapani, G.; Murty, D. S. R.; Balaji, B. K.; Rangawamy, R., Spectrophotometric method for the determination of vanadium in uranium rich hydrogeochemical samples using pyridyl azo resorcinol (PAR). *Talanta* **1993**, *40*, 541-544.
  38. Pribil, R.; Vesely, V., Contributions to the basic problems of complexometry-V mutual masking of iron and manganese. *Talanta* **1961**, *8*, 270-275.

39. Meredith, N. A.; Volckens, J.; Henry, C. S., Paper-based microfluidics for experimental design: Screening masking agents for simultaneous determination of Mn(II) and Co(II). *Anal. Methods* **2017**, *9*, 534-540.
40. Taylor, A. A.; Tsuji, J. S.; Garry, M. R.; McArdle, M. E.; Goodfellow, W., Critical review of exposure and effects: implications for setting regulatory health criteria for ingested copper. *Environ Manage.* **2020**, *65*, 131-159.
41. Leyssens, L.; Vinck, B.; Van Der Straeten, C.; Wuyts, F.; Maes, L., Cobalt toxicity in humans-A review of the potential sources and systemic health effects. *Toxicology* **2017**, *387*, 43-56.
42. Jan, A. T.; Azam, M.; Siddiqui, K.; Ali, A.; Choi, I.; Haq, Q. M., Heavy metals and human health: Mechanistic insight into toxicity and counter defense system of antioxidants. *Int. J. Mol. Sci.* **2015**, *16*, 29592-630.
43. Jaishankar, M.; Tseten, T.; Anbalagan, N.; Mathew, B. B.; Beeregowda, K. N., Toxicity, mechanism and health effects of some heavy metals. *Interdiscip. Toxicol.* **2014**, *7*, 60-72.
44. Jorg, M.; Knirsch, W.; Kern, K.; Schleh, C.; Adelhelm, C., Nanoparticulate vanadium oxide potentiated vanadium toxicity in human lung cells. *Environ. Sci. Technol.* **2007**, *41*, 331-336.
45. Liu, C.; Bi, X.; Zhang, A.; Qi, B.; Yan, S., Preparation of an L-cysteine functionalized magnetic nanosorbent for the sensitive quantification of heavy metal ions in food by graphite furnace atomic absorption spectrometry. *Anal. Lett.* **2020**, *53*, 2079-2095.
46. Rodrigues, N. P.; Rodrigues, E.; Celso, P. G.; Kahmann, A.; Hertz, P. F., Discrimination of sparkling wines samples according to the country of origin by ICP-OES coupled with multivariate analysis. *Lwt* **2020**, *131*.
47. Dalkiran, B., Amperometric determination of heavy metal using an HRP inhibition biosensor based on ITO nanoparticles-ruthenium (III) hexamine trichloride composite: Central composite design optimization. *Bioelectrochemistry* **2020**, *135*, 107569.
48. Liu, Y.; Chu, Y.; Hu, Z.; Zhang, S.; Ma, S.; Khan, M. S.; Lau, C., High-sensitivity determination of trace lead and cadmium in cosmetics using laser-induced

- breakdown spectroscopy with ultrasound-assisted extraction. *Microchem. J.* **2020**, *158*, 105322.
49. Martinez, A. W.; Phillips, S. T.; Butte, M. J.; Whitesides, G. M., Patterned paper as a platform for inexpensive, low-volume, portable bioassays. *Angew. Chem. Int. Ed.* **2007**, *46*, 1318-1320.
50. Curto, V. F.; Lopez-Ruiz, N.; Capitan-Vallvey, L. F.; Palma, A. J.; Benito-Lopez, F.; Diamond, D., Fast prototyping of paper-based microfluidic devices by contact stamping using indelible ink. *RSC Adv.* **2013**, *3*, 18811–18816.
51. Cassano, C. L.; Fan, Z. H., Laminated paper-based analytical devices (LPAD): Fabrication, characterization, and assays. *Microfluid Nanofluidics* **2013**, *15*, 173-181.
52. Songjaroen, T.; Dungchai, W.; Chailapakul, O.; Laiwattanapaisal, W., Novel, simple and low-cost alternative method for fabrication of paper-based microfluidics by wax dipping. *Talanta* **2011**, *85*, 2587-2593.
53. Tai, Y.-L.; Yang, Z.-G., Fabrication of paper-based conductive patterns for flexible electronics by direct-writing. *J. Mater. Chem* **2011**, *21*, 5938–5943.
54. Sánchez-Calvo, A.; Fernández-Abedul, M. T.; Blanco-López, M. C.; Costa-García, A., Paper-based electrochemical transducer modified with nanomaterials for mercury determination in environmental waters. *Sensors and Actuators B: Chemical* **2019**, *290*, 87-92.
55. Chaiyo, S.; Apiluk, A.; Siangproh, W.; Chailapakul, O., High sensitivity and specificity simultaneous determination of lead, cadmium and copper using  $\mu$ PAD with dual electrochemical and colorimetric detection. *Sensors and Actuators B: Chemical* **2016**, *233*, 540-549.
56. Li, M.; Cao, R.; Nilghaz, A.; Guan, L.; Zhang, X.; Shen, W., "Periodic-Table-Style" paper device for monitoring heavy metals in water. *Anal. Chem.* **2015**, *87*, 2555-2559.
57. Guo, C.; Wang, J.; Cheng, J., Colorimetric sensing of copper (II) ions based on the inhibition of biocatalytic growth of gold nanoparticles. *Microchem. J.* **2020**, *157*, 105015.

58. Wu, Q.; He, J.; Meng, H.; Wang, Y.; Zhang, Y.; Li, H.; Feng, L., A paper-based microfluidic analytical device combined with home-made SPE column for the colorimetric determination of copper(II) ion. *Talanta* **2019**, *204*, 518-524.
59. Pratiwi, R.; Nguyen, M. P.; Ibrahim, S.; Yoshioka, N.; Henry, C. S.; Tjahjono, D. H., A selective distance-based paper analytical device for copper(II) determination using a porphyrin derivative. *Talanta* **2017**, *174*, 493-499.
60. Huang, K.; Chen, Y.; Zhou, F.; Zhou, Y.; Jing, T., Integrated ion imprinted polymers-paper composites for selective and sensitive detection of Cd(II) ions. *J. Hazard. Mater.* **2017**, *333*, 137-143.
61. Cai, L.; Fang, Y.; Mo, Y.; Huang, Y.; Xu, C.; Zhang, Z.; Wang, M., Visual quantification of Hg(II) on a microfluidic paper-based analytical device using distance-based detection technique. *AIP Adv.* **2017**, *11*, 85214-85222.
62. Mentele, M. M.; Cunningham, J.; Koehler, K.; Volckens, J.; Henry, C. S., Microfluidic paper-based analytical device for particulate metals. *Anal. Chem.* **2012**, *84*, 4474-80.
63. Quinn, C. W.; Cate, D. M.; Miller-Lionberg, D. D.; Reilly, T., 3rd; Volckens, J.; Henry, C. S., Solid-phase extraction coupled to a paper-based technique for trace copper detection in drinking water. *Environ. Sci. Technol.* **2018**, *52*, 3567-3573.
64. Hofstetter, J. C.; Wydallis, J. B.; Neymark, G.; Reilly, T. H.; Harrington, J.; Henry, C. S., Quantitative colorimetric paper analytical devices based on radial distance measurements for aqueous metal determination. *Analyst* **2018**, *143*, 3085-3090.
65. Cate, D. M.; Nanthasurasak, P.; Riwkulkajorn, P.; L'Orange, C.; Henry, C. S.; Volckens, J., Rapid detection of transition metals in welding fumes using paper-based analytical devices. *Ann Occup Hyg* **2014**, *58*, 413-423.
66. Takahashi, Y.; Danwittayakul, S.; Suzuki, T. M., Dithizone nanofiber-coated membrane for filtration-enrichment and colorimetric detection of trace Hg(II) ion. *Analyst* **2009**, *134*, 1380-1385.
67. Budesinsky, B. W.; Sagat, M., Stability constants of some metal dithizonates. *Talanta* **1973**, *20*, 228-232.

68. Shahat, A.; Ali, E. A.; El Shahat, M. F., Colorimetric determination of some toxic metal ions in post-mortem biological samples. *Sens. Actuators B Chem.* **2015**, *221*, 1027-1034.
69. Qin, L.; Jing-Fong, W.; Greg, E. C.; Robert, E. M.; Pamela, M. S.; Yan, G., Rapid determination of dissolved copper in jet fuels using bathocuproine. *Energy&Fuels* **2003**, *17*, 699-704.
70. Allafchian, A. R.; Farajmand, B.; Koupaei, A. J., A paper-based analytical device based on combination of Thin film microextraction and reflection scanometry for sensitive colorimetric determination of Ni(II) in aqueous matrix. *Bull Environ Contam Toxicol* **2018**, *100*, 529-535.
71. Muhammad, S.; Umer, S.; Waheed-uz, Z.; Rabia, R.; Amna, Y.; Faiza, A.; Jesús, M. A., A rapid method for measurement of nickel and chromium at trace level in aqueous samples. *J Mex Chem Soc* **2011**, *55*, 214-217.
72. Smirnova, S. V.; Samarina, T. O.; Ilin, D. V.; Pletnev, I. V., Solubilization of 4-(2-pyridylazo)resorcinol in hydrophobic-hydrophilic ionic liquids and extraction of heavy metal ions from aqueous solutions. *Moscow University chemistry bulletin* **2015**, *70*, 229-233.
73. Tavallali, H.; Deilamy-Rad, G.; Karimi, M. A.; Rahimy, E., A novel dye-based colorimetric chemosensors for sequential detection of Cu(II) and cysteine in aqueous solution. *Anal. Biochem.* **2019**, *583*, 113376.
74. Kocyla, A.; Pomorski, A.; Krezel, A., Molar absorption coefficients and stability constants of metal complexes of 4-(2-pyridylazo)resorcinol (PAR): Revisiting common chelating probe for the study of metalloproteins. *J. Inorg. Biochem.* **2015**, *152*, 82-92.
75. Shar, G. A.; Bhangar, M. I., Spectrophotometric determination of metal complexes of 1-(2 pyridylazo)-2-naphthol in micellar medium. *Jour. chem. Soc. Park.* **2003**, *25*, 28-33.
76. Electrolytes, EFM, and Chemical Equilibrium.  
<https://drjvazque.files.wordpress.com/2012/2001/tablas-de-formacion-de-complejos>.
77. Izquierdo, A., Determination of the solubility product constants of Ni(II) and



- Cu(II) complexes with N-substituted hydrazinedithiocarboxylic acids. *Polyhedron* **1986**, *5*, 1007-1011.
78. Wuilloud, R. G.; Wuilloud, J. C.; Olsina, R. A.; Martinez, L. D., Speciation and preconcentration of vanadium(V) and vanadium(IV) in water samples by flow injection-inductively coupled plasma optical emission spectrometry and ultrasonic nebulization. *Analyst* **2001**, *126*, 715-719.
79. Wilkins, D.; F., S., 6-Bis(2-pyridyl)pyridine and alkyl derivatives their properties in the formation of ferrous and cobaltous coloured complex cations. *Anal. Chim. Acta* **1953**, *9*, 338-348.
80. Zargoosh, K.; Babadi, F. F., Highly selective and sensitive optical sensor for determination of Pb(II) and Hg(II) ions based on the covalent immobilization of dithizone on agarose membrane. *Spectrochim. Acta A Mol. Biomol. Spectrosc.* **2015**, *137*, 105-10.
81. Wang, Z.; Cheng, K. L., Spectrophotometric determination of iron with 1,10-phenanthroline in the presence of copper. *Microchim. Acta* **1982**, *2*, 115-124.
82. Bai, X.; Zhang, X.; Gu, H.; Li, F.; Huang, W.; Liang, L.; Ye, Z., Highly selective colorimetric sensing of Cu(II) using a schiff Base derivative immobilized on polyvinyl alcohol microspheres. *New J. Chem.* **2018**, 11682-11688.
83. Abraham, J.; Narayana, B., Complexometric determination of zinc(II) using 2,2'-bipyridyl as selective masking agent. *Mikrochim. Acta* **2000**, *134*, 33-35
84. Cesa, S.; Carradori, S.; Bellagamba, G.; Locatelli, M.; Casadei, M. A.; Masci, A.; Paolicelli, P., Evaluation of processing effects on anthocyanin content and colour modifications of blueberry (*vaccinium* spp.) extracts: Comparison between HPLC-DAD and CIELAB analyses. *Food Chem.* **2017**, *232*, 114-123.
85. Jean-Francois, G., Colour effects of co-pigmentation of anthocyanins revisited-I. A calorimetric definition using the CIELAB scale. *Food Chem.* **1998**, *63*, 409-415.
86. Zhang, Y.; Jiang, J.; Li, M.; Gao, P.; Shi, L.; Shuang, S., Bright far-red/near-infrared gold nanoclusters for highly selective and ultra-sensitive detection of Hg(II). *Sensors and Actuators B: Chemical* **2017**, *238*, 683-692.
87. Pham, D. N. K.; Roy, M.; Golen, J. A.; Manke, D. R., The first-row transition-

- metal series of tris(ethylenediamine) diacetate complexes  $[M(en)_3](OAc)_2$  (M is Mn, Fe, Co, Ni, Cu, and Zn). *Acta Crystallogr C Struct Chem* **2017**, *73*, 442-446.
88. Wayne, E. W., Dithizone as an analytical reagent. *J. Chem. Educ.* **1936**, *1*, 369-373.
89. Naracham, V. S.; Ronald, A. N. B., Narayana. Prashant, Hegde. ; Busnur , R. M., Indirect complexometric determination of Thorium(IV) using sodium fluoride as masking agent. *Microchim. Acta* **2002**, *140*, 77-79.
90. Rudolf, P.; Vladimir, V., Contributions to the basic problems of complexometry- V Mutual masking of iron and manganese. *Talanta* **1961**, *8*, 270-275.
91. Duffy, G.; Maguire, I.; Heer, B.; Gres, P.; Ducree, J.; Regan, F., ChromisSense: A colorimetric lab-on-a-disc sensor for chromium speciation in water. *Talanta* **2018**, *178*, 392-399.
92. Sun, X.; Li, B.; Qi, A.; Tian, C.; Chen, L., Improved assessment of accuracy and performance using a rotational paper-based device for multiplexed detection of heavy metals. *Talanta* **2018**, *178*, 426-431.
93. Appendix F: Guidelines for standard method performance requirements. *J. AOAC Int.* **2016**.

## VITA

NAME	Miss Pornphimon Kamnoet
DATE OF BIRTH	2 April 1991
PLACE OF BIRTH	Nong Khai
INSTITUTIONS ATTENDED	Chulalongkorn University
HOME ADDRESS	157 Nammong, Thabo, Nong Khai 43110 Thailand
PUBLICATION	Kamnoet, P., Aeungmaitrepirom, W., Menger, F. R., and Henry, C. S., Highly selective simultaneous Cu(II), Co(II), Ni(II), Hg(II), Mn(II) determination in water samples on microfluidic paper-based analytical devices, <i>Analyst</i> . 2020 (Major Revision).
AWARD RECEIVED	-